Performance Optimisation of Hot Water Cylinders

By:

Angelo Kanishka Goonesekera

A thesis submitted in partial fulfilment of the requirements for the degree of
Master of Philosophy

The University of Sheffield
Faculty of Engineering
Department of Mechanical Engineering

January 2017

Acknowledgements

Contents

Abstract

The systematic depletion of non-renewable energy sources and the current high capital costs of installing renewable energy systems place significant focus on energy efficiency in engineering. The requirement for energy efficiency covers a wide set of disciplines from industrial power generation to home heating and hot water. This study focuses on the operation of domestic hot water cylinders and how to better understand the factors relating to improving the output of its immersed tube coil heat exchangers. It is shown that by improving the output capability of the immersed coil, a domestic hot water cylinder can transfer the energy provided to it by both renewable and non-renewable sources faster to the stored water.

This was an experimental research project, and all the work was completed to BS EN 12897:2006, which ensured that the results were repeatable, transferable and comparable to other cylinders both from the sponsoring company and to others on the market.

The study looked at varying the parameters of height, diameter and pitch of a coil within a test cylinder and measuring the *U* values obtained under operation. In each case the coil tested was placed offset to the cylinder axis with the intention of creating a convective current to improve heat transfer. Special tests separate from the parametric investigation were also carried out to evaluate the impact of adding a chimney to the coil, painting the coil surface black and adding a taper angle to the coil. The test coils were also compared to current commercial heating coils in cylinders.

Certain combinations of parameter changes showed slight improvements in the U values of the coil. The taper angle added to the coil showed no significant improvements and painting the coil surface black was proven to be detrimental to the coils performance. The chimney addition showed signs of improved convection within the cylinder.

The offset test coils when compared with current central commercial coils showed a significant improvement in output per square meter of coil surface area, providing same heat up times with 39% less coil length. The offset design has now been presented to the host organisation of this project and is under review for implementation in a future range of large capacity cylinders.

Nomenclature

A	Area (m^2)
C_d	Discharge coefficient
C_p	Specific heat at constant pressure (J/kg/K)
D_R	Diameter ratio
D	Diameter of coil turns to central axis of tube (m)
g	Acceleration due to gravity (m/s^2)
Gr_L	Grashof number
h	Convective heat transfer coefficient (W/m^2/K)
H	Height or vertical distance (m)
H_R	Height ratio
k	Thermal conductivity (W/m/K)
k_f	Thermal conductivity of fluid (W/m/K)
L	Characteristic length (m)
L_{coil}	Total length of coil helix (m)
m	Mass (kg)
$\dot{m}$	Mass flow rate (kg/s)
n	Number of coil turns
Nu	Nusselt number
P	Calculated heat exchanger performance (kW)
Pr	Prandtl number
$\dot{q}$	Energy generation within the system (W)
Q	Energy transferred (kJ)
Q_{hx}	Mean power output of the heat exchanger (W)
Q_c	Corrected 24 h heat loss (kWh/24h)
Q_{coil}	Coil power(kW)
Q_{conv}	Rate of heat transfer due to convection (W)
Q_{cr}	Rate of radial thermal conduction (W)
Q_{flow}	Flow induced by stack effect (m^3/s)
Q_{rad}	Rate of heat transfer due to radiation (W)
Q_{st}	Declared standing heat loss (kWh/24h)
Q_c	Conduction rate (W)
r	Radius (m)
Re_L	Reynolds number
S_R	Separation ratio
t	Time (s)
T	Temperature (K)
ΔT_{coil}	Temperature difference between the coil inlet and outlet (°C)
u_∞	Free stream velocity (m/s)
U	Overall heat transfer coefficient (W/m^2/K)

V_{40}	Mixed water quantity delivered at 40 °C (l)
V_{hot}	Volume of water drawn off at ≥ (θc + 30)°C (l)
β	Volumetric thermal expansion coefficient (1/K)
δ	Velocity boundary layer
ε	Emissivity
θ_a	Measured ambient temperature at a given position (°C)
θ_c	Average temperature of inlet cold water during the test (°C)
θ_d	Average value of the calculated temperature differentials (°C)
θ_p	Normalised value of average draw off temperature (°C)
θ'_p	Average temperature of the water drawn off at ≥ (θc + 30) °C (°C)
θ_{set}	Target hot water temperature for hot water performance testing = θc + 50 K (°C)
θ_w	Target temperature of stored water for heat loss testing (°C)
μ	Viscosity of fluid (kg/s/m)
ν	Kinematic viscosity (m^2/s)
ρ	Density (kg/m^3)
σ	Stefan-Boltzmann constant (W/m^2/K^4)

Introduction

In a modern household, hot water has almost been taken for granted as much as having running water. The days of heating water separately in pots or jugs for use in sanitary purposes and mixing at point of use in a bath or a wash basin are a distant memory. In contemporary times heating water on a stove or in a jug would be reserved for food or drink preparation. The on demand hot water which most of the developed world enjoys would have been viewed as a luxury a few decades ago. One must only think of how inconvenient it would be to have a fault in a domestic hot water system during winter to understand how important having a reliable supply of hot water is to the modern household.

Types of Hot Water Cylinders

In a typical domestic setting, hot water is obtained by way of point of use electrical heaters, combination boilers or hot water cylinders connected to boilers, electrical heaters or renewable energy sources. Hot water cylinders sometimes referred to as hot water tanks or water heaters are vessels that store potable water obtained from sources such as main pipelines or boreholes. The stored water is maintained at an elevated temperature of 60°C - 65°C and in most cases is mixed with cold water at point of use to a lower temperature to provide water at 35°C - 45°C.

Many different designs of hot water cylinders are available in the market today but they all belong to one of two categories

1. Vented or unpressurised hot water cylinders
2. Unvented or pressurised hot water cylinders

Vented hot water cylinders are open systems where the cylinder is fed by a cold-water tank or cistern which is placed above the cylinder to give the cylinder some head of pressure and ensure that it remains filled. This tank is sometimes referred to as the feed and expansion tank. In most cases the cold-water tank is given a supply from the mains water supply. During the operation of heating, the water in the hot water cylinder will expand and flow back into the cold-water tank by way of its inlet pipe at the bottom of the cylinder. A vent pipe is also connected to the top of the hot water cylinder which terminates above the water line of the cold-water tank. This pipe is present to make the cylinder an open vented vessel. In a typical case the domestic hot water supply pipe is connected to the vent pipe at

the lower part of its height by way of a T connection. Because water in this type of hot water cylinder expands to atmosphere during heating, it is referred to as a vented hot water cylinder.
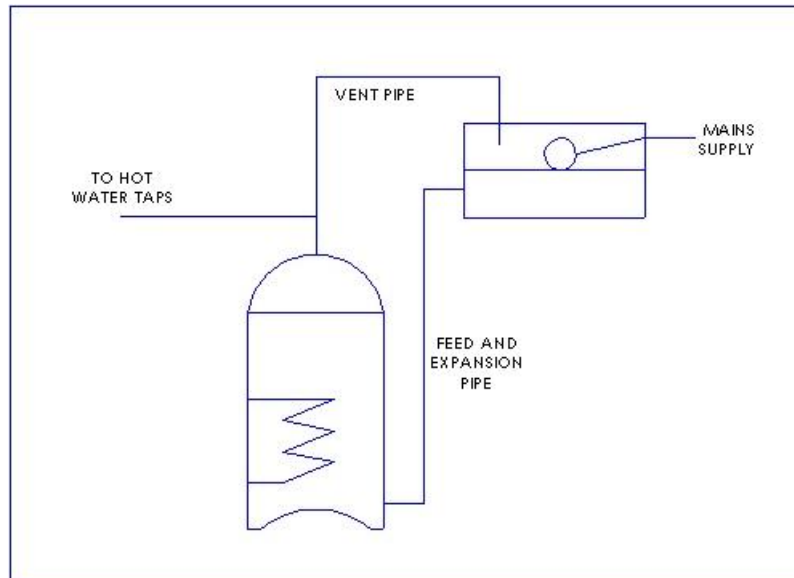
Figure 1.1 – Vented Hot Water Cylinder

Unvented hot water cylinders are considered closed systems of hot water supply. They must have safety components fitted during installation that allows for the cylinder to vent to atmosphere if the safety limit of temperature or pressure within the cylinder is exceeded during operation. The typical safety limits are 90°C for temperature and 7 bar to 10 bar for pressure (Kingspan Environmental, 2014). Unvented hot water cylinders usually have a supply feed direct to the cylinder from the mains water pipeline. A pressure reducing device is fitted at the inlet to the cylinder to regulate the incoming water pressure to protect the cylinder if an increase in mains pressure above a safe limit occurs. At present most pressure reducing valves limit the inlet pressure of the cylinder to 3 bar (Kingspan Environmental, 2014).

A main requirement for unvented hot water cylinders is a mechanism for allowing the water within the cylinder to expand during the heating operation. This is mainly done by including an expansion vessel in the installation of the cylinder. An expansion vessel is a chamber that has a built-in water tight diaphragm which separates the chamber into two sections. One side of the chamber is connected to the hot water cylinder and is therefore in contact with the potable water. The other side of the chamber is pressurised with air. The air in the chamber is pressurised to the same pressure as indicated by the pressure reducing device connected

to the potable water inlet. This allows for the entire volume of the expansion vessel to remain filled with air before the heating operation and then gradually lets it fill with water as the heating begins.

In some instances, a trapped air bubble within the hot water cylinder is also made to work as an expansion volume. A third method is to allow the expanded volume of water to flow out of a waste pipe by way of an expansion relief valve. As with vented hot water cylinders the water is held at an elevated temperature of 60°C - 65°C and mixed with cold water to usable temperatures of 35°C - 45°C at point of use.
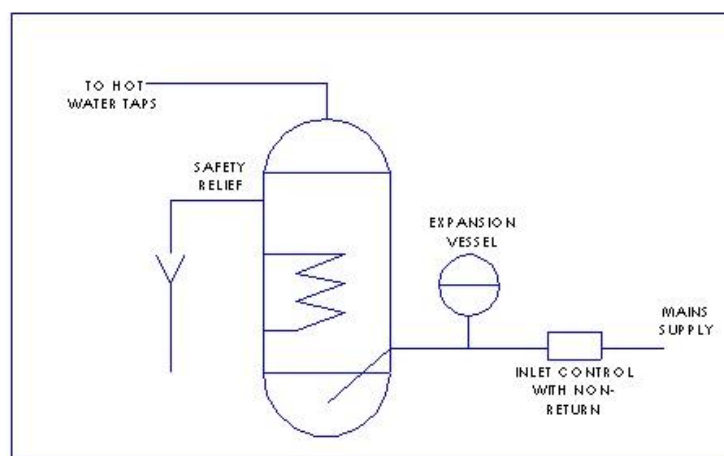
Figure 1.2 – Unvented Hot Water Cylinder

Benefits of Hot Water Cylinders

The main benefit of having a hot water cylinder to provide domestic hot water requirements is that it is better capable of managing higher demands more economically. To deliver higher flow rates of hot water from a hot water cylinder, the key requirement would be to increase the working pressure of the cylinder. This can be done by simply increasing the pre-charged pressure on the expansion vessel integrated in unvented hot water systems and increasing the expansion relief valve opening pressure or increasing the head on the feed and expansion tank of a vented hot water system. To satisfy higher hot water demands combination boilers would most likely require a larger heat exchanger which may not be possible in a domestic setting. In households with more than one bathroom hot water cylinders would be the preferred choice for stable hot water supply at peak demand.

Another benefit that domestic hot water cylinders offer is the option to integrate renewable energy sources for water heating with relative ease. Energy efficiency is a key topic of interest in modern domestic activities. Increasing pressure from legislation (HM Government, 2008) as well as added incentives for higher efficiency (HM Treasury, 2007) illustrate the current focus on energy efficiency and the intention for energy savings to be made where possible.

The Importance of Energy Efficiency and Renewable Energy

A factor closely related with energy efficiency is CO_2 emissions. The total estimated global CO_2 emissions from fossil-fuel combustion and industrial processes for the year 2014 was estimated at 35.7Gtons (Olivier et al., 2015). The total global CO_2 emissions from fossil-fuel combustion and industrial processes for the year 1990 the baseline year for the Kyoto protocol was 22.3Gtons (Global Carbon Project, 2016). That is a 60% increase in CO_2 emissions to date. Global CO_2 emissions are expected to keep increasing (Centre for Climate and Energy Solutions, 2015) even when taking the slowdown in 2012 to 2014 into account (Olivier et al., 2015). The global proven oil reserves have been estimated to be 1700 billion barrels (British Petroleum, 2015). The average worldwide demand for oil and other liquid fuels is in excess of 35 billion barrels an year as of 2016 (International Energy Agency, No Date). This would mean that the global oil reserves have a predicted lifetime of less than 49 years at current usage rates. This places further importance on both development of renewable technologies and more efficient usage of conventional energy sources.

The future of energy production and usage is focused on cleanliness and efficiency. This can be observed from the climate change act of 2008 in which the UK has placed a mandatory requirement that the "net UK carbon account for the year 2050 is at least 80% lower than the 1990 baseline" (HM Government, 2008). Recommendations from the IEA to include mandatory minimum energy performance standard (MEPS) labelling on residential appliances and equipment (International Energy Agency, 2011) would further support investigation into improving energy efficiency. In 2010 the European council also passed the directive that energy using equipment must be labelled with their energy efficiency rating. This creates an easily visible and comparable system for identifying energy usage of appliances (European Commission, 2010).

In the scenario where improvements in energy efficiency do not bring about increased usage, the said improvements can also support low carbon initiatives. In 2011 UK households contributed 14.38% to the national CO_2 emission of 458.6 Mtonnes (Department of Energy and Climate Change, 2012). The energy efficiencies obtained at the household level have the potential to favourably impact the reduction of future national CO_2 emission.

In 2012 over 18% of domestic energy usage was to produce hot water (MacLeay et al., 2010). This is greater than the combined energy needed for appliances (13.88%) and lighting (3.08%). Therefore, water heating for domestic use can be deemed a useful area to investigate for improvements in energy efficiency.

The support for integration of renewable energy in domestic hot water service is further illustrated with the passing of European union directive 2009/125/EC of the European Parliament and of the Council with regard to eco-design requirements for water heaters and hot water storage tanks (European Commission, 2009) and the supplement to Directive 2010/30/EU with regard to the energy labelling of water heaters, hot water storage tanks and packages of water heater and solar devices (European Commission, 2013). The above directives favour the usage of renewable energy and penalise the usage of non-renewable electric energy usage. The directive further supports energy efficiency by limiting the sale of lower efficiency water heaters and hot water storage as part of the timetable of implementation.

Usage of renewable energy in place of fossil fuels is an increasingly attractive and more economical option due to the finite nature of the supply of fossil fuels and their increasing cost with the passage of time (Macrotrends, 2017). As the proven oil reserves are estimated to last under 49 years, further exploration and deeper wells in harsh environments will be required to satisfy demand further than the proven reserves can provide. Economics dictates that this will further affect the price of fossil fuels. In the short term, it is not economically viable to stop using fossil fuels but developing alternative energy sources to be used as substitutions for or complement fossil fuels where possible is beneficial for both extending the period of availability of fossil fuels as well as avoiding the scenario of dependence on a single energy source and the challenges that may arise from the loss of said source.

Another good reason for investigating methods for improving integration of renewable energy with hot water cylinders is that the UK government is backing low carbon technologies both in the non-domestic and domestic settings through schemes such as the renewable heat incentive (RHI). RHI is a government financial incentive that offers participants payments based on the amount of "clean, green renewable heat" that is produced by their systems (OFGEM, 2017).

An added benefit of using hot water cylinders in conjunction with renewable energy sources is that the energy storage medium is non-toxic water. Water is a superior energy storage medium from an environmental point of view as it is a product of biodegradation and hence not harmful to the ecosystem.

Disadvantages of Using Hot Water Cylinders

While hot water cylinders have many benefits compared to alternative sources for domestic hot water supply, they also have some disadvantages. A main drawback for hot water cylinders is the heat loss which occurs during service. A well-insulated hot water cylinder can lose anywhere from 0.9kWh/24hours to 2.3kWh/24hours depending on the size of the cylinder (Kingspan Environmental, 2014). In comparison, a combination boiler does not store hot water and hence the heat loss is not as prominent. However, the detriment of the heat loss can be managed by correctly sizing the hot water cylinder to user needs and using a programmable thermostat to be more in line with usage patterns.

Growth of Legionella is another concern when using hot water cylinders and in most cases where water may become stagnant. However, this too can be managed by ensuring a disinfection cycle is run whenever the hot water cylinder may lay dormant for extended periods. A disinfection cycle is defined as a period when the hot water cylinder is heated to above the legionella bacteria survival temperature for a period.

Energy Sources for Hot Water Cylinders

In the UK market, most of the current hot water cylinders employ two different methods for providing thermal energy. They are;

1. Electrical immersion heaters
2. Immersed helical tubed coils transporting fluid heated at a secondary source.

In some instances the tubed coils can have concentric arrangements of more than one coil. (Kingspan Environmental, 2014)

In most cases the tubed coil heat exchangers are heated by a boiler. When integrated with renewable energy the typical methods of utilizing renewable energy for heating water in cylinders include solar thermal collectors, heat pumps and resistance heating through current generated from photovoltaic cells. Solar thermal collectors and heat pumps are similar in relation to their integration with hot water cylinders as the heat transfer occurs by way of a working fluid travelling through a heat exchanger within the cylinder. Solar thermal collectors are further subdivided into vacuum tube, flat plate and concentrating collectors. In a typical domestic setting the most widely used forms of solar thermal collectors are vacuum tube and flat plate types.

A key benefit of having immersed helical tube heat exchangers in hot water cylinders is that they have low pressure drops in the range of 0.01 to 0.05 bar. This allows for easier integration with solar thermal systems as the heat exchanger in the cylinder only minimally contributes to the overall resistance to flow in the system. This reduces the pumping requirements for the system. Immersed tube heat exchangers are also beneficial for delivering the working fluid from the collectors direct to the internal section of the hot water cylinder. Therefore, investigation into the efficiencies and characteristics of immersed tube heat exchangers for hot water cylinders may be beneficial for better integration of hot water cylinders with renewable energy systems such as solar thermal collectors and heat pumps.

Hot Water Cylinder Design Considerations

The helical tube coil heat exchanger design has been in operation from as far as the 1950s (Range Cylinders, 1950) with little change up to present day. Over the said period the boilers which provide heat to the hot water cylinders have undergone significant change with efficiencies in the range of 65% in 1985 to present efficiencies in the range of 80% (Home Heating Guide, No Date-a, Home Heating Guide, No Date-c). Current condensing boilers are also able to give power outputs in the range of 29kW to 40kW (Ideal Boilers, No Date). These improvements in boilers warrants investigation of the heat exchanger in a hot water cylinder to better exploit the improvement in technology.

Along with efficiency, the time taken to heat the contents of a hot water cylinder is of importance when selecting a domestic hot water system. Current hot water cylinder manufacturers claim cylinder heat up times in the range of 14 minutes to 40 minutes for a range of cylinder capacities from 70litres to 300litres (Kingspan Environmental, 2014, HeatRae Sadia, 2015).

In the broadest terms a good hot water cylinder is characterised by four main qualities. It must be efficient at producing and delivering hot water. In this case efficiency is determined by how well it can transfer the energy supplied to obtain usable hot water above 40°C. It must be reliable meaning the cylinder must be robust and reasonably resistant to failure such as corrosion. The cylinder must be able to deliver the hot water to point of use in the minimum amount of time and the cylinder must be as economical to build as possible.

To reduce the time to deliver hot water to point of use and increase cylinder efficiency, the conventional approach has been to increase the size of the heat exchanger and increase the insulation thus increasing the amount of materials used. This can lead to higher costs of manufacture and distribution which may result in greater expense for end users. Reducing material to reduce the cost of manufacture without proper investigation can negatively impact the performance of the hot water cylinder. The aim of this study is to investigate a method where optimisation of the heat exchanger can lead to reduced material usage with equal or better performance.

Better understanding of the heating mechanisms of the coiled heat exchanger may lead to improvements in efficiency which can further support manufacture of hot water cylinders

through the achievement of higher efficiency banding under the Energy-related Products (ErP) scheme associated with EU directive 2010/30/EU. Higher ErP banding could further support adoption of hot water cylinders by home owners and house builders as the preferred method for satisfying domestic hot water needs.

This body of work is focused around the interaction between the internal coiled tube heat exchanger and the hot water cylinder. It is hoped that the study will bring about an increased depth of knowledge of heating within domestic hot water cylinders and in turn aid the future design of hot water cylinders to be more energy efficient, economical to manufacture and better at delivering the required hot water to satisfy user needs.

The overall objective of this study is to investigate the impact of parameter changes on a single helix heat exchanger coil on the efficiency of the hot water cylinder.

Theory

The study of thermofluids has been a topic of great interest due to its essential role in engineering activity from past to present. Thermofluids incorporates some of the most essential industrial processes such as heat transfer, thermodynamics, fluid flow and combustion. The subsections of heat transfer and thermodynamics are of great importance to engineers working across various fields from nuclear reactors to domestic hot water cylinders and beyond.

Heat Transfer

Conduction

Heat transfer occurs through three main physical mechanisms conduction, convection and radiation. A method of explaining conduction would be to consider it as a transfer of energy from a particle of higher energy to a particle of relatively lower energy (Bergman et al., 2011). The energy transferred being the more energetic particle's internal energy. A key requirement of this method of heat transfer is contact between the particles exchanging energy. In the case of conduction, it is assumed that the particles are not in a state of flux.

The rate of conduction heat transfer can be measured using Fourier's law. For a one-dimensional application the general rate equation will be as stated below (Bergman et al., 2011).

$$Q_C = -kA\frac{dT}{dx} \tag{1}$$

For the conduction rate Q_C (W), k (W/m/K) is the thermal conductivity of the material and A is the area across which the heat transfer takes place. dT (K) is the temperature differential across a finite distance dx (m).

The above rate equation is given in one dimensional form. However, conduction heat transfer can act in three dimensions and vary with time which is considered a transient case rather than the steady case where the rate is constant with time. A general heat transfer rate equation for a three dimensional (x, y, z) transient condition is given as below (Bergman et al., 2011). As it can be observed, solving the general equation can be considerably more complex.

$$\frac{\partial}{\partial x}\left(k\frac{\partial T}{\partial x}\right) + \frac{\partial}{\partial y}\left(k\frac{\partial T}{\partial y}\right) + \frac{\partial}{\partial z}\left(k\frac{\partial T}{\partial z}\right) + \dot{q} = \rho C_p \frac{\partial T}{\partial t} \qquad (2)$$

$\dot{q}$ (W) denotes energy generation within the system. ρ (kg/m³) is the density of the conduction material and C_p (J/kg/K) is the specific heat at constant pressure of the conduction material. $\partial T/\partial t$ is the rate of change of temperature with time.

The heat transfer through the immersed coil and to the storage water can be approximated to a cylindrical tube of small sections. The heat loss from the cylinder walls to the atmosphere is another case that can be approximated to a cylindrical tube. It is important to know that the approximation would contain errors due to geometrical differences which should be addressed with experimental data. The rate equation would be modified for a cylindrical surface as given below.

$$Q_{cr} = \frac{2\pi L k (T_i - T_o)}{\ln\left(\frac{r_2}{r_1}\right)} \qquad (3)$$

Q_{cr} is the rate of radial thermal conduction. T_i and T_o are the temperatures of the inner and outer walls of the cylinder. The length of the cylinder is denoted by L and r_1 and r_2 are the inside and outside radii of the cylinder.

Theory on conduction heat transfer has been introduced as background for this study as it is a component off overall heat transfer. Conduction will not be analysed in isolation as this study will be focused on analysing the overall heat transfer due to all present mechanisms of heat transfer. It is hoped that focusing on overall heat transfer will provide a more meaningful comparison of the coil performance within the study.

Radiation

The heat transfer mechanism of radiation by definition is the energy emitted by matter that is at a non-zero temperature (Bergman et al., 2011). Heat transfer by radiation occurs through electromagnetic waves. A physical medium is not necessary for this process to occur. The heat transfer through radiation will not be investigated within this study. For assessment of the heat transfer due to radiation the equation below can be used (Bergman et al., 2011).

$$Q_{rad} = \sigma A \varepsilon (T_1^4 - T_{sur}^4) \qquad (4)$$

Q_{rad}(W) is the heat transfer due to radiation. T_1(K) is the absolute temperature of the radiative surface and T_{sur}(K) is the absolute temperature of the surrounding space. σ(W/m²/K⁴) is defined as the Stefan-Boltzmann constant and ε is the emissivity of the material. When ε is equal to one the radiator is considered to be a black body. The range for ε lies between one and zero. In the case of a hot water cylinder it is beneficial to make sure the outer surface has as low an ε as possible. The opposite is true for the heating coil in the cylinder.

As with conduction, theory on radiation has been introduced as background for this study as it is a component of overall heat transfer. Radiation will not be analysed in isolation as this study focuses on overall heat transfer with the hope of providing a more meaningful comparison of the coil performance within the study.

Convection

Convection can be defined as the energy transferred by random molecular motion as well as bulk motion of fluid (Bergman et al., 2011). The key identification of convection is that a mass transfer is occurring as part of the energy transfer. Convection is separated into two main sections of forced convection and natural or free convection.

By definition forced convection is the convective heat transfer which occurs when the flow is caused by external means (Bergman et al., 2011). Convection in the absence of an external influence of flow is defined as free convection or natural convection. During free convection the flow observed is caused by buoyancy forces arising from density differences due to temperature differences in the fluid (Bergman et al., 2011).

The rate of convective heat transfer can be obtained using Newton's law of cooling. The one-dimensional rate equation for the convective heat transfer Q_{conv}(W) is given below.

$$Q_{conv} = hA(T_s - T_\infty) \hspace{3cm} (5)$$

h (W/m^2/K) is the convective heat transfer coefficient and T_s(K) and T_∞(K) are the temperatures of the surface of heat transfer and free stream respectively.

The problem lies in determining h. In addition to h being dependent on surface geometry and the conditions of flow, it is also dependent on numerous fluid properties and material properties (Bergman et al., 2011). This problem becomes more complex as the conditions drift away from steady conditions into transient and unsteady conditions.

As a single analytical equation for calculating the value of the convective heat transfer coefficient does not exist, engineers must rely on experiments and published values to determine h for given circumstances.

Knowledge of the practical effects of boundary layers is useful to engineers. The velocity boundary layer δ which influences the convective heat transfer is defined as the thickness from the stationary surface to the point where the velocity is $0.99u_\infty$. u_∞(m/s) is the free stream velocity in a system (Bergman et al., 2011). The thermal boundary layer δ_t is defined as the thickness from the stationary surface to the point where a thermal gradient exists. The thermal boundary layer is considered to exist up to the point where the value of the ratio of

$(T_s - T)/(T_s - T_\infty)$ is equal to 0.99 where T (K) is a point temperature measurement of the fluid (Bergman et al., 2011). These boundary layers grow along the surface of contact between the fluid and the solid body. If the solid body is at a constant temperature, then the effect of the growing thermal boundary layer will be a decrease in the convective heat transfer coefficient.

When investigating convective heat transfer a very important dimensionless number used is the Nusselt number. The Nusselt number (Nu) in practice is the ratio of convection to pure conduction heat transfer. It also indicates the enhancement of heat transfer due to fluid motion (Bergman et al., 2011). Nusselt number can be calculated from the following equation.

$$Nu = \frac{hL}{k_f} \qquad (6)$$

L is the characteristic length of the geometry under investigation. For a pipe this would be the diameter. k_f (W/m/K) refers to the thermal conductivity of the fluid.

Another regularly used dimensionless number is the Prandtl number (Pr). The Prandtl number can be interpreted as the ratio of the momentum of the fluid to thermal diffusivity (Bergman et al., 2011). Prandtl number can be obtained from the relationship below

$$Pr = \frac{C_p \mu}{k_f} \qquad (7)$$

μ (kg/s/m) is the viscosity of the fluid. As Prandtl number decreases the effect of molecular diffusion due to heat plays a more significant role when compared with the molecular diffusion due to momentum.

Fluid dynamics is closely linked to convective heat transfer. When solving problems related to heat transfer, flow regimes are regularly quoted. The three flow regimes are laminar, transition and turbulent. The Reynolds number (Re_L) can be used to determine the flow regime of a fluid. The Reynolds number can be interpreted as the ratio of inertial to viscous forces. Characteristic length plays an important part in the calculation of Reynolds number as

with Nusselt number. The Reynolds number can be calculated as follows. u_∞ is the free stream velocity of the fluid and L(m) is the characteristic length (Bergman et al., 2011).

$$Re_L = \frac{\rho u_\infty L}{\mu} \tag{8}$$

The objective of calculating the above dimensionless constants is to finally calculate the convective heat transfer coefficient and in turn obtain the value for the rate of convective heat transfer. This is possible because the average Nusselt number has a functional dependence with the Prandtl number and Reynolds number (Bergman et al., 2011). If this functional dependence is obtained experimentally the Nusselt number can be determined and the convective heat transfer coefficient can be calculated.

In free convection, the Grashof number plays an important role in determining the convective heat transfer coefficient. The Grashof number (Gr_L) can be interpreted as the measure of the ratio of the buoyancy forces to viscous forces (Bergman et al., 2011). The Grashof number can be calculated as follows.

$$Gr_L = \frac{g\beta(T_s - T_\infty)L^3}{\nu^2} \tag{9}$$

In the above equation β(1/K) is denoted as the volumetric thermal expansion coefficient of the fluid and ν (m^2/s) is the kinematic viscosity. g (m/s^2) is the acceleration due to gravity. In case of free convection T_∞ (K) is the temperature of the quiescent fluid the body is immersed in. If forced convection effects are neglected a functional relationship exists for the Nusselt number with the Grashof number and Reynolds number (Bergman et al., 2011).

The Rayleigh number which is the product of the Grashof and Prandtl numbers is another useful dimensionless number in calculating the heat transfer coefficient. The importance of Rayleigh number is that it can indicate if the buoyancy driven flow has transitioned from laminar to turbulent. This critical Rayleigh number is dependent on the geometry and orientation of the heat transfer surface (Bergman et al., 2011).

Theory on convection has been introduced as background for this study as it contributes to overall heat transfer. The study focuses on overall heat transfer and coil power output. The individual contribution of convection and measurement of non-dimensional numbers associated with it will not be analysed. It is hoped that analysis of overall heat transfer will provide a more meaningful comparison of the coil performance within the study when compared with analyzing the individual mechanisms of heat transfer.

Heat Exchangers

In practice heat exchangers can have complex geometries due to an effort to maximise surface area with overall volume. In such cases, it is useful to have an overall measure of the effectiveness of the heat exchanger. The overall heat transfer coefficient U (W/m²/K) can be used for this purpose. U can be calculated for heat exchangers as given below (Bergman et al., 2011).

$$Q_{hx} = UA\Delta T_m \tag{10}$$

Q_{hx}(W) is the mean power output of the heat exchanger and ΔT_m (K) is the average temperature difference between the heat exchanger inlet and outlet. When a counter flow or parallel flow heat exchanger is analysed the above equation (10) can be solved using the log mean temperature difference of the heat exchanger inlets and outlets. ΔT_1(K) and ΔT_2(K) are the temperature differentials between the fluid streams for the inlet and outlet.

$$Q_{hx} = UA \left(\frac{\Delta T_1 - \Delta T_2}{ln\left(\frac{\Delta T_1}{\Delta T_2}\right)} \right) \tag{11}$$

Stratification

Thermal stratification is the mechanism where heated water within a storage vessel rises to the top section of the said vessel and gradually creates a layer of water at a higher temperature to the rest of the stored fluid. The interface between the hotter layer of water and the colder layer is called a thermocline. When measuring the temperature vertically downwards of a stratified cylinder, a sharp change in temperature is observed when crossing the thermocline (Walmsley et al., 2009). Figure 2.1 shows the typical effect of stratification and the formation of a thermocline within a cylinder. This type of tank is historically used, so that soon after commencing heating, there is a supply of hot water in the tank to be drawn off. The level of stratification will not be quantified within this study. However, some resultant movements of the thermocline will be discussed.
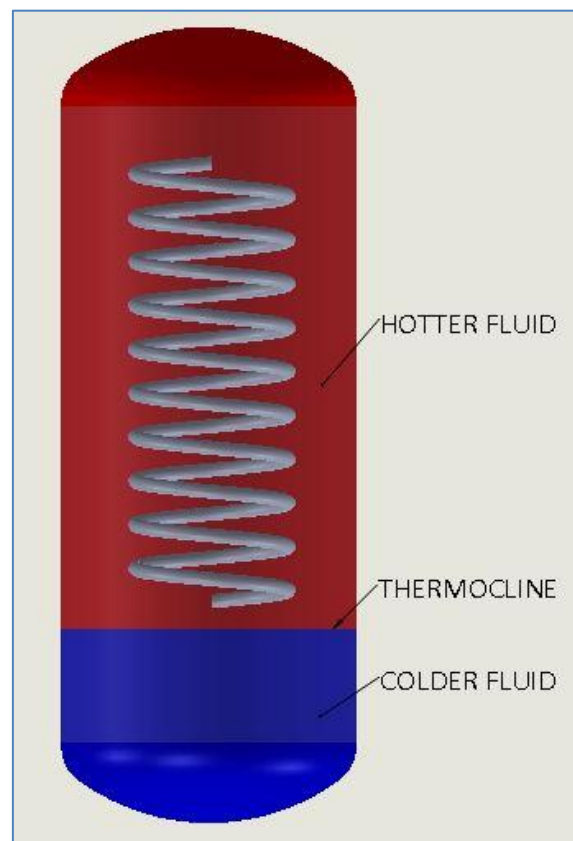
Figure 2.1 – Stratified Cylinder

Stack Effect

The stack effect is defined as buoyancy driven flow which occurs in hollow vertical columns such as buildings and chimneys. As seen in figure 2.2, the warmer fluid rises to the top of the column and colder fluid from outside is drawn into the column. For the stack effect to occur there must be openings in the columns at the bottom and top.

A horizontal plane exists in the column where the pressure difference between the inside of the column and the space outside is zero. This is termed the neutral plane.
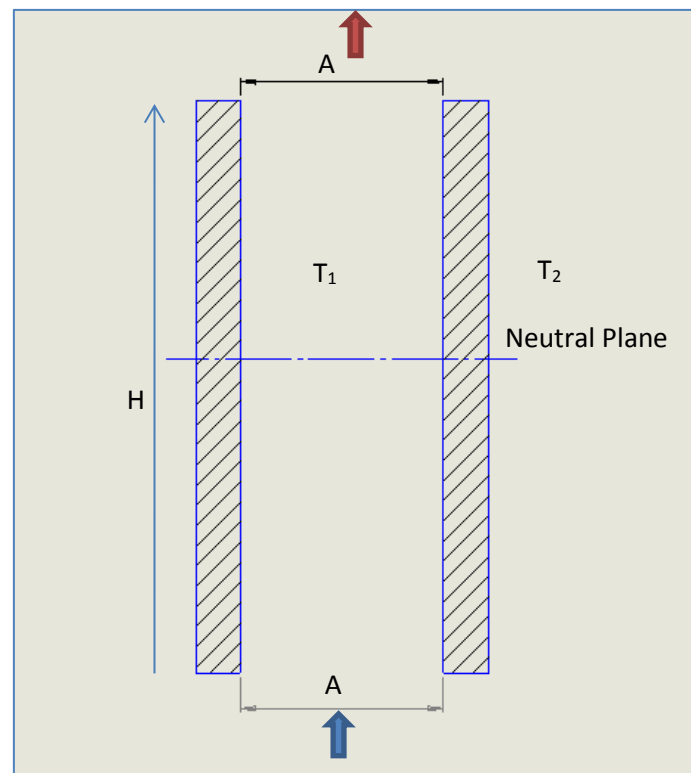
Figure 2.2 – Stack effect in a vertical hollow column

The flow induced by the stack effect Q_{flow}(m³/s)can be calculated as given below (Walker, 2016).

$$Q_{flow} = C_d A \sqrt{\frac{2gH(T_1 - T_2)}{T_1}} \tag{12}$$

C_d is the discharge coefficient and A(m²) is the cross-sectional area of the inlet and outlet. H(m) denotes the vertical distance between the mid-points of the inlet and outlet. T_1

is the temperature inside the hollow vertical column and T_2 is the temperature surrounding the column. In figure 2.2, $T_1 > T_2$.

For a hot water cylinder, the rate of heat transfer with a stratified flow will be lower than one in which convection can take place, and the boundary layer will be thinner, and hence U will be larger. The flow due to the stack effect has not been analysed in depth in this study due to practical considerations. However, the result of introducing a stronger flow across the coil using the principles of the stack effect is investigated.

Literature Review

In the modern home, hot water cylinders play an important role in satisfying domestic hot water needs. Even with the improvements in combi-boiler technology and heat interface units for district heating, hot water tanks remain ubiquitous.

Hot water tanks have been the focus of much investigation both in the past and present day. With a large body of work focused on the hot water cylinder's interaction with solar heating systems. The key importance of the hot water tank lies in the fact that in most domestic settings it would be the primary thermal energy storage option. In many cases the domestic hot water tank could be the only thermal energy store. Its importance is further cemented as the hot water tank is also one of the key components in a domestic heating system that a householder comes into direct contact with.

Mechanisms of Heat Transfer in Hot Water Cylinders

Domestic hot water tanks are host to a complex combination of heat transfer mechanisms. Previous studies have focused on trying to map and explain these heat transfer mechanisms. Heat transfer is categorised into three main physical mechanisms of conduction, convection and radiation.

Conduction

Conduction can be observed throughout a hot water cylinder. The energy transferred from a heat exchanger wall section to its thermal boundary layer would be an example of the role of conduction in heating systems. The heat transfer across the insulation foam is another important impact of conduction in hot water cylinders. Much focus has been given to reducing the thermal conductivity of the insulation for better energy efficiency through reduced heat loss. In most cases the preferred insulation of expanded polyurethane foam used for hot water cylinders will have a closed cell structure to reduce its thermal conductivity (BASF Chemicals, No Date, BASF Chemicals, 2014). A closed cell foam is designed to trap insulating gas bubbles within the foam structure in order reduce thermal conductivity (AB Building Products, 2017).The energy efficiency banding of storage hot water cylinders are also closely influenced by the result of better insulation due to the energy efficiency rating being determined by the heat loss of a cylinder (European Commission, 2013). Another important case of thermal conduction is the heat transfer that occurs along the cylinder walls. The

influence of conduction in this case can have a further impact on thermal stratification within the cylinder (Cole and Bellinger, 1982).

Radiation

Even though radiation heat transfer is present in a hot water tank at all times, little investigation into its proportions relative to conduction and convection has been published. When considering the heat loss of a cylinder it is important to factor the radiation heat transfer when considering the accuracy of calculations (Kingspan Environmental, 2016b).

Convection

Convection has been the most investigated mechanism of heat transfer associated with hot water cylinders. In hot water cylinders as well as many other engineering applications special interest is given to the convection process occurring between a bounding surface in contact with a fluid that it is at a different temperature to the surface. The water/glycol mix flowing through a tube heating coil in a hot water tank is an example of this. If the fluid is pumped, then the convection occurring between the inner wall of the coil and the flowing fluid would have a component of forced convection. If the heating system is a gravity system i.e. the fluid through the coil is not pumped then the heat transfer within the coil would be free convection (Hounsfield Boilers, 2016).

During the hot water draw-off process the heat transfer from the outlet pipe to the surrounding area would have a component of forced convection within the pipe and free convection outside the pipe. In a typical hot water tank heated by a tubed coil, the heat transfer between the surface of the tube exposed to the inside of the tank and the fluid contained within the tank will be a combination of free convection, conduction and radiation.

As mentioned above the heat transfer occurring in hot water cylinders has a complex interaction between the different physical mechanisms. However, in the broadest sense the heat transfer can be separated into the heat input by connection to an energy source such as a gas boiler, electrical resistance heater or solar thermal collector and heat output by heat loss from the store or through mass transfer during the usage of hot water at the taps. Previous work focused on efficiency has looked at improving fluid circulation around the heat exchangers or maintaining or improving the stratification within tanks particularly with hot water tanks connected to solar thermal collector systems.

Some investigation has also been carried out regarding the metallic shell of the hot water tank and its effect on stratification. The results have stated that if the ratio of the sum of the heat capacities of the stored fluid volume and the tank shell to the heat capacity of the stored fluid volume is less than 1.02, the rate of heat conduction along the tank wall is small and achieving stratification is easy. However, when the ratio is above 1.1 achieving stratification will be difficult. (Cole and Bellinger, 1982)

Review of Work Done on Heat Transfer

Armstrong et al. highlight that conflicts of interest are present between the thermal performance and sanitary requirements of domestic hot water tanks. Traditionally better stratification would be desired for higher thermal performance. A more uniform heating of the complete contents of the tank is preferred to avoid the growth of legionella (Armstrong et al., 2014). The optimum growth temperature for Legionella is 37°C to 42°C (World Health Organisation, 2007).

Between 48.4°C and 50°C growth is limited. The Decimal reduction time or the time required to kill 90% of microbes, for Legionella is 80 to 124 minutes at 50°C or 2 minutes at 60°C (World Health Organisation, 2007). Armstrong et al further discusses that the position of the heat source and thermostat are the key factors regarding the effectiveness of tank sterilisation during the heating cycle. Due to the rapid rate of sterilisation observed above 60°C, achieving a uniform tank temperature above sterilisation temperature even for a short time would prove effective in maintaining the hygiene of the hot water provided it does not cool down to the Legionella growth temperature.

Heat transfer within the coil

Knowledge of the nature of the flow within a tube coil heater would be of some value when investigating heat transfer in modern domestic hot water cylinders. In most hot water cylinders the heat exchanger is a helical coiled tube connected to a boiler or renewable energy source. Numerous studies have been done on the flow and heat transfer in helical tubes as reviewed by Berger and Talbot (Berger et al., 1983). Some of their findings include the fact that flow in finite elbows such as those found on the coil entry and exit legs are almost always developing flows and that the location of maximum axial velocity is shifted to the outer wall. Berger and Talbot also introduce that the local Nusselt number attains its maximum at the outer bend and its minimum at the inner bend. These results did not apply to horizontal

curved pipes. Nusselt number is the dimensionless temperature gradient at the surface of heat transfer and can be interpreted as the ratio of convection to pure conduction heat transfer (Bergman et al., 2011).

Additional work done on helical tubes also indicates that coil pitch, curvature and Reynolds number substantially influence the development of turbulent thermal fields. The uniformity of thermal field is also reduced as the flow becomes more turbulent downstream. As the flow proceeds downstream the average circumferential Nusselt numbers oscillate and this oscillation is further increased by increasing the coil pitch, curvature or the Reynolds number of the fluid (Lin and Ebadian, 1997). These findings can be useful to a coil tube heat exchanger designer in determining the desired type of flow for the heat exchanger. For an example if the designer wishes to have more mixing within the coil then a tighter radius and higher pitch would be suitable.

Work on horizontal tubes

An approach to understand the heating coil inside a domestic hot water cylinder would be to first approach a turn in the coil as a straight horizontal tube. This simplified view of the coil would not be very accurate but it has two benefits. Firstly, it reduces the number of variables required to consider when investigating the heat transfer characteristics. Secondly it opens a larger and in many cases more precise library of previous studies to aid understanding. For an example the work done by Atmane et al can be used to gain understanding of how a single horizontal tube would behave when heated within a fluid. The study indicates that at a Rayleigh number to the order of 6×10^6 when a vertical confinement is present above the heated horizontal tube at approximately the distance of the diameter from the tube surface, the natural convection heat transfer can undergo a transition from stable to unstable. At smaller separations of 1/5 the tube diameter and larger separations of 3 times the tube diameter this transition disappears (Atmane et al., 2003). Therefore, at an optimum distance of a vertical confinement the benefits of forced convection may come into play.

Further investigation of the effects of vertical confinement on a single submerged heated tube indicated the formation of a vortex which wrapped around an apparent meandering plume originating from the tube surface. The vortex tended to form halfway between the vertical confinement which in this case was the surface of the liquid and the surface of the tube. When the separation distance was under two times or over eight times the tube diameter, the influence of the vertical confinement was not repeatable.(Kuehner et al., 2012)
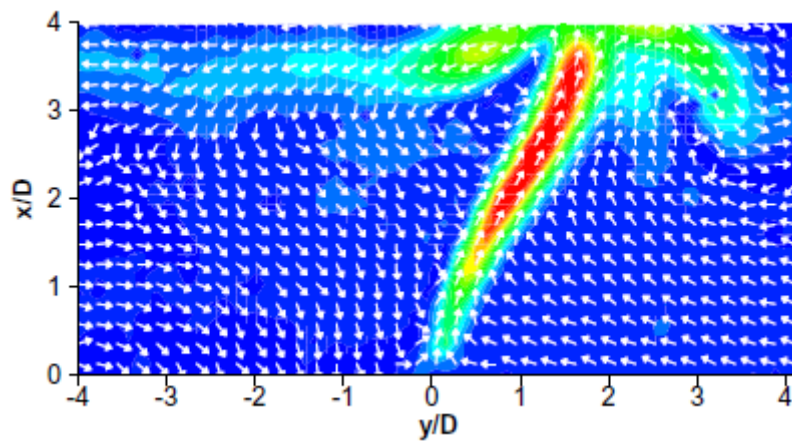
Figure 3.1 - Velocity contours for a vortex wrapped around a thermal plume as observed in the study (Kuehner et al., 2012)

Yaghoubi et al. investigated the influence of a nearly adiabatic ceiling on an array of three horizontal tubes 13mm in diameter as depicted in figure 3.2. The effect of the neighbouring cylinders and the near adiabatic ceiling resulted in the separation of the thermal plume from the centre tube and the formation of a recirculation region even for larger distances between the ceiling and the array. Shorter separation distances between the tubes also resulted in the combination of the thermal boundary layers of the three tubes. The local Nusselt numbers of the tubes in the array tend to vary similar to individual tubes as the tube spacing is increased.(Yaghoubi et al., 2009)
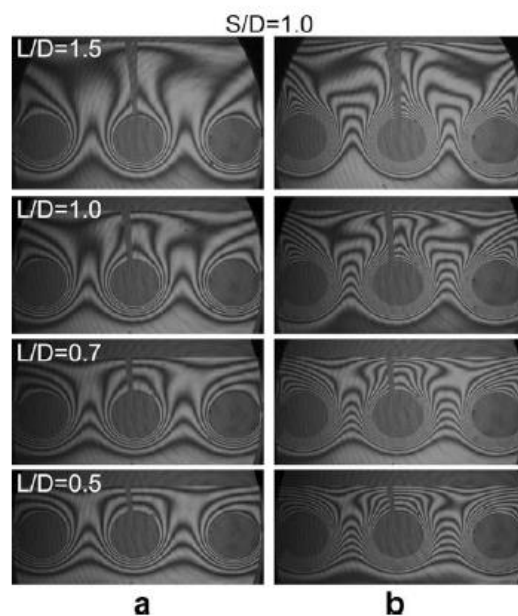
Figure 3.2 - Interferograms obtained from the study for (a) Ra=2500 and (b) Ra=6000 (Yaghoubi et al., 2009)

Persoons et al. have also investigated the influence of having a vertical array of tubes in the heat transfer and flow patterns around isothermal horizontal tubes. As with horizontal tube arrays, oscillating plumes could be observed. A strong periodicity was also present in the local heat transfer rate on the upper tube with an overall heat transfer enhancement of 10% compared to a single tube (Persoons et al., 2010). Further work by O' Gorman et al. suggest that the increase in heat transfer could be attributed to a stronger mixing and reduction of the thermal boundary layer thickness due to the impinging plume from the bottom tube (Gorman et al., 2010).

Work on immersed coils

Whilst it is beneficial to gain an understanding of the key factors influencing the heat transfer around tubes when designing heat exchangers for domestic hot water tank, it is also important to understand the interaction between the heat exchanger and the stored water within the tank.

Work has been carried out on various heat exchanger designs and configurations. Comparisons on the relative benefits of finned tubes with smooth tubes have been carried out by Mote et al. Their work has shown that from a performance perspective finned integron tube is superior to standard un-finned tube (Mote et al., 1989). However, where cost is a key driver the integron tube would be a less attractive option.

Investigations into the merits of heat exchanger orientation have also been carried out in previous studies. Tests have been carried out under operating conditions similar to thermal stores where the heat within a cylinder is extracted through an immersed heat exchanger rather than by extracting the stored volume itself. These tests indicate that the most beneficial orientation of a helical coil would be if its central axis was horizontal when immersed in a vertical tank. The reason for this being that a horizontal orientation would impact the stratification set up within the tank less negatively (Mote et al., 1991). A horizontal orientation would be less important if maintaining the stratification within the cylinder is not critical. Work done by Chauvet and Nevrala also indicate that when a finned heat exchanger is running in reverse to standard operation i.e. absorbing heat from the store as with thermal stores the heat transfer coefficient used should be higher at low Rayleigh numbers for steady state natural convection than when the coil is expelling heat (Chauvet et al., 1993a).

Further work by Chauvet and Nevrala investigated the impact of baffle plates in conjunction with horizontally oriented coils. Horizontal plates when sized and placed appropriately could improve stratification. Vertical plates placed around and below the immersed horizontal coil proved ineffective in creating recirculation. However an increase in overall heat transfer coefficient could be observed when a rectangular duct was placed around the coil under test (Chauvet et al., 1993b). Further work on horizontal coils with encapsulating baffles also suggests that close attention must be given to the attachment of the buoyant plume whether it is positive or negative. It also suggests that the width of the encapsulating baffle be kept small (Kulacki et al., 2007).

Investigation has also been carried out on vertically oriented heat exchanger coils with baffles close to or around the coil. Only a modest increase of 2.5% to 3% in heat discharge performance was observed for a vertical coil with an open ended cylindrical baffle placed symmetrically below it as seen in figure 3.3 (Mote et al., 1992).
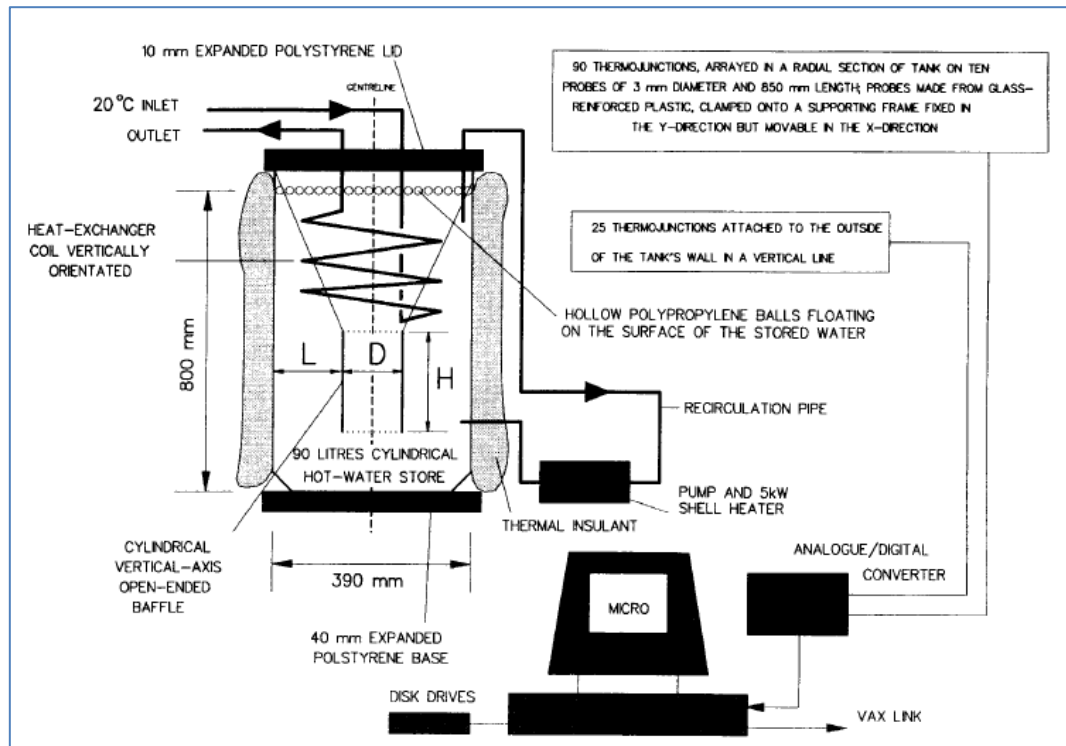
Figure 3.3 – Position of baffle below vertical coil (Mote et al., 1992)

Simulation work done by Devore et al. on a centrally located coiled heat exchanger running in charging mode show that when the hot inlet on the coil is at the top, stratification is promoted within the cylinder. When the coil is enclosed by a symmetrical baffle with a section of the coil protruding above the baffle the thermal stratification is lost. However when the bottom of the baffle is restricted the storage water regains a better level of stratification (Devore et al., 2013). Commercial designs are interested in the effect of baffles in hot water cylinders to promote recirculation. In electrically heated cylinders baffles are seen as a legionella preventative method and hence beneficial to the sanitary performance of the hot water tank during operation (Axcell, 1993).

Effects of heat loss

Heat loss in domestic hot water tanks are of significance in both scientific and commercial investigation. In scientific studies on the thermal performance of hot water cylinders and

particularly in studies related to solar hot water applications the heat loss is often approximated as uniform and in some cases neglected completely. In commercial applications heat loss has high importance associated with the marketing of hot water cylinders due to the implementation of energy labelling regulations (European Commission, 2015) and customer demand for energy efficient products. Heat loss measurements are an integral part of certification of hot water cylinders. In the United Kingdom hot water cylinder heat loss performance is tested in accordance with the British standards BS EN 12897:2016 for unvented hot water cylinders and BS 1566-1:2002+A1:2011 for copper open vented hot water cylinders (British Standards Institute, 2016, British Standards Institute, 2002). The test requires that a minimum of 85% of the cylinder be heated to 65°C and kept at that temperature for 48 hours. During the test period temperature probes are used to sense the increase in air temperature around the cylinder and the heat loss is calculated from the readings. As previously mentioned commercial cylinders typically have heat loss between 0.90 and 2.3kWh/24hours.

Heat loss from a hot water cylinder is quite complex to model due to the transient nature of local convection within the tank during cooling and the non-uniform heat loss that occurs as a result (Fernández-Seara et al., 2011).

Furthermore the impact of radiation heat loss is also important when considering the total loss from a hot water tank (Fernández-Seara et al., 2011). Just as heat loss in hot water cylinders is affected by the convection within the cylinder, the heat loss from the cylinder can in turn initiate convection within the cylinder as well (Fan and Furbo, 2012). Further investigation on domestic hot water cylinders also indicates that the impact of fittings, pipes and the bottom of the tank is quite significant on the measured heat loss. One study suggests that the heat loss from the exposed areas can be as high as 17% of the overall heat loss of the cylinder and among those areas pipework is the largest contributor (Simpson and Castles, 1992). A separate study observes that a large percentage of the heat loss was from the bottom of the cylinder (Cruickshank and Harrison, 2010).

In addition to understanding the critical factors affecting heat loss from a cylinder it would be useful to have some appreciation for the insulating materials used on cylinders as well. Modern domestic hot water cylinders are usually sold with a factory applied insulation layer

of expanded polyurethane foam. In many cases the foam is either sprayed onto the cylinder (Kingspan Environmental, 2017a) or injected between the hot water tank and an outer case (Kingspan Environmental, 2017b). A study on the relative benefits of commonly available hot water tank insulation material was carried out by Omer et al. and polyurethane foam placed third highest on thermal diffusivity among the non-composite insulation types. Fibreglass has the highest diffusivity and vacuum insulated panels (VIP) had the lowest at just over a third of the polyurethane value. In practice VIP is not considered an attractive material due to the loss of vacuum during handling and installation as well as its high production cost. Expanded polyurethane is considered the best compromise for hot water cylinders on cost, performance and robustness.

Current work on the blowing agents used in expanded polyurethane foams are focused on improving both thermal performance and reducing environmental impact. This can be seen with the derivation of polyol blowing agents from rapeseed oil which also give a low 0.02W/mK conductivity (IFS Chemicals, 2016).

Stratification

Stratification in hot water cylinders and particularly in solar domestic hot water cylinders is considered a very desirable state. Many studies have focused on the mechanisms to improve stratification in hot water storage cylinders. Other studies have investigated the factors influencing stratification and methods to minimise disturbing the existing stratification during draw off operations. Heat loss within the tank can set up convection currents where the cooler fluid travels downward along the walls and the warmer fluid travels upwards in the central region. The rising central plume is responsible for establishing the stratification (Fan and Furbo, 2012).

Under draw-off conditions where hot water is extracted from the upper part of the tank and cold water is replenished from the lower part of the tank, the effects of obstacles to flow such as horizontal baffles have also been investigated with regards to promoting stratification and they have proven beneficial (Altuntop et al., 2005). Numerical analyses suggest that a higher aspect ratio of cylinder would aid stratification. An exergy based non-dimensional parameter was used to determine the level of stratification. When the parameter was equal to 0 the tank was considered to be perfectly stratified and when it was equal to 1 the tank was considered to be perfectly mixed. Within the confines of the study an aspect ratio change of 2.5 to 3 would yield a 22.57% increase in stratification and that value would increase to 30.69% if the aspect ratio was increased to 5 (Ievers and Lin, 2009). However, a cylinder with a 5 to 1 height to diameter would not be practical both in terms of storage volume and ease of manufacture.

The implementation of thermal diodes across the entire internal cross section also showed a beneficial improvement in stratification during the cooling of a hot water cylinder. However the thermal diode showed reverse stratification during the heating as the heat exchanger is typically at the bottom of a tank (Rhee et al., 2010). Therefore, a thermal diode across the entire cross section of a hot water cylinder would be detrimental to operation.

In hot water cylinders heated by immersion elements it is advisable to have the immersion heater as low down as possible to ensure the lowest parts of the cylinder are being sterilised during operation. However placing the immersion heaters at the bottom can adversely affect the thermal stratification in the tank (Armstrong et al., 2014).

Mantle heat exchangers show a distinct advantage in maintaining thermal stratification over immersed heat exchangers in hot water tanks (Han et al., 2009). Under conditions of high solar fraction the mantle inlet should be placed towards the top of the mantle for better stratification at the cost of a small amount of thermal performance (Knudsen and Furbo, 2004). Solar fraction is defined as the portion of the total conventional heating load delivered by the solar thermal energy system (United States Department of Energy, No Date).

Storage Cylinder Contents Draw-off

The draw off operation is very important for domestic hot water tanks. The quality of the householder's experience is directly affected by the contents of the drawn-off water. The most beneficial circumstance would be if the householder can use the complete heated contents of the storage tank at the stored temperature. Therefore, maintaining stratification and reducing mixing during draw off would be ideal. For vertically directed inlet jets at low flow rates of draw-off the effects of horizontal baffles do not affect the mixing within the tank. However, at higher flow rates the presence of a single baffle has proven beneficial. Additional baffles have negligible further effect (Aviv et al., 2009).

Experimental results on a 150l cylinder show that complete cylinder thermal uniformity can occur during the draw off stage due to mixing caused by the inlet jet as well as the effects of convection (Amara et al., 2003). Having a distributed flow through the inlet pipe, a large inlet pipe diameter, having the inlet ports at the end of the cylinder and directing the inlet jet towards the bottom of the tank all proved beneficial in reducing the amount of mixing during draw off (Lavan and Thompson, 1977). The influence of the position of the inlet and outlet has been further studied by Fernández-Seara et al. They have observed that withdrawing the hot water from the top of the tank rather than from the bottom with a tube extending to the top is better for performance. For the inlet it is better to have a side entry tube in the shape of an elbow with the inlet jet impinging on the bottom of the cylinder compared to a side entry inlet with the water jet directed at the side walls or with a bottom entry inlet with the water jet directed upwards (Fernández-Seara et al., 2007a). In all cases the inlet should be located towards the bottom end of the tank to reduce disruption to stratification and ensure higher temperature hot water is drawn-off. The importance of maintaining a low inlet position is proved further by Jordan and Furbo (Jordan and Furbo, 2005).

Cylinder Pressurisation

Most of the unvented or pressurised hot water cylinders available in the market have one of two distinct thermal expansion methods. The first and most common is the usage of a gas filled membrane expansion vessel (Caleffi S.p.A., 2013) usually connected to the cylinder through the water inlet pipe (Kingspan Environmental, 2014). The other method is termed as integrated expansion where the thermal expansion is accommodated by a void in the cylinder (Kingspan Environmental, 2016b). Several patents exist for variations of the aforementioned integrated expansion (Hales, 1993, Powell and Hales, 2004, Pringle, 2008) but they all centre around trapping an air bubble at the top of the cylinder and separating the air water interface with a non-porous material in order to reduce the dissolving of oxygen contained in the air bubble with the stored water. The sizing of expansion vessels for heating systems is also introduced in the British standards (British Standards Institute, 1989) and manufacturer product data sheets (Caleffi S.p.A., 2013). The size of the expansion vessel is influenced by the system pressure, system operating temperature and the pre-charge of the expansion vessel.

Cylinder Heating Times

Much work has been carried out on the charging or heating up of hot water tank using a variety of methods from immersed heat exchangers to mantle heat exchangers and immersion heaters. These studies have mainly focused on maintaining cylinder stratification with little attention paid to the rate of tank heat up. Heat up time is a key factor in both commercial consideration of hot water cylinders (Kingspan Environmental, 2016b) and when testing hot water cylinder in accordance with the British standards (British Standards Institute, 2016). The two main standards in use for hot water cylinders are BS EN 12897:2016 for unvented hot water cylinders and BS 1566-1:2002+A1:2011 for copper indirect cylinders. An essential test for complying with the standards requires heating the hot water cylinder to 60°C from a starting temperature of 10°C or 15°C based on the standard used. The time taken for the heating operation is measured and used to determine the coil power output which must be stated on the cylinder data label (British Standards Institute, 2016, British Standards Institute, 2002).

Previous studies have suggested that heating time is directly related to the heating power and cylinder pressure has a slight impact on the heat up time (Fernández-Seara et al., 2007b) other studies have showed that under practical conditions stratification can be completely lost

during the heating up period (Amara et al., 2003). However focused study has not been carried out to minimise the heat up time in a practical setting. A workshop conducted by Ipsos MORI and the Energy Saving Trust highlighted a consideration against using hot water cylinders. A commonly raised requirement by the participants of the workshop was the availability of instant hot water on demand, as opposed to having to wait for a hot water tank to heat up. Furthermore, in a survey conducted by Ipsos Mori and the Energy Saving Trust, 80% of the respondents selected a gas boiler as their first choice for the heating system they would consider for the future. Just over 50% of the total respondents specifically opted for a combination boiler with some citing the disadvantage of having to wait for hot water cylinders to heat up (Ipsos MORI and Energy Saving Trust, 2013). The barrier to selecting a hot water cylinder for future domestic hot water needs could be overcome by reducing the heating up times currently associated with hot water cylinders.

Performance Measurement Per the British Standards

The British standards for vented and unvented hot water cylinders uses the equation below to determine coil power (British Standards Institute, 2016). The amount of water drawn off above 30°C of the cold-water temperature is also featured in the coil power (P) equation. This suggests that in practice the volume of usable hot water delivered is an important factor for the end user.

$$P = \frac{(\theta_p' - \theta_c) \cdot V_{hot}}{14.3t}$$

(13)

θ_p' is the average temperature of the water drawn off at $\geq (\theta_c + 30)$°C and θ_c is the temperature of the inlet cold water. V_{hot} is the volume in litres of water drawn off at $\geq (\theta_c + 30)$°C. t is the time in decimal minutes taken to heat the contents of the cylinder from θ_c to θ_{set} and θ_{set} is the target hot water temperature.

The energy Q (kJ) transferred to the water can be calculated using equation (14)

$$Q = m \cdot C_p \cdot \Delta T$$

(14)

m is the mass (kg) of the water and ΔT (°C) is the temperature differential during heating.

For the case of draw off water above 40°C equation (14) can be re-written as given below

$$Q = (\rho \cdot V_{hot}/1000) \cdot C_p \cdot (\theta_p' - \theta_c)$$

To present the final coil power in kW, the time value must be presented in seconds. Therefore equation (13) can be re-written as given below

$$P = \frac{(\rho \cdot V_{hot}/1000) \cdot C_p \cdot (\theta_p' - \theta_c)}{t \cdot 60}$$

Substituting the values of 999.8 (kg/m³) and 4.192 (kJ/kg/K) for ρ and C_p respectively for water at 10°C (Engineeringtoolbox.com, No Date), equation (13) can be derived. The above calculation method doesn't consider any draw off water volume below θ_c+30°C. It is not clear from the British standard at which temperature ρ and C_p values are taken. However, the values at 10°C appear to be the best fit to obtain the coefficient 14.3 as observed in equation (13)

Emphasis is also placed on determining how much mixed hot water above 40°C can be obtained from a hot water cylinder. The quantity of mixed hot water is calculated using the equation below. Mixed hot water volume will not be considered within this study as the draw off volume is deemed a sufficient factor of analysis.

$$V_{40} = V_{hot} \times \frac{(\theta_p - 10)}{30} \tag{15}$$

θ_p is calculated as

$$\theta_p = (\theta_{set} - 10) \times \frac{(\theta_p' - \theta_c)}{(\theta_{set} - \theta_c)} + 10 \tag{16}$$

Heat loss is another important aspect considered in the British standards. The standards require a cylinder to be placed in a still test area and heated to 65°C ± 3°C and maintained at that temperature for a minimum period of 48 hours. During the test period, the energy input to the hot water cylinder is measured. Temperature measurements of the air around the hot water cylinder are also taken over the entire test period with three temperature probes (British Standards Institute, 2016).

The temperature differential between the storage water θ_w and the average of the ambient air temperature measurements θ_{a1}, θ_{a2} and θ_{a3} is taken. The average value of the calculated temperature differentials is denoted as θ_d.

The equation below is then used to calculate the heat loss (Q_{st} in kWh/24hours) of a hot water cylinder (British Standards Institute, 2016). Q_c is the average energy consumed during a 24-hour period of the test. The effect of heat loss from the cylinder is not investigated within this study as the test duration is comparatively low compared to the testing duration per the standard.

$$Q_{st} = \frac{Q_c \times 45}{\theta_d} \qquad\qquad (17)$$

The impact of heat loss on comparing coil performance is also considered to be negligible as the cylinder is heated to the same target temperature for each test and is well insulated. The same cylinder is used to test the different coils compared. It is assumed the heat loss affects all tests in a very similar manner.

There are certain limitations in the British standards testing method when it comes to exploring possible efficiency improvements. The standards are in place to provide a set method for testing hot water cylinders and hence most of the parameters cannot be varied to investigate the effect of said parameters on the overall efficiency. The objective of the standards is also to benchmark products based on end user requirements. The draw-off volume and coil power rating are examples of this. Due to this overall efficiency measures like U values on heat exchangers are not considered within the scope of the standards.

Renewable Energy

Hot water cylinders are an important part of most domestic renewable energy systems. Water being a non-toxic fluid is ideal for storing thermal energy. As an added benefit the energy stored in water can be used as is without transfer into another medium. Most commercial hot water cylinders designed for renewable heat input tend to have two or more separate heat exchangers (Kingspan Environmental, 2014). In most cases the bottom most heat exchanger will be used for the renewable input. Apart from photo voltaic panels all other compatible renewable heat inputs would use a working fluid which is typically a water/glycol

mixture in the heat exchanger on the collector side of the system and then pump the fluid through the cylinder heat exchanger. Flat plate thermal collectors and vacuum tube array collectors tend to run through a pumping station which also acts as a controller for the system (Kingspan Environmental, 2015). Air source heat pumps (ASHP) and ground source heat pumps (GSHP) would have the controllers built into the unit but the principle of energy transfer is the same.

At times when the supply of solar energy exceeds the demand such as in summer, solar thermal systems must bypass the energy collected to a secondary store of sufficient size such as a swimming pool or in the last instance to a thermal dump (Kingspan Environmental, No Date). Heat pumps can remove the electrical energy input and stop the energy capture cycle in similar situations. Solar thermal and heat pump energy can also be routed to thermal stores as another storage solution. This can allow for several energy sources to directly transfer heat into a large volume of water typically more than 300 litres. Individual services such as radiators or underfloor heating tubes in a house can then extract heat from the thermal store through a heat exchanger. Most of the literature presented previously has investigated the heat transfer and stratification characteristics of hot water storage tanks under thermal store operations.

Biomass boilers can be fitted to hot water cylinders to generate domestic hot water as well (Land Energy, No Date). A biomass boiler generates heat by burning renewable materials such as wood pellets (Bioenergy Technology Ltd, No Date). These types of boilers are sometimes called solid fuel boilers. The biomass boiler can either heat the storage water by running it through a heat exchanger in the combustion chamber or by running a working fluid through the heat exchanger in the combustion chamber and the circulating the fluid through a immersed heat exchanger in the storage tank or a heating mantle around the storage tank (ResDevon, 2015).

Photovoltaic panels are used to a lesser degree for providing domestic hot water. However it can be used to power electrical immersion heaters (HeatRae Sadia, No Date) to heat the stored water. Even though the immersion heater is 100% efficient the overall energy conversion process is not very efficient (Centre for Alternative Technology, No Date).

Sizing of a domestic renewable energy system is an important aspect in its efficiency. If a solar thermal collector system is oversized, during peak supply the additional energy captured would need to be stored or dumped to protect the system. Sizing of a renewable energy system for peak efficiency depends on a series of factors. The most important factor to ascertain is the total hot water requirement. The size and weight of the system are other practical considerations. A single flat plate collector can be 44kg and over $2.4m^2$ in surface area (Kingspan Environmental, 2016a). A biomass boiler can be considerably bigger than a conventional boiler and may also require storage for the fuel (The Green Age, No Date).

The heat exchanger in a domestic hot water cylinder must be correctly sized for the renewable energy system as well. When domestic hot water storage tanks are used in conjunction with solar thermal systems a minimum of $0.1m^2$ of heat exchanger area is recommended for every $1m^2$ of collector area (HM Government, 2013). Auxiliary heat sources are almost always present on solar thermal and heat pump systems to provide energy when the renewable source is weak or unavailable. In most cases the auxiliary source will be an electric immersion heater or gas or oil boiler (Kingspan Environmental, 2014). In the case of solar thermal collectors, guidance is set in place to ensure that the renewable resource is given a sufficient volume of dedicated storage to ensure it preferentially heats the storage volume. A minimum of 25 litres for every $1m^2$ of collector area is recommended (HM Government, 2013).

At $1000W/m^2$ of solar irradiance Flat plate solar thermal collectors can have an efficiency of approximately 72% (Arcon Sunmark, 2017) compared to vacuum tube solar collectors which can be around 70% efficient (Kingspan Environmental, No Date). However, these values are highly variable with the ambient temperature. The overall system efficiency will be influenced by the pump and storage method used as well. In comparison photovoltaic panels have an approximate efficiency 17% (Viessmann, 2016). However, the mechanism for energy conversion is different to solar thermal collectors.

Improvements in Gas Boilers and the Limitations of Stratification

Domestic gas boilers have undergone significant improvements within the last 30 years. These improvements can be seen in both efficiency and available power output. From the back boilers which were a common sight to today's condensing gas boilers the technology used has moved forward considerably. In the mid-1970s to early 1980s boilers such as the Baxi

Bermuda 551 had efficiencies as in the range of 65% and power outputs of 10kW to 16kW (Home Heating Guide, No Date-a). Top of the range boilers in the same era had approximately 23kW in output power (Home Heating Guide, No Date-c). Comparatively recent non-condensing boilers manufactured in the early part of the last decade have efficiencies in the range of 79% with power outputs to hot water in the range of 31kW (Home Heating Guide, No Date-b). The newest boilers which tend to be the condensing type, have a wide range of power outputs from 18kW up to 40kW (Baxi, 2016).

Most of the previous work on domestic hot water cylinders has been focused on the interaction of the tanks with solar thermal collectors. It has been shown that stratification is beneficial in improving the efficiency of such systems. In domestic solar thermal systems the heat exchanger is usually placed at the bottom of the cylinder. When the water in the cylinder stratifies, it allows for the hottest water to collect at the top of the cylinder and is extracted from here for the householder's requirements. It also allows for the relatively cooler water to remain at the bottom of the cylinder in contact with the heat exchanger. This enables more efficient heat transfer into the cylinder even when the collector temperatures are relatively low. However, this approach is mainly focused on the temperature difference between collector temperatures and store temperatures. The higher temperature differences are beneficial for conduction and the resulting natural convection. It doesn't consider the benefits in heat transfer that may arise from introducing stronger flow across the outer surface of the heat exchangers and achieving an induced forced convection and potentially increasing the heat flux across the heat exchanger. Furthermore as high energy inputs would impact the established stratification within a hot water storage tank (Baek et al., 2011) and therefore modern day boilers could disrupt the storage stratification during operation.

The investigation proposed by the author focuses on promoting an induced forced convection across the coiled tube heat exchanger in a domestic hot water cylinder. It is hoped that non-concentrically placed helical coil heat exchanger will set up a convective current within the hot water cylinder. Thus, benefitting the coil from a higher heat flux and depositing the hottest water at the top of the cylinder adjacent to the outlet port for end use.

Previous studies that have focused on coils have used central coils or horizontal coils. Commercial products have focused on central coils. The concept of a non-concentric or offset

coil has not been presented in scientific or commercial sources the author reviewed and hence is a novel approach to hot water cylinder design.

Methodology

Test Apparatus

The test apparatus used for the study is broadly separated into two sections. The test cylinder and the test rig.

A test cylinder was required for the study primarily as the housing for the heat exchanger coils that were to be tested. This was to give realistic result which would follow as closely as possible to the current commercial offerings. It would also help if the results of the study were to be commercialised. The second reason for building a test cylinder was to be able to swap the different coil designs or investigate different positions of a given design and test them in the same cylinder hence reducing any variability. The test cylinder was also required if any flow visualisation work would need to be carried out.

The design considerations for the test cylinder

1. Deviation from a commercial cylinder would have to be minimised
2. The cylinder would require a facility to easily switch heat exchanger coils
3. The cylinder would require the facility to house more than one heat exchanger coil
4. The cylinder would require the facility to modify the vertical positioning of a given heat exchanger coil
5. There should be provision to view the inside of the test cylinder when it is operating
6. There should be two perpendicular viewing angles for viewing the inside of the cylinder if future particle image velocimetry (PIV) study was to be carried out
7. The fittings on the cylinder would need to be a standard and easily available type for both plumbing and measurement equipment
8. The cylinder should be able to withstand normal operating pressures of unvented hot water cylinders without leaking or rupturing
9. The cylinder should be capable of resisting corrosion to a reasonable degree
10. The cylinder should be well insulated
11. The cylinder should be stable. Especially when filled with water.

Detailed design parameters

Capacity

The first detail decided upon was the capacity of the cylinder. It was decided that the test cylinder would be modelled after a 180 litre Kingspan Tribune HE cylinder. The capacity of 180

litres was selected as it was a middle capacity cylinder in the Tribune HE range. The standard range starts at 90 litres and the largest cylinder is 300 litres. Another reason for selecting the 180-litre variant was because it was one of the sizes in high demand by end users.

Material

The material selected was 316L stainless steel. Copper was an alternative material choice. However stainless steel was selected over copper to minimise the heat transfer both along the vessel walls and as loss into the atmosphere. Another key reason was that stainless steel could withstand higher pressures for comparative vessel wall thicknesses. As the intention was to incorporate viewing windows on the cylinder, stainless steel would be more suitable for adding large flanges while remaining sturdy.

Vessel diameter

The vessel diameter selected was 453mm. This was to mirror the range tribune HE 180 litre cylinder. The standard nominal diameters of domestic hot water cylinders in the United Kingdom are 375mm, 400mm and 450mm with a largest proportion of stainless steel cylinders being 450mm (Kingspan Environmental, 2017b, Kingspan Environmental, 2017a)

End caps or spinnings

Convex Torispherical domed ends were used to cap the cylindrical body. The domed ends are colloquially called spinnings as they were spun into domes from flat sheets. The spinning diameter was 453mm to allow for a butt weld with the body diameter. The Torispherical shape was selected to improve robustness under pressure and increase ease of welding whilst having thin wall thicknesses.
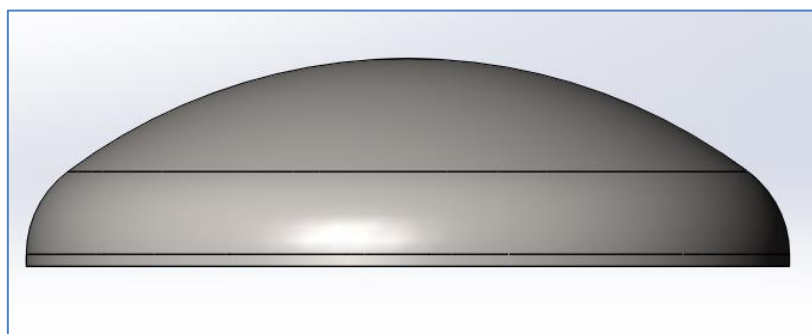

Figure 4.1.1 – Stainless steel spinning

Cylinder connections

The bosses used for pipe connections had a 22mm bore to accept 22mm tube. 22mm tube is a plumbing standard in the United Kingdom. The connection bosses use a compression fitting method with a 22mm nut and olive. The material used for the pipe connection bosses were 316L stainless steel to be welded to the cylinder body. The thread form on the connection bosses is a proprietary Kingspan 22mm, 14 threads per inch Whitworth form. This thread form was used due to its good locking capabilities and compatibility with other products in the Kingspan Range. Every tube connection on the body of the cylinder had an extended stub into the cylinder. This stub was a 316L stainless steel tube with an internal diameter of 22mm. the stub extended 50mm into the cylinder body. The length of 50mm was selected to allow for connecting components such as feed tubes either with a straight brass connector or plastic push fit connector.

A connection for fitting an electrical immersion heater was included. The connection boss has a 1 ¾" BSP female thread for accepting an immersion heater of 1 ¾" connection diameter. The fitting size 1 ¾" is an industry standard for stainless steel hot water cylinders. A 2 ¼" standard also exists for immersion heaters. However, they are mostly for copper hot water cylinders. If an immersion heater used in copper cylinders was to be used in a stainless-steel cylinder, the immersion heater would leak over time due to galvanic corrosion.

Temperature and pressure relief valve and thermocouple connections

A ½" bore diameter female NPT threaded connection was used for fitting the temperature and pressure relief valve (PTRV) and K type thermocouples along the body of the cylinder. The NPT thread was selected as the pressure tight joint was made on the thread and hence added an extra layer of security and because the PTRV and thermocouples wouldn't need to be replaced regularly. ½" NPT was also the standard for the PTRVs used by Kingspan cylinders. ½" NPT thermocouple adaptors could also be readily sourced.

The thermocouple probes connected were named as shown in figure 4.1.2
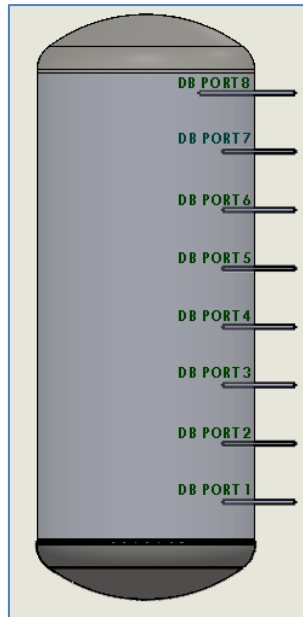
Figure 4.1.2 – Naming of side wall temperature probes

The vertical separation distance between the thermocouples ports was 122mm and the vertical separation between the coil connection ports was 96mm. The two values were offset to reduce the risk of coil turns touching temperature probes. The measuring tips of the probes DB port 1 to 7 had entry depth of 66mm from the cylinder wall and DB port 8 had an entry depth of 116mm.

Water inlet pipe and diffuser

Two types of water inlet pipe were used during testing. The pipe diameter used was 22mm. The main design consideration of the inlet pipe was to ensure that the water was injected at the very bottom of the cylinder and as close to the centre of the body when viewed from above. A polypropylene diffuser was fitted to the inlet pipe to promote an even flow during draw off tests. The diffuser used was identical to that which is used in the products marketed by Kingspan Environmental.
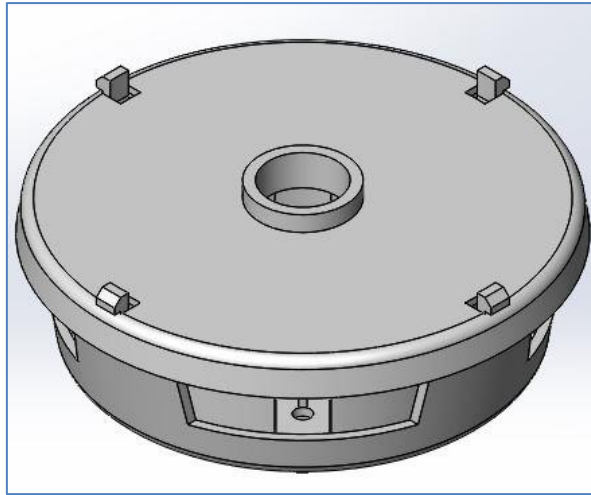
Figure 4.1.3 – Diffuser used on inlet pipe

Positioning of coil connection and cold water inlet pipe bosses

As indicated in figure 4.1.4 the coil bosses were placed within and angle of 75° from the central axis of the test cylinder. The angle was to allow for the connection of standard coil used in the Kingspan Tribune range of cylinder which was the benchmark for this study. This layout of connection bosses was repeated 8 times along the body of the test cylinder to facilitate the coil to be positioned at different heights. The cold-water inlet boss was also placed as it would appear on the commercial product. For testing, the ports at each horizontal level were number as 1 to 8 from bottom to top. This selection of coil boss positions allows for the connection of the standard commercial "coil in coil" design as well as single helix coils or intertwined helix coils. The single helix coil can be fitted to any one of the three vertical rows of coil boss connections. The connections not used were capped during testing to prevent leakage.
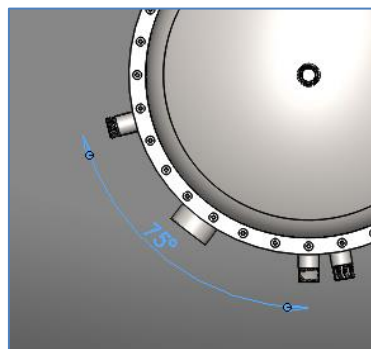
Figure 4.1.4 – Coil boss angle

Main viewport

As mentioned previously the test cylinder required a method for viewing the internal space during operation. This was achieved by including a slot shaped viewport 876mm tall and 384mm wide. The design considerations for the viewport were

1. Enable maximum viewing angle and height
2. Minimise protrusion of viewport
3. Minimise addition of thermal mass through the addition of a viewport flange
4. Minimise addition of internal volume
5. Provide a method for sealing viewport

The viewport was designed to have a maximum protrusion of 60mm in the radial direction from the cylinder body. This was the minimum radial protrusion that could be achieved practically as the flange was to be welded on to the test cylinder body. Keeping the protrusion to a minimum also minimised the additional thermal mass and increase of internal volume. The flange thickness selected was 20mm this was to ensure that the flange did not warp during welding as a flat surface was required to seal the flange. The flange had the facility to be secured with 38, M16 bolts. In the first instance a cover plate, sealing ring and sealing gasket were manufactured for the viewport. This was replaced later by an insert described later in this chapter. The material used for the viewport flange was mild steel to make fabrication easier. Stainless steel was not a viable option due to the thickness of the material and the machining capability available.
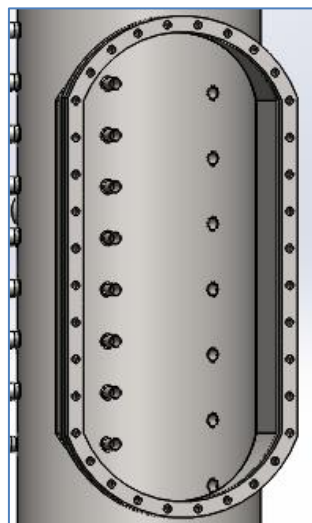
Figure 4.1.5 – Main viewport

Secondary viewport

The top spinning on the cylinder was fitted to the body using a flanged connection similar to the main viewport. This enables two perpendicular viewing angles of the internal space of the test cylinder. The secondary viewport flange is also constructed from mild steel plate 5mm thick. The flange can be secured with 32, M5 bolts. All viewports double as access hatches.
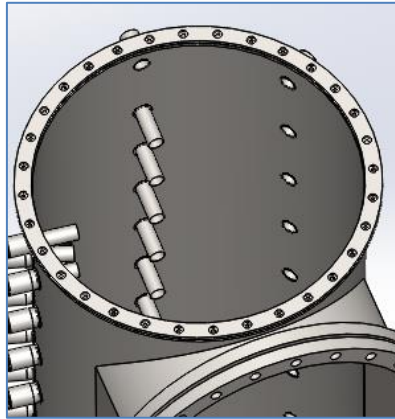
Figure 4.1.6 – Secondary viewport

Cylinder stand

The cylinder is comprised of two convex domed ends. A stand is required for the cylinder to be placed vertically. A ring of stainless steel sheet 372mm in diameter and 65mm in height was welded concentrically to the bottom spinning to give the test cylinder a stable horizontal base. This stand is referred to as a skirt in cylinder manufacture.

Fabrication process

A 3D model for the test cylinder was developed in Solidworks and corresponding engineering drawings were generated from the model. The CAD model was a valuable first step as it allowed for discussion on feasibility and practicality of manufacture across departments at the host organisation, Kingspan Environmental limited.

The test cylinder body was constructed of 3mm thick, 316L stainless steel sheet. All welding processes carried out were Tungsten Inert Gas (TIG). The sheet was cut to 1424mm X 976mm. Once cut, holes corresponding to the locations of the connections were punched on the sheet. The sheet was then passed through a roller to give the cylinder a diameter of 453mm. The two straight edges of the curved body were butt welded together. The holes in the cylindrical body were flared out to give them a flat upstand for accepting the flat connection edge of a boss. 50mm lengths of stainless steel tube were welded to the 22mm connection bosses to be welded to the cylindrical body. The bosses with connection stubs were fitted onto the flared holes and welded in place. The skirt was tack welded to the bottom spinning and a 22mm compression connection boss without a connection stub was connected to the top spinning. A 5mm thick circular flange was welded to the top circular edge of the cylindrical body and another to the circular edge of the top spinning. The bottom spinning was welded onto the bottom end of the cylindrical body. The main viewport was cut on the cylindrical body and the viewport flange was welded on. A flat flange cover was fabricated for the main viewport from mild steel. Sealing gaskets for the flanges were fabricated from 3mm thick textured rubber sheet. The main viewport was sealed with the flange cover, sealing gasket and M16 bolts. The secondary flange was sealed with a gasket and M5 bolts.

Figure 4.1.7 – Fully welded test cylinder prior to foaming

To test the integrity of the welded joints the cylinder was pressure tested. If any leaks were discovered during this process the test cylinder would be sent back to welding for patching. The cylinder was filled from its lowest connection boss with the remaining connection bosses on the body being capped with pressure tight fittings. Once the cylinder was full and the water was overflowing from the top most outlet, the outlet was capped and the cylinder internal pressure was increased by pumping more water into it. The pressure was monitored by a gauge on the filling controls. The test pressure was 10 bar and the cylinder had to be held at that pressure for 15 minutes. 10 bar is approximately 2 times the cylinder operating pressure. Once the cylinder passed pressure testing, the welds on the stainless steel were chemically de-scaled using a Hydrofluoric and Nitric acid mixture and left to passivate in air. Passivation is the process of exposing chemically de-scaled stainless steel to oxygen to re-form the passive oxide layer which protects the steel from corrosion. When this process is done in standing air it is called auto-passivation. The welds on the mild steel were mechanically descaled and coated with a corrosion resistant paint. The mild steel could not be chemically de-scaled as it would corrode. The completed cylinder was insulated with expanded polyurethane foam sprayed on to its bare surface. The average foam thickness on completion was 50mm which was the standard foam thickness for domestic hot water cylinders.

Curve insert manufacture

The addition of a large viewport on the test cylinder created the challenge of significantly deviating the design of the test cylinder from a commercial cylinder of comparable capacity, diameter and height. The viewport would be essential for possible future flow visualisation work. However, the test cylinder needed to be modified for all other testing. The modification would be required to bring the test cylinder's storage volumes closer to its commercial counterpart the Tribune HE 180 litre cylinder. The viewport changed the internal geometry of the test cylinder by adding an extruded space to its internal cylindrical shape. In addition to volume and geometry changes the viewport also created a large face for heat loss. Additional lagging of the viewport cover in its current form would also affect the stability of the entire cylinder.

The solution employed to bring the test cylinder in line with commercial cylinders was to have an insert placed in the viewport space. This insert would need to be removable if flow visualisation work was to be carried out. The design considerations for the insert were as follows

1. The insert must create a watertight seal
2. The insert must be able to be insulated
3. The insert must be able to displace the additional volume of water that the viewport would have filled up with
4. The insert must restore a cylindrical face to the inside of the test cylinder
5. The thermal mass of the insert must be kept to a minimum

The curvature insert was manufactured with 1mm duplex stainless steel. Duplex stainless was utilised for its rigidity even with low gauges of metal sheet. The sheet thickness was selected as 1mm to keep the thermal mass as low as practically possible. The top, bottom and side walls of the insert had the same shape and curvature of their corresponding surfaces on the viewport flange. The insert wall dimensions were marginally smaller to ensure that the insert would be able to be fitted into the viewport without interference while still displacing as much volume as possible. The back wall of the insert has a curvature of radius of 226mm almost identical to the rest of the cylinder inner wall. The front face of the insert was flat with holes corresponding to the bolt holes on the flange.

The curvature was manufactured as a combination of four parts. The fastening hole positions and a central hole for the front face was programmed into a computer numerical control punch machine. A sheet of stainless steel was punch using the programme. Prior to punching the sheet, based on calculated dimensions the front plate outer edge was marked on the sheet. The outline on the sheet was cut using an angle grinder. The central hole on the front sheet was flared out for welding a connection boss at the end of the curve insert fabrication process.

Figure 4.1.8 – Front face sheet of curvature insert

The shapes of the top and bottom curve were marked on another stainless-steel sheet and cut out using an angle grinder. The outlines had an extra strip on the edge which was folded back and acted like a welding tab. The welding tab had thin slots cut in it to allow for the weld tabs to be folded before the piece was rolled into a curve.

Figure 4.1.9 – Top and bottom curve base piece

A flat outline of the back curved face connected to the side walls with weld tab extensions was outlined on a sheet of stainless steel and cut with a guillotine and angle grinder. The sheet

was fed into a rolling machine and rolled to give it the required curvature. Folds were placed on the lines of the weld tabs and the edge of the side walls where it met the back curved face.

Figure 4.1.10 - Side wall and back face piece

The four fabricated parts were assembled together and tacked in place. The front face of the insert would need to remain as flat as possible during welding to minimise warping due to heat. For this reason, the front sheet was tacked onto a rigid flat welding table. Once tacked up the part was fully welded and a coil connection boss was welded to the flare on the front face.
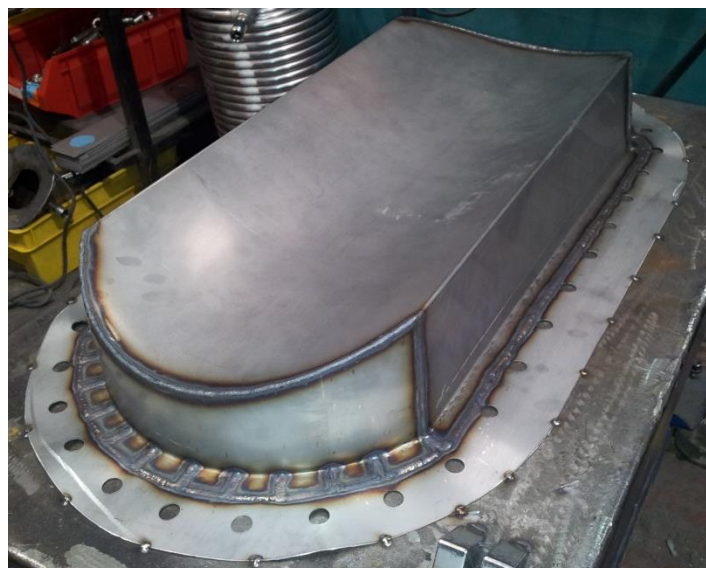
Figure 4.1.11 – Assembled curvature insert

The insert was fastened by placing the gasket on the viewport flange rim then slotting the insert in and placing the flange ring on the outer face. Once all the holes were aligned an M16 bolt could be fed through and fastened with a nut at the back of the flange rim. All the bolts required and equal level of fastening and hence the torque setting for tightening the bolts was 14 Nm. The bolts also need to be fastened in an alternating pattern with 4 corner bolts being fitted lightly to hold the entire fixture and then diametrically opposite bolts being fastened with the pattern following a clockwise or anticlockwise progression. The gasket was permanently fixed to the flange rim with their holes aligned to minimise the movement of the gasket and make assembly and disassembly more convenient.

The insert was pressure tested with water to discover if any leaks were present prior to fitting it on the test cylinder. A boss connection hole was punched in the front face of the insert and a 22mm compression boss was fitted. The water inlet hose was lightly fitted to the connection boss to allow air to escape and the insert was slowly filled. Once the insert was full the connection hose was tightened and the pressure was increased to 1 bar. Excessive pressure must be avoided when pressure testing the insert as it may bow due to the pressure being on the convex face rather than the concave face. Once the insert passed the pressure test it was drained and the welds were chemically de-scaled and the insert was auto-passivated. After de-scaling the connection boss on the front face of the insert was removed along with a plate of approximately 100mm x 100mm around it. The internal space of the insert was filled with expanded polyurethane foam of the same composition as the external insulation of the cylinder. By adding this insert the storage volume of the cylinder was reduced from 205litres to 180litres.

Figure 4.1.12 – Completed cylinder on test

Coil manufacture process

The coils tested were manufactured using 22mm outer diameter tube made of copper. The total length of tube also called 'undeveloped' length was determined based on the number of coil turns, diameter of the coil helix and the required leg lengths at the start and end of the helix. 150mm per coil leg was set as the standard for this study and the coil legs were trimmed down to the exact required length at the end of the forming process. The coil helical section length L_{coil}(m) was determined using the equation below. D is the diameter of a coil turn to the central axis of the tube and n is the number of coil turns.

$$L_{coil} = \pi D n \qquad (18)$$

Once the undeveloped length of the coil is determined, straight sections of tube were cut to the required undeveloped length. A solid cylindrical 'pusher' bar was fitted to the back end of the straight tube and the tube was rested on to the guide track of the forming machine. A curved guide piece made from a solid cylindrical bar capable of fitting inside the tube was fitted to the front end of the straight tube. Two rollers held the tube in place and a third roller pushed against the tube to give it a continuous bend. The guide piece was used to allow for a smooth engagement of the forming rollers and to protect the tube from damage when first engaged by the roller. Prior to the bending operation, the straight tube was fed past the forming roller to the required leg length. Once the straight section was fed through, the bending roller engaged to give the tube a radius. The formed tube passed over a horizontal guide roller whose vertical position could be varied in relation to the bending roller. This height adjustment determines the gap between coil turns which further determined the coil height and pitch. The only variables that could be adjusted on the machine were total tube length fed, radius of the tube bend and gap between turns in a coil. If the incorrect tube length was supplied for a given radius, then the coil would be formed with the incorrect number of turns and in most cases an incomplete final turn.

As a post process, a 90° bend was placed at the point where the helical section of the coil meets the coil leg. This was done so the coil inlet and outlet could be mounted on the cylinder in a vertically straight line. The coil leg length can be further trimmed after this operation. The amount trimmed off the coil legs must be equal to maintain a vertically straight coil within the cylinder. The amount trimmed off the coil legs also determined the amount the coil helix central axis is offset from the cylinder central axis.
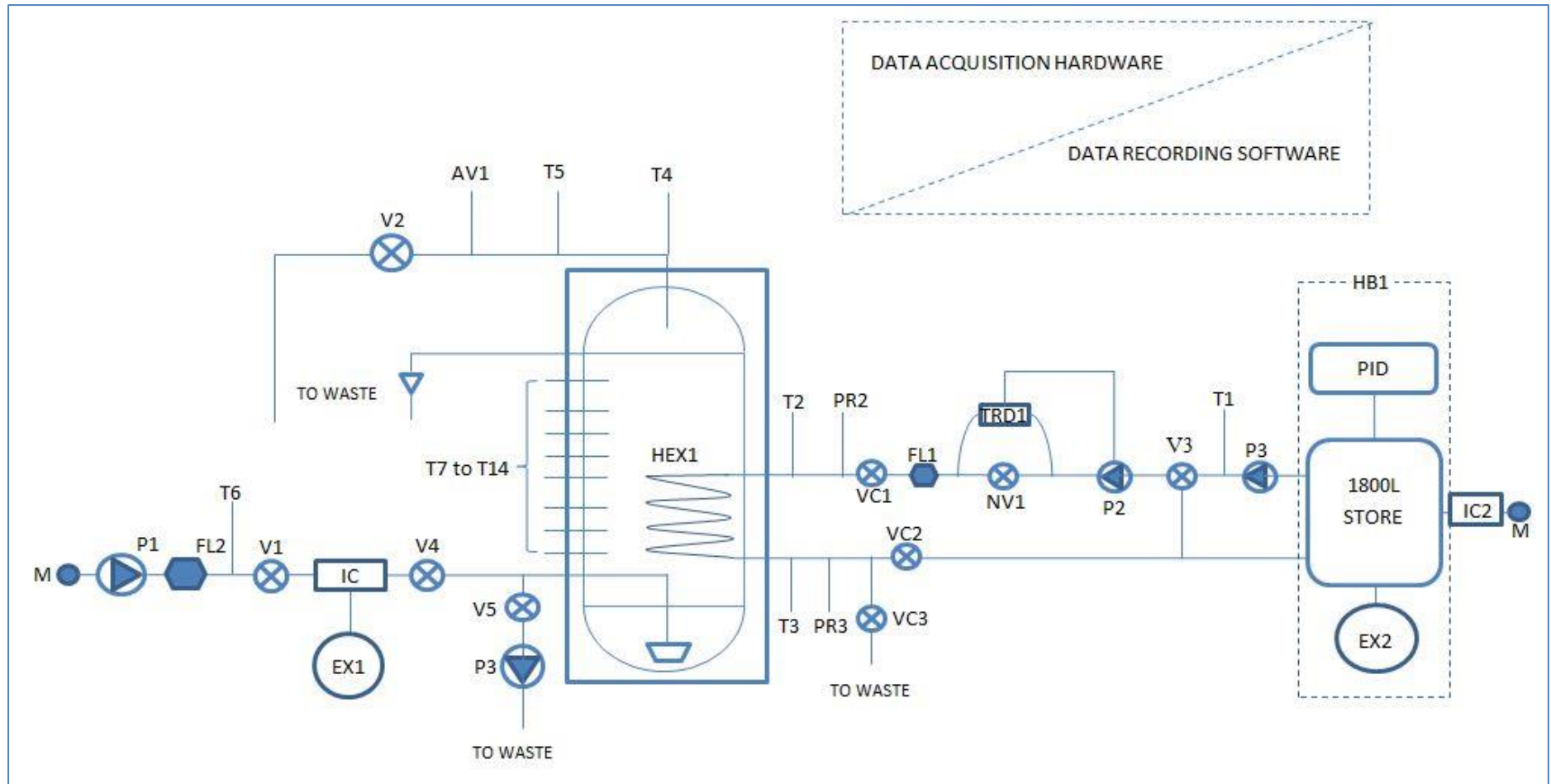

Figure 4.1.13 – Coil forming machine

Test Rig

Figure 4.2.1 – Schematic of Test Rig Used

A key component for testing the hot water tank developed above is the rig within which it was housed. The test rig has four main sections.

1. Heat battery and heat delivery system to the coil under test
2. Cold water supply and control
3. Test cylinder temperature measurement and hot water draw off system
4. Data acquisition and data recording system

Most the components of the test rig were available for use at the thermal test labs at Kingspan Environmental limited. The test rig was evaluated to determine its suitability for the type of testing in this study. Where required the existing system was added to or modified.

Heat battery and heat delivery system

The key component of the heat battery is an array of three 600 litre capacity insulated hot water cylinders. The total battery hot water volume of 1800 litres is considered sufficient for testing without unduly cooling down as the battery volume to test cylinder volume is 10:1. A test would approximately run for 30minutes with the coil flow rate of 15 litres/minute. Each tank is heated by a 3kW titanium immersion heater. Titanium immersion heaters were selected for this process due to their corrosion resistance under elevated temperatures. The integrated thermostats on the immersion heaters were disconnected and the tanks were thermostatically controlled by a remote K type temperature sensor with a reading accuracy of ±1.5°C ±0.25% and range of -100°C to 250°C. A proportional integral derivative (PID) controller was used to control the electrical energy input into the immersion heater through a control box powered by mains electricity. The control set point for the hot water tanks was 82°C. selection of this value was influenced by the British standard EN12897:2006. The PID controller used had a control accuracy of 0.5% of the control range which was ±0.41°C. The heat battery operating pressure was maintained at 2.5bar. An expansion vessel EX2 with a volume of 200 litres was fitted to the heat battery system to accommodate the expansion of water over the heat up temperature range. Vessel EX2 was pre-charged with an air pressure of 1.5 bar on one side of a fitted membrane. The other side of the membrane would accommodate the volume of expanded water. As the system pressure climbs over 1.5 bar the membrane within the expansion vessel will compress the pre-charged air. When an expansion vessel is open to atmosphere the total internal volume will be comprised of air at the pre-

charged pressure. The aforementioned section of the heat battery was deemed completely suitable for the requirements of testing and was used without making any further modifications.

Two separate pipework configurations of series and parallel were available for the heat battery. In series flow configuration, the heat battery had a single inlet and single outlet. The hot draw connection of the cylinder with the inlet was connected to the cold-water inlet of the adjacent cylinder. The hot draw connection of the second cylinder was connected to the cold inlet of the next cylinder. The hot draw connection of the third cylinder was connected to heat battery outlet. The water returning to the heat battery would enter the first cylinder through its cold inlet and the flow would force water across the heat battery and out of the hot water draw off connection in the third cylinder. This section off pipework was used as available.
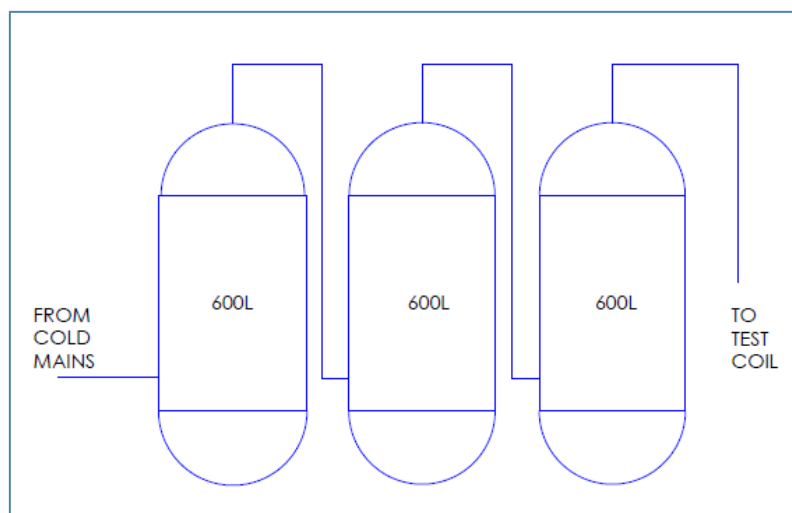
Figure 4.2.2 – Series pipework configuration

In parallel flow the inlet to the heat battery was branched into three 22mm diameter tubes and fitted to the inlets of each 600-litre hot water tank. The outlets of the tanks were independently connected to the outlet of the heat battery. Flow regulators were placed on the outlets of each hot water tank to ensure that each constituent cylinder in the heat battery was contributing equally to the overall outflow of the heat battery. The benefit of running the test in parallel mode was that a higher flow rate could be delivered to the heat exchanger. This section of pipework was also left unmodified for use.
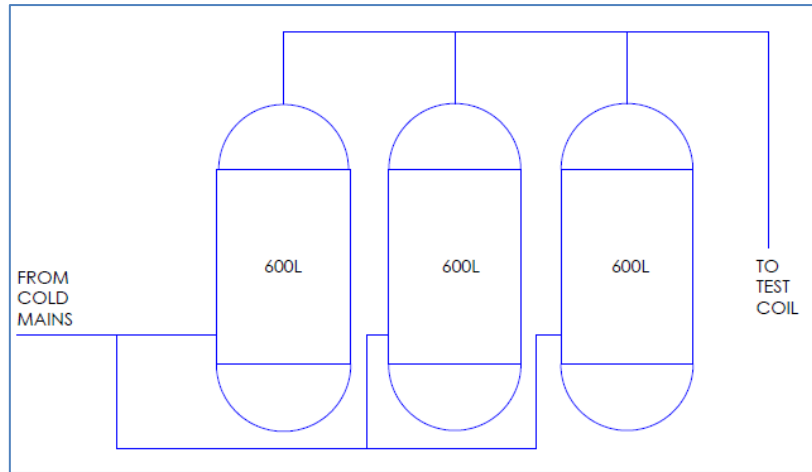
Figure 4.2.3 – Parallel pipework configuration

A 3-speed circulation pump P3 was installed on the outlet line of the heat battery. The pump used was a Grundfos UPS2 25-40/60 130 central heating pump rated for a liquid temperature range of 2°C to 95°C. The circulator pump is important to remove stratification in the heat battery cylinders when tests are not running. This ensures that the entire volume of the heat battery is at the target temperature. If a circulator pump is not present, a well-defined thermocline would be present in large cylinders such as the 600 litre cylinders within the heat battery. If a thermocline crosses the outlets of the cylinders a sudden drop in temperature would be witnessed in the water flowing through the heating coil. This would cause anomalies in the test as well as to render the test invalid if tolerances were exceeded. By ensuring the total volume is at the desired temperature better estimations can be made regarding the number of tests that can be completed before the heat battery needs to recover. It also allows for a greater number of tests to be carried out on a single charge of the heat battery.

An immersed RTD temperature probe T1 was fitted to the outlet pipework leg of the heat battery. Probe T1 is used to measure the flow temperature to the test cylinder heat exchanger coil. Temperature probe T1 has an accuracy of ±0.31°C at 80°C and ±0.18°C at 15°C. All RTD temperature probes used in this rig carry the same level of accuracy.

Valve V3 is placed on a T connection to divert the flow of water from the heat battery to the coil or back into the heat battery inlet. A 3-way valve was used for this purpose as it was sufficient due to a single inlet dual outlet requirement. A dial temperature gauge was in place on the pipework to the test cylinder for a quick access reading of the line temperature. This

was for indication only. The above components were deemed suitable for testing and used as available.

A variable speed pump P2 was installed on the heat battery outlet/coil inlet leg of the pipework. This pump was used to increase the flow into the coil to 15 litres/minute. The pump was controlled by a differential pressure transducer TRD1 with pressure signals obtained from the inlet and outlet side of the double regulating valve NV1. The flow rate through the coil could be varied by varying the pressure difference across NV1. This set up required no further modification and was used as available.

A turbine type Apollo RN3/20/5 high accuracy flow meter FL1 was fitted to the coil inlet leg of the pipework. The flow meter, FL1, was used to measure the flow rate across the heat exchanger coil. FL1 was capable of measuring flow rate to the accuracy of ±0.5% of the reading.

Quarter turn valves VC1 and VC2 were installed on the coil flow and return legs of the pipework to isolate the coil from the rest of the heating circuit to exchange the coil on test. The actual connection to the coil connection bosses were made by flexible pipes that could be disconnected form the cylinder at a point after the T1 and T2 temperature probes. Flexible pipe was the preferred choice when making the final connections to the coil inlet and outlet as well as the cold-water inlet to the tank. The reason for this preference was due to the varying locations of the coil and cold inlet connections for different tests.

K type temperature probes T2 and T3 were placed immediately adjacent to the coil inlet and coil outlet connections respectively. This was one of the modifications made to the existing rig. Prior to the addition of T2 and T3 the test rig had no method of measuring the coil power using energy balance. T2 and T3 were used to find the temperature difference across the coil under test. T2 and T3 have a reading accuracy of +0.89°C and +0.76°C at 60°C and 82°C respectively.

As the coils were regularly changed for the tests, the issue of introducing air into the heating circuit needed to be addressed. The heat battery cylinder pipework contained an automatic vent for dispelling air that had been introduced into the system. However, it is best practice to minimise the amount of air introduced and rely on the automatic air vent as a last resort.

Ingress air can be a significant detriment to a sealed pumped system. It can reduce the performance of heat exchangers and damage seals on pumps. To reduce the amount of air introduced into the heating circuit during coil change process once the coil was fitted on the test cylinder and the heating circuit was reconnected, valve VC1 and VC3 would be opened and VC2 shut. Pump P3 would be switched off and pump P2 would then be turned on. Most of the air within the coil would then be forced out of the pipe with valve VC3. Once an even flow of water was being discharged, VC3 would be shut and the pump would be switched off and VC2 opened. As a process of preventative maintenance, the bleed valve on pump P2 would also be opened during the coil change air discharge process.

Inlet pipework

The cold-water main is connected to the cylinder at M on the inlet pipe work as depicted in figure 4.2.1. A pump P1 is fitted in line if the flow rate needs to be boosted if a high demand situation occurs. In general pump P1 would only be used for larger cylinders above 250 litres as the British standards call for higher draw off flow rates (British Standards Institute, 2006). For testing the 180-litre test cylinder, pump P1 would not be used except for in exceptional cases of low mains water pressure.

A turbine type Apollo RN3/20/5 high accuracy flow meter FL2 was fitted after pump P1 on the cold-water inlet pipework. Flow meter FL2 was used to measure the flow rate of the cold-water inlet to the cylinder. Flow meter FL2 is identical in design to FL1.

An immersed RTD temperature probe T6 was fitted to the cold inlet pipe to measure the inlet water temperature from the mains supply. In certain instances such as during the hottest summer months, the mains flow water must be by-passed through a chiller or cold store to reduce the inlet water temperature to within the acceptable range of the British standards.

An inlet control set IC was installed to limit the maximum inlet water pressure allowed into the cylinder. The inlet control set also houses two non-return valves which are required to avoid backflow into the mains water system. When the cylinder is heated up it has elevated pressure as a result of temperature. This pressure may exceed mains water pressure and conditions for back flow would be setup. The maximum pressure setting of the inlet control set is 3 bar. The inlet control set also acts as a safety against cylinder damage due to excessive pressure. The inlet control set can withstand 16 bar of water pressure. A pressure gauge was

also fitted on the inlet control set to be used for indication only. The inlet control set used also had an expansion vessel port. This allows for an expansion vessel to be fitted to the cold-water pipework to accommodate for the thermal expansion of water over the heating temperature range. The expanded water from the cylinder will flow back through the inlet pipework past the inlet control set and into the expansion vessel. During the hot water draw off process the water in the expansion vessel will be discharged back into the cylinder. The volume of the expansion vessel used was 24 litres.

Quarter turn valves V1 and V4 were placed on either side of the inlet control set IC. The purpose of these valves were to isolate the mains water supply from the test cylinder whilst having the functionality of the inlet control set or to isolate both the inlet control set and mains water supply from the test cylinder. The above inlet pipework was used as available for this study.

A section of pipework which terminated at waste was added to the water inlet pipework through a T connection. The purpose of this branch was to allow for draining the cylinder. Quarter turn valve (V5) was added to isolate the draining pipework from the main water inlet pipework during testing. A 3-speed pump was also added to the draining pipework to assist with draining the test cylinder.

Draw-off pipework

A 22mm diameter copper draw off pipe was connected to the hot outlet of the test cylinder. An immersed RTD temperature probe T4 was fitted on the pipe by way of a T connection. The probe T4 was placed such that the sensor tip would fit through the hot water draw off boss and be immersed in the cylinder 25mm below its highest point. This was a requirement of the British Standard BS EN 12897:2006. This is one of the key temperature readings during the test. This probe determines when the cylinder is up to temperature during the heating phase and the starting cold temperature of the cylinder. The draw-off pipework also included an immersed RTD temperature probe T5, 150mm away from T4 further downstream on the pipework. T5 was utilised to read the temperature of the water being drawn off from the cylinder. An automatic air vent AV1 was also available on the pipework after T5 to expel any trapped air in the cylinder. AV1 is useful during the cylinder fill phase. This section of pipework was used as available as it satisfied the needs of testing.

During the fill phase once the cylinder is full and discharging from the outlet pipe the cold-water flow is maintained further until the sound of air expelling from AV1 stops. This ensures that any trapped air in the cylinder has been removed. Trapped air bubbles within the cylinder can significantly affect the temperature readings, especially if they are trapped around a probe tip. A quarter turn valve V2 was available on the outlet pipework to seal the test cylinder and allow for its pressurisation. Water flowing out of the test cylinder was discharged to waste.

Discharge pipework was fitted to the temperature and pressure (T&P) relief valve as well. The T&P valve used would fully discharge if the temperature exceeded 90°C of the pressure exceeded 7 bar. The discharge pipe had a vertically downward section and a tundish was placed on it. A tundish allows for viewing the flow through a pipe as it has an open section. This was required both as a safety requirement and to confirm that the test didn't run under a cylinder failure mode.

Data acquisition and recording
Three main types of data acquisition hardware modules were utilised during testing.

1. Signatrol SL7101 data loggers
2. Metra-smart flow totaliser, counter and display (flow computers)
3. Pico Log TC-08 data loggers

Signatrol SL7101 data logger
Two Signatrol SL7101 data loggers are used for collecting sensor signals during test. One logger was used for the primary loop or heating side of the test apparatus and the other was used for the secondary loop or load side. The sensors read from the primary side of the rig were heat battery outlet temperature T1, the output of the Metra-smart flow counter connected to coil flow rate sensor FL1 and pressure sensors PR2 and PR3. The secondary loop sensors were read by a second Signatrol SL7101 logger. The inputs on the second logger were from temperature probes T4, T5 and T6 and the output of the Metra-smart flow counter connected to cylinder inlet flow sensor FL2. The SL7101 loggers also had a LCD displays that cycled between the readings of the sensors for a quick view of the logged information without having to access the computer software interface.

Metra-smart flow totaliser, counter and display

Two Metra-smart flow computers were used to connect the output of the flow meters FL1 and FL2. This was done to have a visual display of the flow meter during test without having to access the computer software interface. The flow computers had analogue to digital converters that displayed the flow rate to an accuracy of 0.1 of a litre/minute on its LCD screen. The signals from the flow meters were routed through the flow computers and onwards to the Signatrol SL7101 data loggers for recording.

The Signatrol SL7101 loggers and flow computers were housed in an IP6 rated cabinet with custom wiring to power and initialise the units. A single toggle switch was used to initiate data capture on the both loggers simultaneously and ensure the data tables were synchronised.

Pico technology TC-08 thermocouple data loggers

Two TC-08 thermocouple data loggers were used during testing. One logger received inputs from the eight K type thermocouples T7 to T14 measuring the internal temperature of the test cylinder. The other TC-08 module captured data from the T2 and T3 thermocouples measuring the coil flow and return temperatures.

The TC-08 units and SL7101 units were connected to the same PC and the synchronisation of their data tables was carried out manually by way of computer time stamp to the closest second.

The data logged by the Signatrol SL7101 modules were recorded on a PC by the TempIT-PRO software which was written for the modules by Signatrol. The output from the TC-08 modules was recorded by the PicoLog data acquisition software. All read rates for software used were set to one reading per second.

Testing Method

The test method used for evaluating the performance of the heat exchanger coils closely followed the method outlined in Annex A of the British standard BS EN 12897:2006. The decision to fulfil the testing requirements for the above-mentioned standard as part of the overall test method was governed by the following

1. The ability to compare results with historical data published by hot water manufacturers
2. Commercialisation of results would require conformance to the British standards. It is also required for product certification by approved third parties and energy labelling of the product

The scope of British standard BS EN 12897:2006 deals with the performance requirements and test methods for indirectly heated, unvented storage water heaters up to a capacity of 1000 litres (British Standards Institute, 2006). A water supply pressure of 0.5bar to 10bar is considered within this standard and hot water cylinders tested in accordance with this standard must have control and safety devices which prevent the stored water from exceeding 100°C.

The test requirements as per Annex A of the standard is as follows

Test Clause	Test description
A.4.1	Hot water performance
A.5.1	Hot water capacity
A.5.2	Reheat performance (primary heating power)
A.4.2	Primary heater pressure drop
A.6	Temperature control

Table 4.3.1 – Performance testing requirements outlined within BS EN 12897:2006 (British Standards Institute, 2006)

Testing within this study will cover all the above points apart from A.6 which is related to the functioning of safety devices on a storage water heater.

The similar British standard BS 1566-1:2002+A1:2011 was excluded from consideration as it dealt with performance of copper cylinders for open vented service.

Some of the key test parameters for testing in accordance with BS EN 12897:2006 are indicated below.

1. The heat source must be capable of providing a primary water flow temperature of (80 ±2) °C. The set point on the heat battery for testing purposes is 82°C. This value was chosen to compensate for any losses that may occur in the hot water tanks and delivery pipework.

2. The default flow rate across the heat exchanger coil must be 0.25 litres per second. This value can be changed depending on the intended conditions of use. However, the default value of 0.25 litre per second was selected for the purposes of this study

3. All flow rates must be measured to an accuracy of 0.01 litres per second

4. The primary flow meter FL1 must be calibrated for water at 80°C

5. The temperature sensors used must be capable of measuring temperature to an accuracy of ±1°C

6. Temperature probe T1 must be positioned just prior to the bypass valve V3

7. Temperature probe T4 which detects the stored water temperature the must be positioned inside or on the hot water cylinder 25mm below the hot water outlet. For this study the author opted to have probe T4 inside the test cylinder for a more reliable result.

8. Temperature probe T5 which detects the temperature of the water discharged must be sited no more than 150mm from the cylinder outlet

9. Temperature probe T6 which detects the temperature of the mains inlet water must be sited no more than 150mm from the cylinder inlet

10. Pressure sensors measuring the pressure drop across the heat exchanger coil must have a reading accuracy of ±2%

11. The test cycle can commence when the temperature at temperature probe T4 is between 13°C and 15°C both inclusive. For this study, the requirement was further clarified as needing 3 consecutive readings within this range for the test cycle to commence.

12. The timer for recording the reheat time must be started when temperature probe T4 detects a temperature of 15°C and must be stopped when T4 detects a temperature of 60°C. When the T4 reaches the target of 60°C the heat source must be disconnected from the heat exchanger coil

13. One minute of stabilisation time must be allowed for the system after it reaches 60°C before the hot water draw off process can commence.

14. Hot water draw off volume is calculated from when draw off commences to the first instance when temperature sensor T5 reads a temperature of 40°C or less

Coil fitting process

The first step of rig preparation is to fit the coil to be tested to the test cylinder. The coil is the primary focus of this study and care must be taken during this operation to minimise any anomalies during the test. Below is the process checklist the author followed for exchanging the heat exchanger coil in the test cylinder assuming another coil had previously been fitted. It is assumed that all viewports are sealed for testing.

1. Ensure the test cylinder is drained down to its lowest point and resting on its base on a stable surface no more than 100mm from floor level

2. Disconnect all pipework from the test cylinder. When disconnecting the coil connections remove the top connection first. Place a container no less than 10 litres below the second connection and then remove the pipework. Allow the water in the coil to empty under the force of gravity

3. Using a socket wrench with ratchet capability and a 24mm drive socket, loosen the M16 bolts on the front viewport. Loosen the bolts such that diametrically opposite bolts are loosened alternately

4. Once all the bolts are loosened a powered drill with socket adaptor can be used to completely remove the bolts. Be cautious of the weight of the insert and sealing ring during the bolt removal process.

5. Remove the viewport insert and sealing ring and place aside safely

6. Ensure sufficient lighting is directed toward the inner space of the test cylinder when removing or replacing the coils

7. A 22mm compression straight connector is the method used to fit coil ends to the test cylinder internal connection stubs. Loosen the nuts on the connection stub ends to

release the coil complete with the straight connector. Loosening the nuts on the coil end while the coil is fitted may damage the coil. It is advisable to loosen both top and bottom nuts first and release the coil legs simultaneously.

8. Prepare the coil to be installed by fitting its end with a 22mm straight connector. Ensure the internal connection stub on the cylinder has a nut and compressed olive available. If not fit a nut and olive and use a free straight connector to compress the olive to point of sealing

9. Align the connection stubs ends with the bore of the straight connectors on the coils and fasten the connector to the stub with the available nut

10. Connect the mains water source M through IC to the lower connection of the coil and slowly fill the coil with water until discharged from the upper coil connection. Valve V1 can be fully opened but the flow must be controlled by valve V4

11. Seal the upper coil connection with a blanking cap and PTFE thread seal

12. Once sealed fully open valve V4 and allow the coil to pressurise to a maximum of 3bar as set by IC. Check for leaks and if present diagnose, correct and check again

13. Once the coil has been checked shut valve V4. Remove the cap on the coil and the cold-water inlet pipe. Be cautious, the coil is under mains pressure. A container will be required to collect the water inside the coil

14. Replace the viewport insert and sealing ring and seal with M16 bolts

Performance test procedure

To commence the testing procedure, the test cylinder must be fitted with a heat exchanger coil as outlined above. The rig must be set up as depicted in figure 4.2.1. With all components fitted and sensors connected to their respective data acquisition modules. The PC logging the data must be switched on and the software opened and accessible. To prepare for testing, the Signatrol SL7101 modules must be cleared and reset to await the trigger to begin logging. A new file must be created for the PicoLog software and the software must be ready to record. Listed below are the main activities in the test procedure. It is assumed that the heat battery and delivery pipework are in standby mode i.e. valve V3 is set to the re-circulation position meaning the primary flow bypasses the test cylinder and pump P3 is operating.

1. Ensure the heat battery temperature reading display on the PID controllers is between 78°C and 82°C both inclusive. Confirm with the reading of T1 on the TempIT Pro real-

time display screen. If the reading is outside the range the test cannot be run. The heat battery will require troubleshooting in this situation. If the reading is within the range the testing process can commence. Special attention must be given to the heat battery during testing if the displayed temperature is close to the bottom end of the range as this is an indication that the heat battery may be running low on hot water at the target temperature range and may need time to recover.

2. Reset the flow computers to zero. Close valve V5. Open valve V2, V1 and V4 in that order. Allow the cylinder to fill. The reason for opening valve V2 first is to ensure that a clear path is available for the air in the cylinder to escape before the filling process. It is good practice to gradually open quarter turn valves. It reduces shock to the system and helps the longevity of the valve

3. When water discharges from the cylinder outlet pipework immediately shut valve V2 and turn pump P1 on. The flow computer display counter for FL2 will slow down and gradually stop at a value. Record this value as the cylinder capacity. Once recorded, switch off the pump, open valve V2 and close valve V4

4. On the heating side, close valve VC2 and open valve VC1 and VC3.

5. Turn diverter valve V3 such that the flow is completely going through the coil. Once a steady flow of water is discharging past valve VC3, close valve VC3 and switch off pump P3. This step is carried out to expel the air within the coil if it has been exchanged since the last test. If the rig is to be kept idle for any amount of time after this step, then set valve V3 to bypass the coil and turn pump P3 on allowing recirculation of the heat battery

6. Open valve VC2 and switch pump P2 on. Adjust the pump power setting until 15litres/minute is seen on the display of the flow computer connected to flow meter FL1. A small amount of fine tuning can be carried out with the NV1 if required. Switch off pump P2, set valve V3 to recirculate the flow directly back to the heat battery and turn pump P3 on

7. Open valve V4 and adjust it until 15litres/minute is seen on the display of the flow computer connected to flow meter FL2. Valve V1 should be completely open during this step

8. Reset the counter on the flow computer connected to FL2 and then flush the test cylinder with an amount of water equal to its capacity

9. With valve V4 open observe when the reading on temperature sensor T4 exceeds 13°C. At this point close valve V2 and turn on pump P1. When the flow rate reading on the FL2 flow computer display reads zero turn off pump P1 and close valve V1

10. Reset all the data loggers and synchronise the two Signatrol SL7101 loggers with the toggle switch and set all the loggers to commence recording

11. Turn pump P3 off, set valve V3 to direct the primary flow through the coil and turn pump P2 on. Confirm that the flow rate through the coil is 15 litres/minute by consulting the TempIT Pro software and the flow computer display connected to FL1

12. Monitor the readings of temperature sensor T4. At the first instance that T4 records 3 consecutive temperature readings of 15°C or higher start the stopwatch for recording the cylinder heat up time

13. While the cylinder is heating up record the pressure readings on the PR2 and PR3 displays for calculating the pressure drop across the coil. This value is useful for designers of heating systems as it will help in estimating the pumping requirements for that system

14. Monitor the readings of temperature sensor T4. At the first instance that T4 records a temperature of 60°C stop the stopwatch for recording the cylinder heat up time and start the 1 minute timer for test cylinder stabilisation.

15. Immediately switch off pump P2, set the bypass valve V3 to re-circulate directly back to the heat battery and switch on pump P3

16. Reset the counter on the flow computer connected to FL2 and after the 1 minute stabilisation period open valve V1 and V2

17. Monitor the readings of temperature sensor T5. At the first instance that T5 records a temperature of 40°C, record the volume of water that has passed through FL2 as displayed by the flow computer connected to FL2

18. Continue draw off process until temperature sensor T4 reads a temperature of 15°C or lower. Once this target is reached close valve V1 and save the electronic data files

19. If the test cylinder needs to be emptied for the coil change process, then open valve V5 and switch on pump P3. Once water stops discharging from the outlet, switch off pump P3 and close valve V5

Interpretation of the Results

As per British standard BS EN 12897:2006 the coil power is calculated with equation (13)

In addition to the above calculation the author also proposes evaluating the coil power Q_{coil} with the following equation.

$$Q_{coil} = \dot{m}C_p\Delta T_{coil} \qquad (19)$$

$\dot{m}$ (kg/s) is the mass flow rate through the coil and ΔT_{coil} (°C) is the difference between the coil inlet and outlet temperatures. The mass flow rate is calculated using the volume flow rate measured by FL1. When converting volume flow rate to mass flow rate, the density of water at 82°C was selected.

It would also be useful to understand the overall heat transfer coefficient of the coils. Equations (10) and (11) were used for this purpose.

For comparison, the test cylinder was compared to a commercial cylinder of very similar design. This was to confirm if the test cylinder performance was on par with its commercial counterpart. If the results of the two cylinders are similar, then the test cylinder can be considered a good representation of the existing commercial offering. It would also confirm that the test cylinder behaves in a similar way to the commercial cylinder under laboratory conditions.

Calculating UA

Five different methods were used to determine the UA values or product of the U value and area for different coils.

Method 1 – LMTD analysis

The first method dealt with the coil as a heat exchanger with counter flow. It was assumed that counter flow was achieved by the fluid inside the coil travelling from the top to the bottom of the helix and the fluid on the outside of the coil moving upwards due to buoyancy forces. The UA values were calculated using a log mean temperature difference method (LMTD). The diagram below illustrates the assumptions made for the calculation. The coil input temperature was considered as (T_{h1}) and the cylinder probe reading closest to the height of the coil inlet as (T_{h2}). The coil outlet was considered as (T_{c1}) and the probe closest in height to the coil outlet as (T_{c2}). Using the above method, the UA values for the different coils were obtained. The kW ratings for the coils calculated were used to check if the assumption that the coil acted like a counter flow heat exchanger was correct.
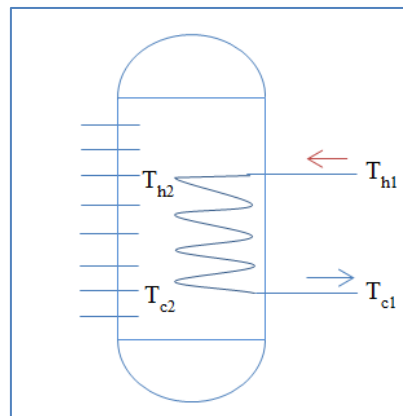
Figure 4.4.1 – Probes used for LMTD method

The equation for calculating *UA* is given below.

$$Q_{coil} = UA \left(\frac{(T_{h1} - T_{h2}) - (T_{c1} - T_{c2})}{\ln \left(\frac{T_{h1} - T_{h2}}{T_{c1} - T_{c2}} \right)} \right) \tag{20}$$

The table below indicates the T_{h2} and T_{c2} probe positions for different coil inlet and outlet ports.

Coil Connection Port Used for Inlet or Outlet	Corresponding Temperature Probe
1	DB Port 2
2	DB Port 3
3	DB Port 3
4	DB Port 4
5	DB Port 5
6	DB Port 6
7	DB Port 6
8	DB Port 7

Table 4.4.2 - Temperature probes corresponding to coil connection ports

Method 2 – mid-coil analysis

The second method looked at the average temperature of the coil and its surroundings. This method used the temperature reading of the probe closest to the middle of the coil in terms of height. Equation (21) was used to determine the UA value for the coil. The average of the coil flow and return temperatures which was considered the average temperature of the fluid within the coil. The UA values obtained were analysed against the corresponding coil power values.
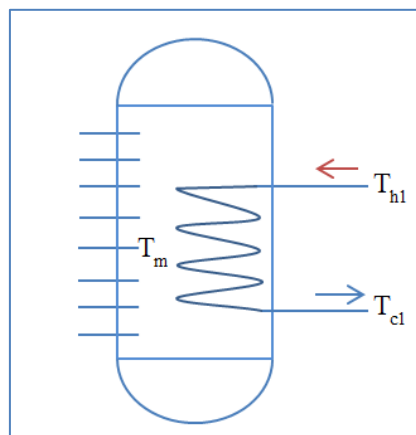
Figure 4.4.2 – Probe used for mid-coil method

$$Q_{coil} = UA\left(\left(\frac{T_{h1} + T_{c1}}{2}\right) - T_m\right) \qquad (21)$$

Test Reference	Corresponding T_m Temperature Probe
KTP003B	DB Port 5
KTP004B	DB Port 2
KTP006C	DB Port 4
KTP008C	DB Port 4
KTP009C	DB Port 3
KTP0010C	DB Port 4
KTP0011C	DB Port 3
KTP0012C	DB Port 3
KTP0013C	DB Port 4

Table 4.4.3 – T_m Temperature probes corresponding to tests

Method 3 – Coil average analysis

With the focus of refining the method followed above a third method was used which followed a similar process for obtaining UA. Instead of selecting the probe closest to the middle of the height of the coil, this method used the average value of the probes closest to the top and bottom of the coil height. The probes closest to the top and bottom of the coil height would be the same as those selected for the LMTD method as shown in figure 4.4.1. The UA value was obtained from equation (22)

$$Q_{coil} = UA \left(\left(\frac{T_{h1} + T_{c1}}{2} \right) - \left(\frac{T_{h2} + T_{c2}}{2} \right) \right) \qquad (22)$$

Method 4 – Probe average analysis

A fourth method was employed to further refine the selection process of obtaining UA for the different coils in the parametric study. In this method, the average value of the seven side wall temperature probes was taken. This excluded the lowest temperature probe DB port 1 which was not included in the calculation since its readings remained relatively stable and at a low temperature throughout the heating period. This indicated that the heat transfer towards probe DB1 was comparatively small and selecting it could lead to obtaining erroneously high UA values overall.
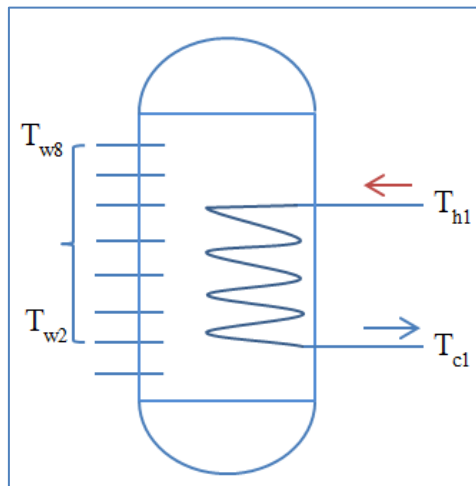
Figure 4.4.3 – Probes used for probe average method

UA was calculated using equation (23) below.

$$Q_{coil} = UA\left(\left(\frac{T_{h1} + T_{c1}}{2}\right) - \left(\frac{\Sigma_2^8 T_{wi}}{7}\right)\right) \tag{23}$$

Method 5 – Selecting the best fit probe for a given coil

It was postulated that due to the geometry of the coil and the positioning within the cylinder, the side wall probes may register the temperature change differently during the heating cycle for different coils.

Based on this the fifth method of calculating UA varies the probe used to measure the cylinder side temperature to match the trend of the coil output power value for its respective coil. All possible probe configurations are considered for each type of coil and the best fit for the UA trend with coil output power is selected. The UA is calculated using equation (24) below. T_b is the temperature of the best fit probe selected.

$$Q_{coil} = UA\left(\left(\frac{T_{h1} + T_{c1}}{2}\right) - T_b\right) \tag{24}$$

Parametric Study

The parametric study carried out is the key component of this study. The investigation focused on varying the parameters of diameter, number of coil turns and coil height of the test coils. The overall tube length was kept as similar as possible. Small variations in tube length were accepted as all coil turns had to be complete for manufacture. The diameter of the tube was kept constant at 22mm. A few exceptional cases of comparatively high surface area were also tested for comparison.

The material selected for the construction of the heat exchanger coils was copper. The other choice for fabrication material was 316L stainless steel. Copper was chosen over stainless steel due to availability of the suitable fabrication facilities for copper whilst fabrication with stainless steel yielded unfavourable results such as repeated and significant tube kinking. The test matrix for the parametric study is given below. The term flow refers to the connection port where heated fluid enters the coil and return refers to the connection port where the fluid exits the coil. The base coil was selected as the coil used in experiment KTP006. The area value for the coils was non-dimensionalised based on this. Subsequent tables and bar charts will include baseline coil data highlighted in red for clear comparison.

Experiment Number	Coil Details			Connection Ports		Non-Dimensional Coil Area
	Diameter	Height	Turns	Flow	Return	
KTP003	320	672	12	8	1	2.59
KTP004	180	288	10	3	1	1.21
KTP006	165	480	9	6	1	1.00
KTP008	150	672	11	8	1	1.11
KTP009	150	384	11	5	1	1.11
KTP010	235	672	8	8	1	1.27
KTP011	235	384	7	5	1	1.11
KTP012	235	288	7	4	1	1.11
KTP013	155	672	20	8	1	2.09

Table 4.5.1 – Parametric Test Matrix

For analysis, a few comparison ratios are defined. All measurements are in mm.

Diameter ratio (D_R)

$$Diameter\ Ratio\ (D_R) = \frac{Diameter\ of\ the\ coil}{Diameter\ of\ the\ cylinder} \qquad (25)$$

Height ratio (H_R)

$$Height\ Ratio\ (H_R) = \frac{Height\ of\ the\ coil}{Height\ of\ the\ cylinder} \qquad (26)$$

Separation ratio (S_R)

$$Separation\ Ratio\ (S_R) = \frac{Vertical\ gap\ distance\ between\ two\ consecutive\ coil\ turns}{Diameter\ of\ tube} \qquad (27)$$

Measurement of total energy within cylinder

The total energy of the cylinder was calculated using equation (14). The volume used to calculate the mass used for this analysis was 154.6 litres. The volume below DB Port 1 probe was excluded due to the negligible temperature variation observed during the test. The cylinder starting temperature was taken as the first value above 17°C. 17°C was selected as the cut in value because it was close to 15°C but may avoid noise that may occur during the test start process. ΔT was calculated by taking the average of the temperature probes DB Port 2 – DB Port 8 and T4 and then subtracting the cylinder start temperature from the calculated value. Test data was analysed from when T4 registered the initial temperature to when it first registered 60°C or above.

Special cases

Separate tests were also carried out to investigate factors which do not fall into parametric variation. The tests include the following.

1. Test to assess the influence of a circular chimney enclosing the coil
2. Impact of painting the coil gloss black
3. Impact of adding a taper angle on the helical coil

Error Analysis

Part of experimental work is the acknowledgement that physical quantities cannot be measured exactly. Listed below are the individual errors for the different measurement equipment used during testing. Using the individual error percentages and equipment used for a given output the error for a given measurement can be calculated by using the sum of the error percentages.

Instrument	Tolerance	Measurement Range	Individual Error %
K Type Thermocouples	+0.76 °C	82°C	0.93%
K Type Thermocouples	+0.81 °C	70°C	1.16%
K Type Thermocouples	+0.86 °C	60°C	1.43%
TC-08 Data Logger	+0.61 °C	60°C	1.02%
TC-08 Data Logger	+0.58 °C	70°C	0.82%
TC-08 Data Logger	+0.55 °C	82°C	0.69%
RTD Temperature Sensors	±0.31°C	82°C	0.76%
RTD Temperature Sensors	±0.18°C	60°C	0.60%
Signatrol Datalogger (temperature)	0.1°C ±0.1%	82°C	0.22%
Signatrol Datalogger (temperature)	0.1°C ±0.1%	60°C	0.30%
Flow meter	±0.50%	15LPM	1.00%
Flow totaliser and rate counter	±0.10%	15LPM	0.20%
Signatrol Datalogger (flow rate)	±0.01%	15LPM	0.02%
Pressure Sensor	±0.30%	2.5bar	0.60%

Table 5 – Measurement instrument error

Coil output power values
The instrumentation used to measure the output were the following

- K type thermocouples X 1 for the coil inlet measuring at an average close to 82°C

- K type thermocouples X 1 for the coil outlet measuring at an average close to 70°C

- TC-08 data logger X 1 for the coil inlet and outlet measuring at an average close to 82°C

- TC-08 data logger X 1 for the coil inlet and outlet measuring at an average close to 70°C

- Flow meter X 1 for coil flow rate

- Flow totaliser and rate counter for coil flow rate X 1

- Signatrol datalogger measuring flow rate X 1

$$Possible\ error\ =\ 0.93\%\ +\ 1.16\%\ +\ 0.69\% + 0.82\% + 1.00\% + 0.20\% + 0.02\%$$

$$= 4.82\%$$

Coil output power values (BS EN 12897: 2006)
The instrumentation used to measure the output were the following

- RTD probe X 1 for the coil inlet measuring at an average close to 82°C

- RTD probe X 1 for the cylinder temperature measuring at 60°C

- RTD probe X 1 for the draw-off temperature measuring at 60°C

- Signatrol datalogger measuring temperature at 82°C X 1

- Signatrol datalogger measuring temperature at 60°C X 2

- Flow meter X 2

- Flow totaliser and rate counter X 2

- Signatrol datalogger measuring flow rate X 2

$$Possible\ error =\ 0.76\%\ +\ 0.6\%\ + 0.6\% + 0.22\% + 0.6\% + 1.00\% + 0.20\% + 0.02\%$$

$$= 4.00\%$$

UA value for LMTD method

The instrumentation used to measure the output were the following

- K type thermocouples X 1 for the coil inlet measuring at an average close to 82°C

- K type thermocouples X 1 for the coil outlet measuring at an average close to 70°C

- TC-08 data logger X 1 for the coil inlet and outlet measuring at an average close to 82°C

- TC-08 data logger X 1 for the coil inlet and outlet measuring at an average close to 70°C

- K type thermocouples X 2 for the cylinder temperature measuring at a maximum of 60°C

- TC-08 data logger X 2 for the cylinder temperature measuring at a maximum of 60°C

- Coil power possible error

$$Possible\ error\ =\ 0.93\%\ +\ 1.16\%\ +\ 0.69\% + 0.82\% + 2.86\% + 2.04\% + 4.82\%$$

$$= 13.32\%$$

UA value for all other methods

The instrumentation used to measure the output was the following. When taking the average measurement, the highest possible error is considered.

- K type thermocouples X 1 for the coil outlet measuring at an average close to 70°C

- TC-08 data logger X 1 for the coil inlet and outlet measuring at an average close to 70°C

- K type thermocouples X 1 for the cylinder temperature measuring at a maximum of 60°C

- TC-08 data logger X 1 for the cylinder temperature measuring at a maximum of 60°C

- Coil power possible error

$$Possible\ error\ =\ 1.16\%\ + 0.82\% + 1.43\% + 1.02\% + 4.82\%$$

$$= 9.25\%$$

Draw-off volume over 40°C

The instrumentation used to measure the output was the following.

- RTD probe X 1 for the draw-off temperature measuring at 60°C

- Signatrol datalogger measuring temperature at 60°C X 1

- Flow meter X 1

- Flow totaliser and rate counter X1

- Signatrol datalogger measuring flow rate X 1

$$Possible\ error\ =\ 0.60\%\ + 0.30\% +\ 1.00\% + 0.20\% + 0.02\%$$

$$= 2.12\%$$

Cylinder heat up time

The instrumentation used to measure the output was the following.

- RTD probe X 1 for the draw-off temperature measuring at 60°C

- Signatrol datalogger measuring temperature at 60°C X 1

- RTD probe X 1 for the coil inlet measuring at an average close to 82°C

- Signatrol datalogger measuring temperature at 82°C X 1

- Flow meter X 1

- Flow totaliser and rate counter X 1

- Signatrol datalogger measuring flow rate X 1

$$Possible\ error\ =\ 0.6\%\ + 0.3\% + 0.76\% + 0.22\% + 1.00\% + 0.20\% + 0.02\%$$

$$= 3.1\%$$

Results

The results obtained from testing show the impact of parameter changes on the performance of the coil heat exchanger within the cylinder. Some information on the nature of the heating and draw off process as well as the influence of the coil surface condition also comes to light.

Comparison of Test Cylinder to Commercial Cylinder

One of the earliest tests conducted was to compare the performance of the test cylinder to a commercial cylinder of comparable storage volume. The coil in the test cylinder was selected to exactly match the coil in the commercial cylinder. The commercial cylinder performance data was obtained from the test result database available at Kingspan Environmental limited. This investigation was done to determine the amount of variation in performance between the test cylinder and commercial cylinder. Less variation would mean that any results obtained in the parametric study if beneficial to performance, could be applied to the commercial product with more ease. The results of the tests are given in table 6.1.

Test Reference	Time (Decimal Minutes)	Volume Over 40°C litres	BS EN 12987 Coil Power (kW)
KTP002B	31.25	205.90	18.89
LTR000147T5	32.28	182.10	18.14
KTP006C	37.13	168.60	13.34

Table 6.1 – Comparison of test cylinder to commercial cylinder

When comparing test KTP002B to LTR000147T5 it is observed that the coil power as calculated by the method in BS 12897:2006 is 4.1% higher for KTP002B. Thus, the time to heat the contents of the cylinder from 15°C to 60°C is 3.3% higher for LTR000147T5. A significant difference in draw-off volume is seen with KTP002B having 13.1% more volume drawn off.

Draw-off and Heat up Behaviour

Prior to evaluating the performance of the coil, it would be beneficial to get a general understanding of the nature of the heating and draw-off process. A comparison of the general draw-off profile of cylinders with varying coil heights is carried out below to ascertain if any significant differences exist in their heating and draw-off profiles.
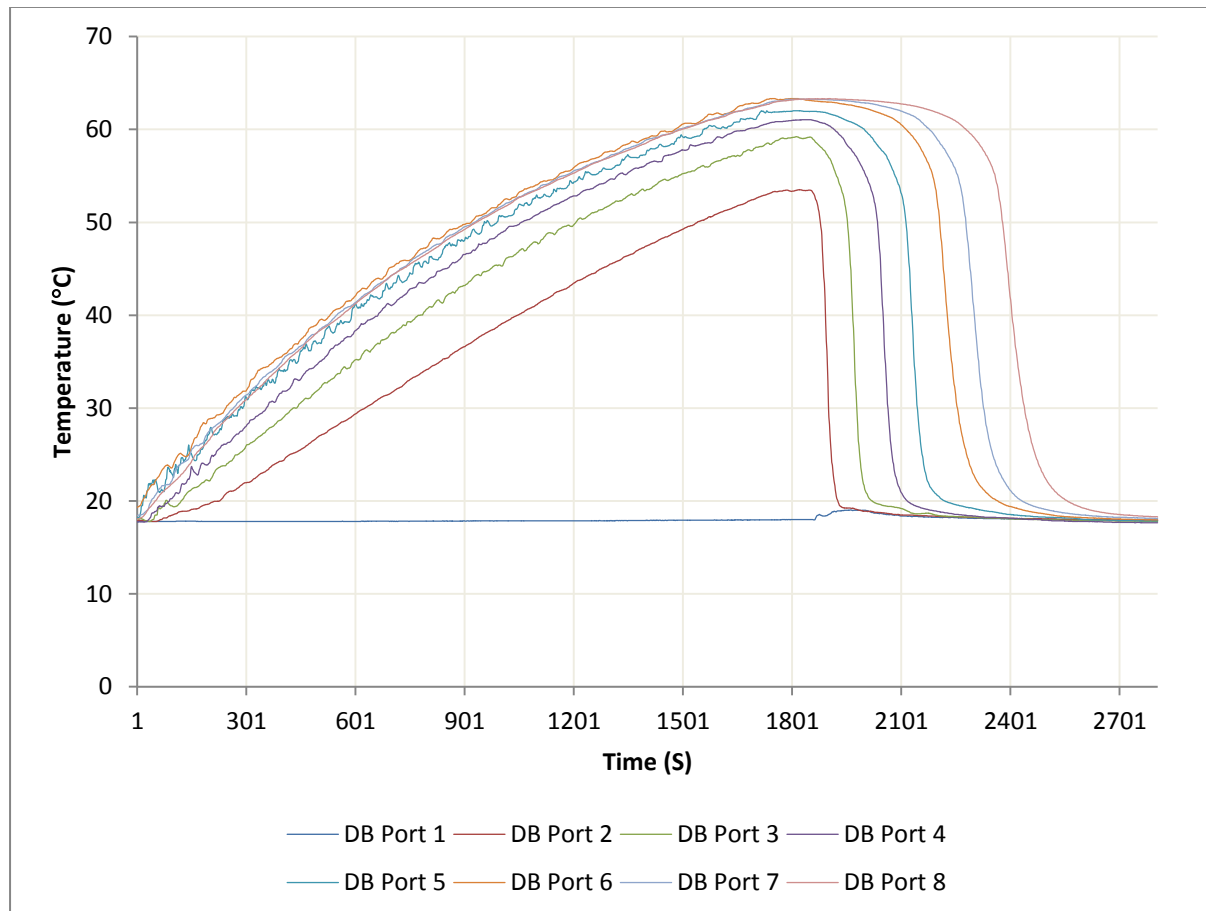

Figure 6.1 – Heating and draw-off profile of cylinder with $D_R = 0.52$ and $H_R = 0.55$

The lines on the graph represent the temperature readings taken by the side wall probes on the test cylinder. The probes are numbered starting with DB Port 1 at the bottom up to DB Port 8 at the top. Figure 6.2 shows their relative positioning within the cylinder.
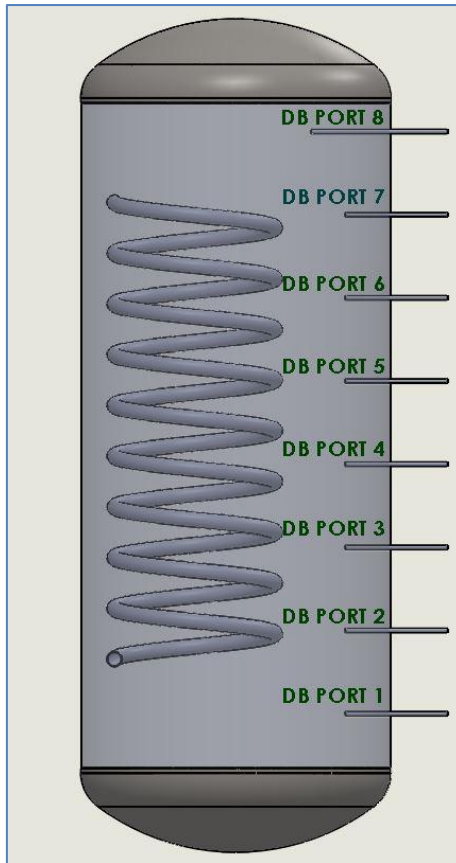
Figure 6.2 – Positon of coil and probes for test in figure 6.1

The cylinder is heated up for the first 1800 seconds. The wide spacing between DB port 2 and DB port 3 as well as the noticeable spacing between DB port 3 and the curves of the probes above it indicate the presence of a clear thermal gradient during heating. There is some indication of stratification setting up during the stabilisation period after heating and before draw-off commences. The first visible sign of a thermocline is further down the cylinder at the height in-between DB port 1 and 2. During testing the full volume of the cylinder does not heat up to the desired 60°C temperature. However, a considerable portion of the top part of the cylinder is at the desired temperature.

The bottom of the cylinder remains at starting temperature during the entire heat up time. During draw off a slight increase in the temperature at the bottom section of the cylinder can be observed. This is most likely caused by volume of water which has been warming up within the pipework being pushed into the cylinder and past DB Port 1. The slight increase in temperature at DB port 1 drops back down as the draw off process progresses.

It is observed that the draw off process has piston behaviour. Piston behaviour is defined as the scenario where the inlet water pushes the storage water evenly with minimal mixing. The existing thermocline is not disrupted by the incoming cold water. The thermocline crosses the side-wall probes in series starting with DB Port 2. This even movement of the thermocline would be observed as a sudden change in temperature read at the side wall probe at the time the thermocline crosses the probe. During draw off this would be a sudden drop in the observed temperature at each side wall probe. The reason for such well-defined piston behaviour is most likely due to the diffuser regulating the inlet jet effectively and minimising mixing of cold inlet water with the hot tank water.

Figure 6.3 depicts the heating and draw-off curve of a coil with diameter ratio 0.52 and height ratio 0.24. Figure 6.4 indicates the position of the coil in relation to the side wall temperature probes for the draw-off curve in figure 6.3
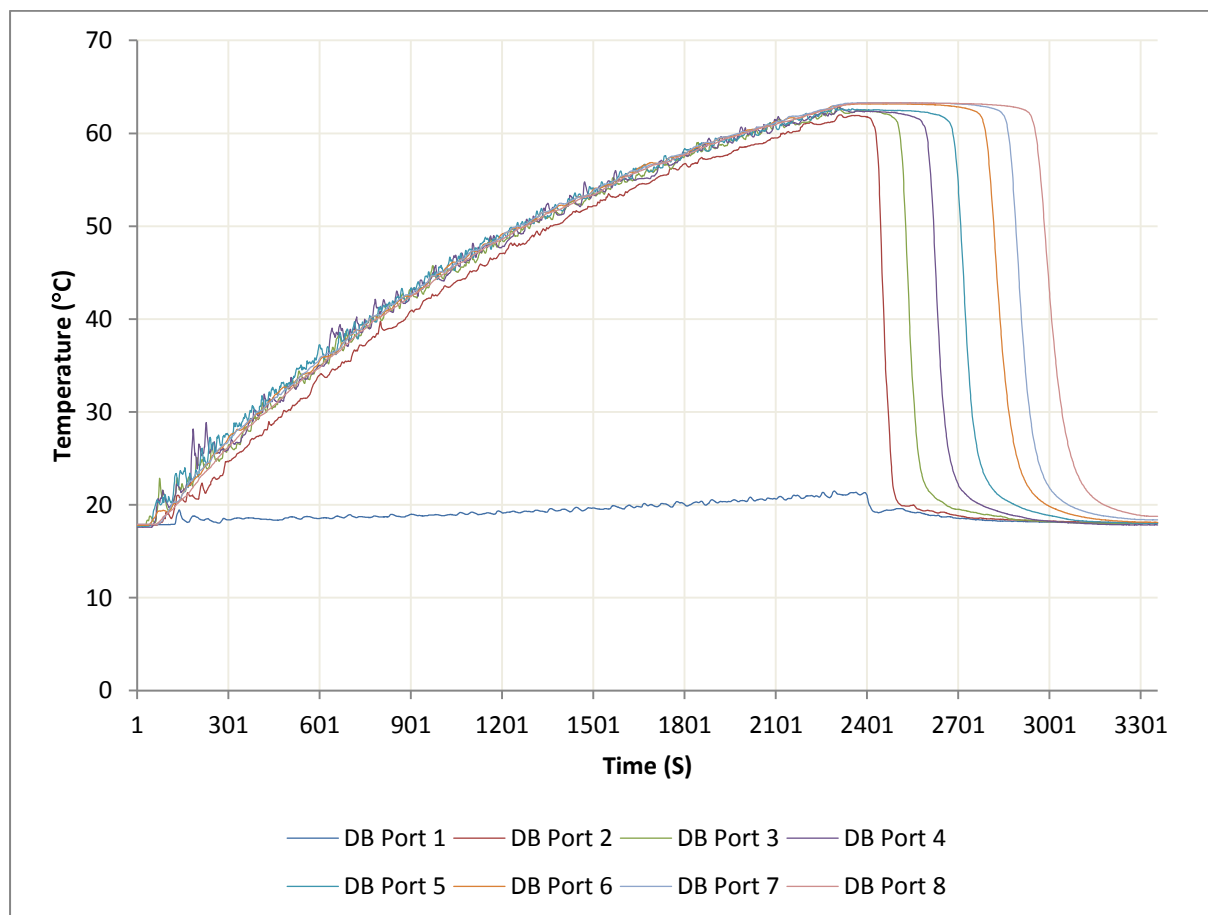
Figure 6.3 – Heating and draw-off profile of cylinder with $D_R = 0.52$ and $H_R = 0.24$
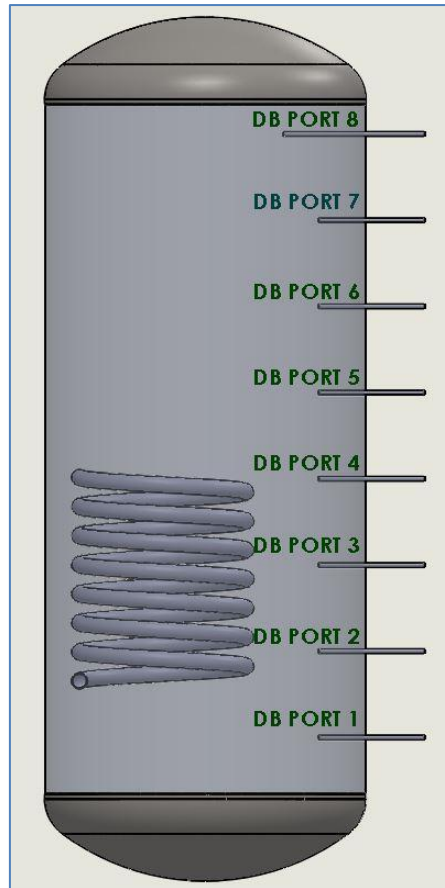
Figure 6.4 – Positon of coil and probes for test in figure 6.3

A well-defined thermal gradient is not observed with this coil in comparison to figure 6.1. The thermocline still seems to be between 1 and 2. The draw off volume of this test is 7.9 litres more than the test used for figure 6.1 which would also suggest that the thermocline has lowered giving a larger volume of hot water. The temperature difference across the thermocline has reduced in comparison as the temperature reading on DB port 1 seems to have increased during this test. The temperature gradient at the upper section of the cylinder during heating is much flatter than the temperature gradient seen in figure 6.1. No visible temperature difference can be observed from DB port 3 to DB port 8. This could be due to the high output power, low height ratio and low position of the coil concentrating the power output in a small area at the bottom of the cylinder causing the water to heat quickly in the concentrated area allowing a rapid expansion and strong buoyancy driven flow and heat transfer.

Characteristics of Consecutive Tests Conducted on a Given Coil

Once the general nature of the heating and draw-off of the test cylinder is investigated it is beneficial to investigate the effect of running tests consecutively with the similar operating conditions. It is hoped that such an investigation would lead to better understanding if any significant variation occurs as a result of repeated testing.

Four tests from the parametric study test matrix were selected for evaluation. The tests were selected to offer a range of coil surface areas, diameters and heights. Figure 6.5 presents the results of the evaluation.
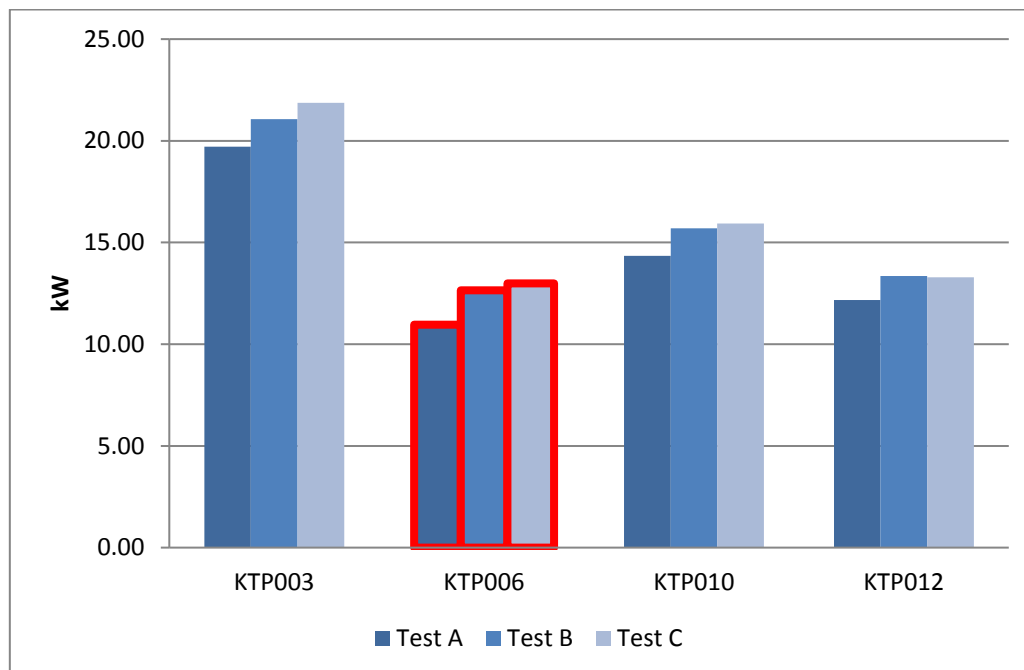
Figure 6.5 – Coil power for consecutive tests with varied coil parameters

It is observed from figure 6.5 that the first test in a series tends to have a comparatively lower coil power rating in comparison to the subsequent tests. The kW rating tends to stabalise as more tests are carried out. This effect is also noticeable as seen in figure 6.6 where the heat up plots for tests A, B and C are investigated. The first test has a lower rate of temperature increase compared to the other tests.
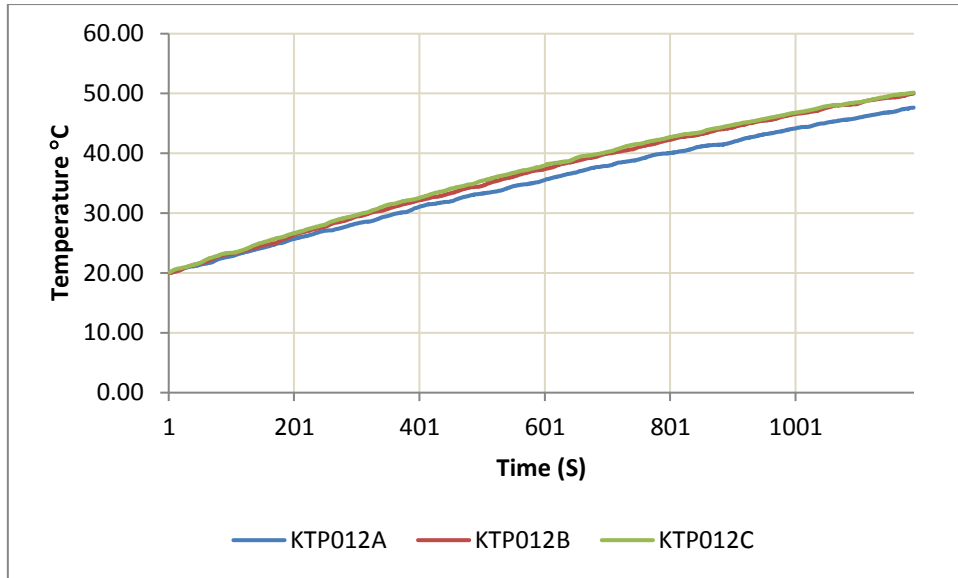
Figure 6.6 – Heat up plot for consecutive tests of KTP0012

An evaluation of U values across the first three tests for KTP010 and KTP006 also indicates a similar pattern as seen in figure 6.7. The first test has a comparably lower U value compared to subsequent tests as expected.
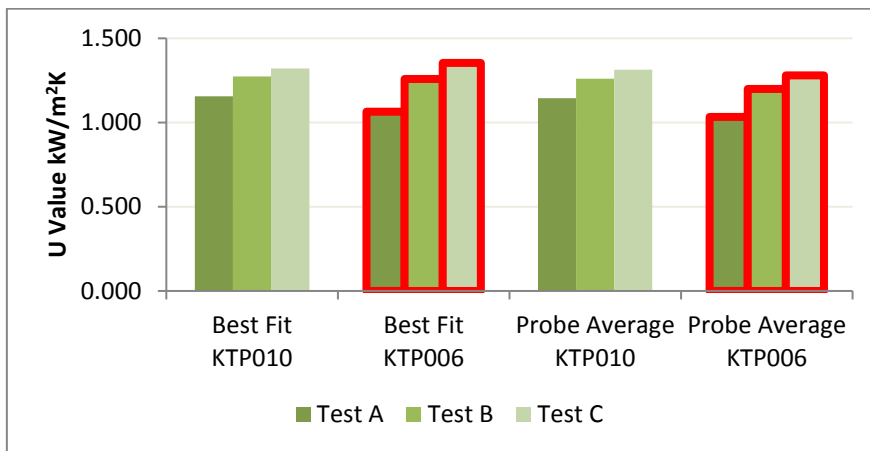
Figure 6.7 – U values for the first three tests of KTP010C

Based on the above results, the third test for each coil in the parametric study will be used as the representative value for comparison of the thermal properties. In the event a third test is not available, the results of the second test will be used.

UA Comparison and UA Calculation Method Selection

U values are a useful quantity for evaluating heat exchangers. It provides an insight into the effectiveness of a heat exchanger independent of the heat exchanger area. U values are also ideal for comparing heat exchangers with dissimilar areas.

Prior to progressing to U value analysis, it would be helpful to compare the UA values or the product of the U values with the area of the heat exchanger. For the coils within the parametric study this would serve as a valuable sense check as the UA values are expected to have similar variation in trend to the kW rating for their corresponding coils. A U value for a coil is a measure of the overall heat transfer for a unit area for a unit temperature difference ($W/m^2/K$). Therefore, the UA is the overall heat transfer for the coil for a unit temperature difference (W/K). Within this study the coil inlet is externally maintained at a set temperature and the cylinder start and end temperatures are the same for all the tests. Therefore, the cylinder average temperature is similar for all tests with small variations taken to account for differences in the position of the thermocline. A higher UA value would allow more heat energy to pass across the surface area of the coil and hence the coil outlet temperature would decrease more than if the UA value was lower. Since the coil power for given flow rate is determined by the temperature difference between the coil inlet and outlet temperatures as given in equation (19) with a higher difference giving a higher power value, it can be assumed that an increase or decrease in UA should show a similar change in coil power output or coil kW rating. Below are the results from the five methods which were employed to calculate UA for this study.

Log mean temperature difference (LMTD) method

The suitability of using the LMTD method to calculate UA for the parametric study is investigated below. Figure 6.8 shows the coil power in kW arranged in ascending order for the coils in the parametric study. Figure 6.9 gives the UA values of the coils measured using the LMTD method. The UA values are arranged to correspond with their respective coil power values in figure 6.9. It is expected that the trend in the two charts would be similar if the LMTD method is suitable for calculating UA for this study.
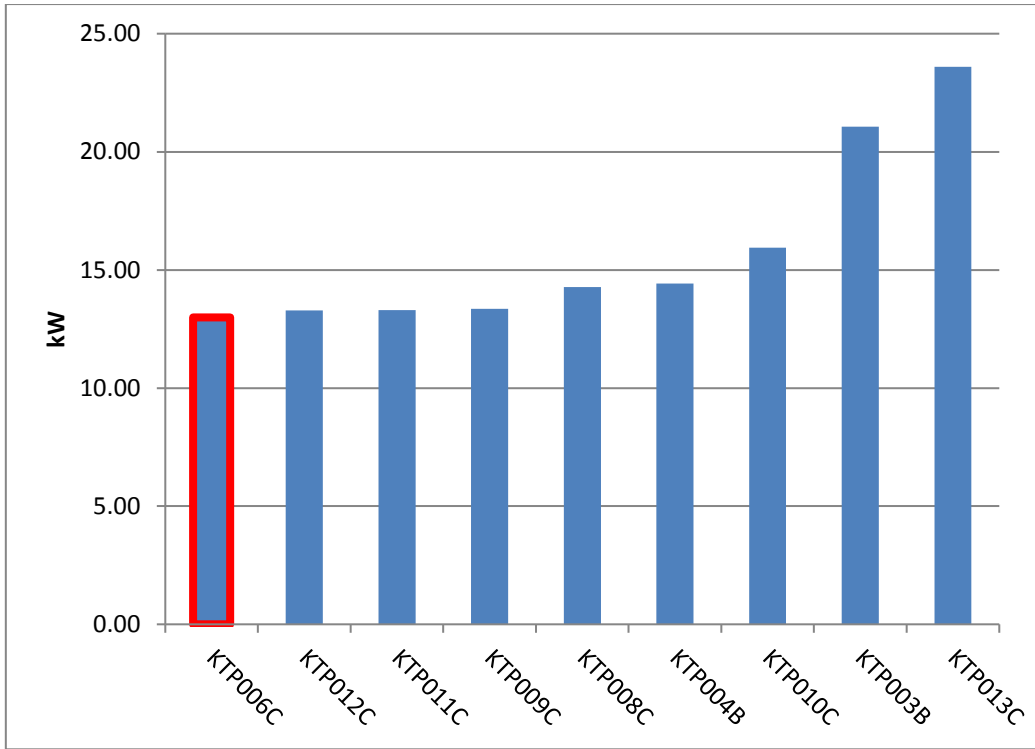
Figure 6.8 – Coil power values for tests arranged in ascending order
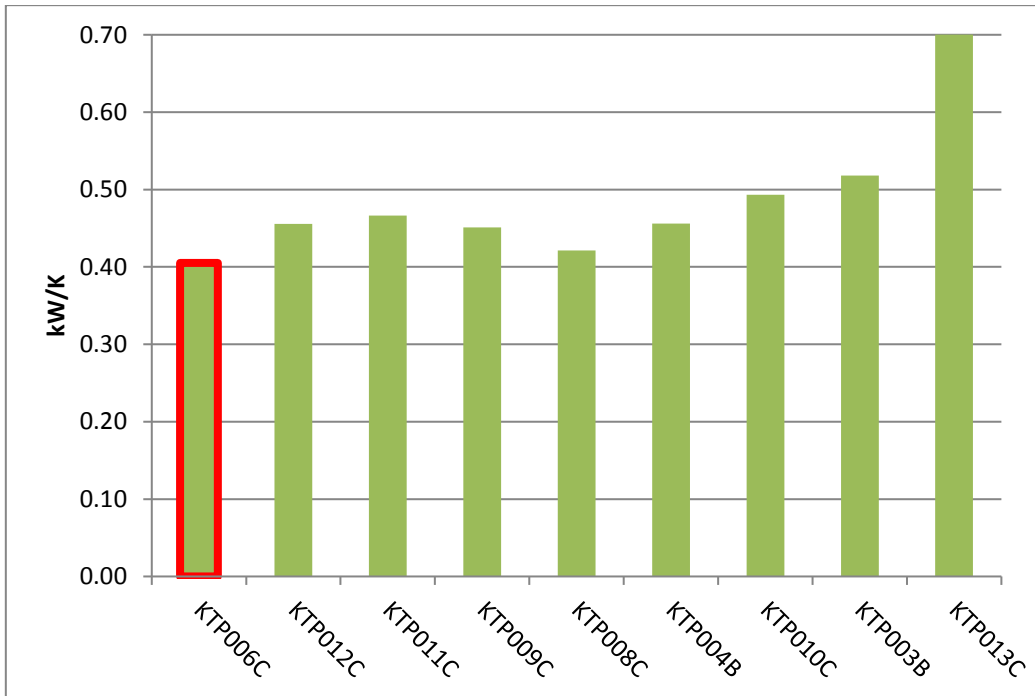
Figure 6.9 – Coil UA values calculated using LMTD method

When comparing figures 6.8 and 6.9 it is observed that the UA values obtained from the LMTD method do not follow the trend of the coil power values. Therefore, the LMTD method is considered unsuitable for calculating UA for this study.

Mid-coil method

The analysis below explores the suitability of using the mid-coil method for calculating UA for the parametric study. Table 6.2 shows the power output of the coils tested in the parametric study along with their corresponding UA values. The table is arranged in ascending order of coil power with the lowest output in the first row. The percentage increase in coil power from one coil to its subsequent coil in the row below is given. The percentage change for the UA values is also presented in the same manner.

Test Reference	Coil Power (kW)	UA Mid Coil Method (kW/K)	% Increase in Coil Power	% Increase in UA
KTP006C	12.99	0.4229	0.0%	0.0%
KTP012C	13.29	0.4524	2.3%	7.0%
KTP011C	13.30	0.4527	0.1%	0.1%
KTP009C	13.35	0.4340	0.4%	-4.1%
KTP008C	14.27	0.4695	6.9%	8.2%
KTP004B	14.42	0.4544	1.1%	-3.2%
KTP010C	15.94	0.5769	10.5%	26.9%
KTP003B	21.07	0.7724	32.2%	33.9%
KTP013C	23.60	0.8359	12.0%	8.2%

Table 6.2 – UA values obtained from the mid-coil method

The variation in UA values with the corresponding change in coil power values was more in agreement for the mid-coil method compared to the LMTD method. However, the UA values did not follow the trend of the coil power values when the difference in coil power was small as seen with the tests KTP009C, KTP011C and KTP004B, KTP008C.

Coil average method

The suitability of using the coil average method is analysed below. Table 6.3 gives the coil power and corresponding UA of the parametric tests. The results in table 6.3 are arranged in ascending order of coil power as in table 6.2. The percentage change in coil power and UA values are presented in the same way as in table 6.2. As with the previous methods, the trend in the variation of UA values calculated were compared against the trend in the variation of coil power values.

Test Reference	Coil Power (kW)	UA Coil Average Method (kW/K)	% Increase in Coil Power	% Increase in UA
KTP006C	12.99	0.3986	0.0%	0.0%
KTP012C	13.29	0.4544	2.3%	14.0%
KTP011C	13.30	0.4622	0.1%	1.7%
KTP009C	13.35	0.4438	0.4%	-4.0%
KTP008C	14.27	0.4547	6.9%	2.5%
KTP004B	14.42	0.4468	1.1%	-1.8%
KTP010C	15.94	0.5384	10.5%	20.5%
KTP003B	21.07	0.7224	32.2%	34.2%
KTP013C	23.60	0.7922	12.0%	9.7%

Table 6.3 – UA values obtained from the coil average method

The variation of UA values compared with the variation of the coil power is less in agreement for this method over the mid-coil method. Variation in UA values does not follow the variation in coil power values for the tests KTP004B, KTP008C and KTP009C. This is a similarity shared with the mid-coil method. The coil average method will not be used to obtain U values for comparing coil parameters.

Probe average method

The probe average method was used with the hope of capturing the probe readings that were more critical to the calculation of UA values and having the effect of the said probes represented in the final temperature value. Table 6.4 gives the coil power values in ascending order alongside the UA values calculated using probe average method. The percentage increase values are presented the same way as with the two previous methods.

Test Reference	Coil Power (kW)	UA Probe Average Method (kW/K)	% Increase in Coil Power	% Increase in UA
KTP006C	12.99	0.4121	0.0%	0.0%
KTP012C	13.29	0.4536	2.3%	10.1%
KTP011C	13.30	0.4601	0.1%	1.4%
KTP009C	13.35	0.4461	0.4%	-3.0%
KTP008C	14.27	0.4483	6.9%	0.5%
KTP004B	14.42	0.4598	1.1%	2.6%
KTP010C	15.94	0.5350	10.5%	16.4%
KTP003B	21.07	0.7454	32.2%	39.3%
KTP013C	23.60	0.7655	12.0%	2.7%

Table 6.4 – UA values obtained using the probe average method

For coil powers above 14.5kW and large coil heights and areas, the UA value variation with coil power variation was in better agreement for this method compared with the mid-coil method. A similar relationship is seen with the coil average method. This method offered an acceptable variation in UA values with variation in coil power for most tests. However, it was not able to satisfactorily mirror the variation in UA values with variation in coil power for the lower output coils.

Best fit method

The best fit method was used to overcome the shortcomings present in the previous methods. It was hoped that by selecting the probe that would give a result closer to the expected result regarding kW variation, would also lead to the selection of the probe most representative of the geometry of the coil.

Test Reference	Coil Power (kW)	UA Best Fit Method (kW/K)	% Increase in Coil Power	% Increase in UA
KTP006C	12.99	0.4359	0.0%	0.0%
KTP012C	13.29	0.4524	2.3%	3.8%
KTP011C	13.30	0.4527	0.1%	0.1%
KTP009C	13.35	0.4541	0.4%	0.3%
KTP008C	14.27	0.4695	6.9%	3.4%
KTP004B	14.42	0.4723	1.1%	0.6%
KTP010C	15.94	0.5387	10.5%	14.0%
KTP003B	21.07	0.7330	32.2%	36.1%
KTP013C	23.60	0.8359	12.0%	14.0%

Table 6.5 – UA values obtained using the best fit method

The variation in UA values obtained from the best fit method is in good agreement with their corresponding coil power values. The percentage change in coil power is closely matched by the percentage change in UA values. The U values obtained from this method are selected as the main set of values for comparing coil parameters.

Further analysis of the probes selected as the best fit probe show variations of one or two probe positon offsets from the mid coil probe. Table 6.6 gives the mid coil probe position and the probe selected as the best fit probe. It also shows the relative offset of the best fit probe with the mid coil probe.

Test Reference	Mid Coil Probe	Best Fit Probe	Relative Position of Best Fit with Mid-Coil
KTP003B	5	4	1 Probe Position Below
KTP004B	3	7	4 Probe Positions Above
KTP006C	4	6	2 Probe Positions Above
KTP008C	5	5	Same Probe
KTP009C	3	5	2 Probe Positions Above
KTP010C	5	4	1 Probe Position Below
KTP011C	3	3	Same Probe
KTP012C	3	3	Same Probe
KTP013C	5	5	Same Probe

Table 6.6 – Difference in position of mid-coil probe and best fit probe

When comparing the position of the best fit probe with the mid-coil probe the best fit probe was within the height of the limit of the coil or within 55mm of the top of the coil. The test KTP004B was the exception. A significant offset can be observed for KTP004B. Figure 6.10 shows the positon of the best fit probe in relation to the coil tested in KTP004B.
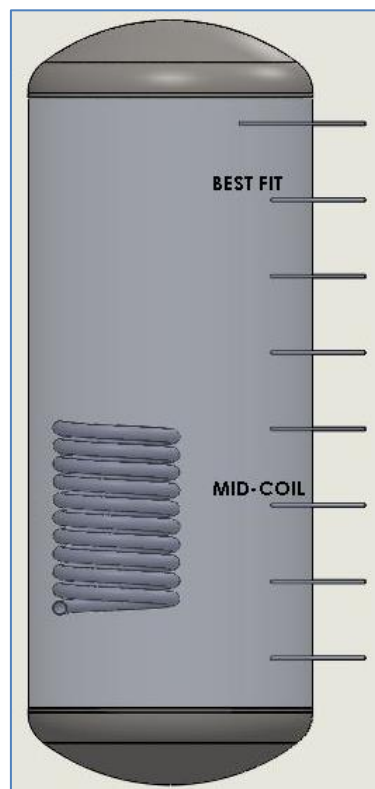

Figure 6.10 – Probe coil and probe positions for KTP004B

U Value Analysis

Once the UA values are calculated from the above method the overall heat transfer or U values can be calculated for a given coil. The U values are used to determine the effectiveness of a coil with regard to heat transfer. For analysis within this section the best fit method has been used as the method for calculating of U Values of the coil.

Effect of coil height on U values

Among the many parameters that can be modified on a helical coil, height is considered a key parameter. Table 6.7 below gives the U value variation for a variation in height. The area and diameter have been kept constant for the coils compared. It is hoped that the analysis below will offer some insight on how to best vary the coil height to obtain better U values and by extension better heat transfers for a given temperature range.

Test Reference	Dimensionless Area	Diameter Ratio (D_R)	Height Ratio (H_R)	U Values kW/m² K
KTP006C	1.00	0.36	0.39	1.354
KTP009C	1.11	0.33	0.31	1.270
KTP008C	1.11	0.33	0.55	1.313

Table 6.7 – U value comparison of a coil with D_R = 0.33 and varied height

A 3.5% increase in U value is observed for a 77% increase in height ratio. As seen in table 6.7 a coil which would occupy close to a third of the cylinder height would have a small increase in U Value when the its height occupied just over half the cylinder height.

The analysis was repeated for a coil with a higher diameter ratio. This was done to investigate if the changes seen in coil height variation were dependent on diameter and level of offset.

Test Reference	Dimensionless Area	Diameter Ratio (D_R)	Height Ratio (H_R)	U Values kW/m² K
KTP006C	1.00	0.36	0.39	1.354
KTP012C	1.11	0.52	0.24	1.269
KTP011C	1.11	0.52	0.31	1.270

Table 6.8 – U value comparison of a coil with D_R = 0.52 and varied height

The U value observed for a variation in height ratio of 29% was negligible.

Effect of coil diameter on U values

Diameter is another key parameter selection for coil heat exchangers. The investigation below will look at the impact diameter may have on the U values of a coil. In hot water cylinders, selection of coil diameter may be influenced by non-performance related factors such as position of immersed water supply tubes. Knowledge of the impact coil diameter has on U values would be useful when designing hot water cylinders with such constraints. The height of the coils compared has been kept constant and the variation in area has been kept to a minimum.

Test Reference	Dimensionless Area	Diameter Ratio (D_R)	Height Ratio (H_R)	U Values kW/m² K
KTP006C	1.00	0.36	0.39	1.354
KTP004B	1.21	0.40	0.24	1.211
KTP012C	1.11	0.52	0.24	1.269

Table 6.9 – U value comparison of a coil with H_R = 0.24 and varied diameter

An increase of 4.8% in U value can be seen for a 30% increase in diameter ratio.

A greater height ratio was selected and the analysis was repeated. This was carried out to see if the impact on U values due to changes in coil diameter are dependent on coil height.

Test Reference	Dimensionless Area	Diameter Ratio (D_R)	Height Ratio (H_R)	U Values kW/m² K
KTP006C	1.00	0.36	0.39	1.354
KTP008C	1.11	0.33	0.55	1.313
KTP010C	1.27	0.52	0.55	1.322

Table 6.10 – U value comparison of a coil with H_R = 0.55 and varied diameter

The increase in U value is negligible when the diameter ratio is increased by 58% for height ratios of 0.55.

Effect of coil pitch on U value

The parameter of coil pitch was analysed alongside corresponding U values. It was expected that the U value increase with increasing pitch up to an optimum value and then a reduction of U value occurs. This is based on the idea that with increase in pitch the boundary layers of individual coil turns would be less likely to combine while maintaining the benefit of induced flow past a given turn caused by the rising thermal plume below. It is believed that at some maximum value the effect of the rising thermal plume from coil turns below would become negligible. The variation in pitch is analysed using the value of separation ratio (S_R).

Figure 6.11 shows the U values of coils for different values of separation ratio. The chart is organised in ascending order for the value of separation ratio.
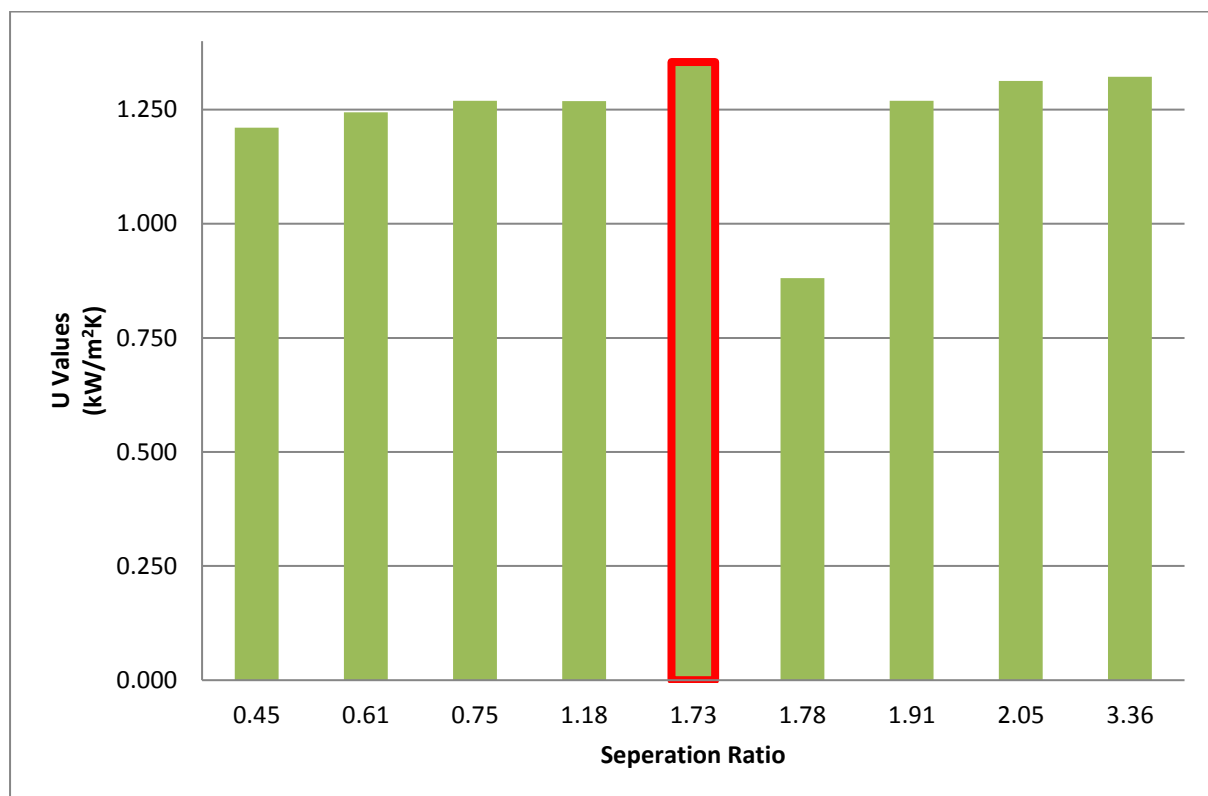

Figure 6.11 – Variation of U value with separation ratio

Apart from the anomaly seen at separation ratio 1.78, figure 6.11 tends to show a gradual increase of separation ratio up to S_R = 1.73 and then a gradual decrease. The increase and decrease is small.

Highest and lowest U values

The following section looks at the coils with the highest U values and those with the lowest. It is hoped that this analysis will provide some insight on the common characteristics that promote increases in U value as well as the factors that inhibit the increase. All U values in this section are determined using the best fit method outlined previously in the text. Table 6.11 gives the three highest U value coils in the parametric study arranged in ascending order of U value and table 6.12 gives the three lowest U values in in descending order.

Test Reference	Dimensionless Area	Diameter Ratio (D_R)	Height Ratio (H_R)	U Values kW/m² K	Separation Ratio (S_R)
KTP008C	1.11	0.33	0.55	1.313	2.05
KTP010C	1.27	0.52	0.55	1.322	3.36
KTP006C	1.00	0.36	0.39	1.354	1.73

Table 6.11 – Highest U values based on best fit method

A common factor observed with the three coils above is a relatively high separation ratio. Both the diameter ratio and height ratio for the highest U value coil appears to be very close proportions. D_R is 9% over a third and H_R is 18% over a third. In the broadest sense the highest U value coil occupies a little over a third of the cylinder height and occupies a slightly larger proportion of the cylinder diameter. Coil KTP006C has close to 38% of the cylinder height above its highest point. In comparison coil KTP008C and KTP010C have 22%. The relatively greater vertical obstruction seen in KTP008C and KTP010C has been compensated for by a larger separation ratio.

Test Reference	Dimensionless Area	Diameter Ratio (D_R)	Height Ratio (H_R)	U Values kW/m² K	Separation Ratio (S_R)
KTP013C	2.09	0.34	0.55	1.244	0.61
KTP004B	1.21	0.40	0.24	1.211	0.45
KTP003B	2.59	0.71	0.55	0.881	1.78

Table 6.12 – Lowest U values based on best fit method

The lowest U value coil KTP003B has a comparable separation ratio with the highest U value coil KTP006C. However, KTP003 has considerably less vertical spacing above the coil and horizontal spacing around the coil. Both KTP013C and KTP004B have very low separation ratios.

The visual comparison of the highest U value coils and lowest U value coils are respectively given below in figure 6.12 and figure 6.13.

KTP008C   KTP010C   KTP006C
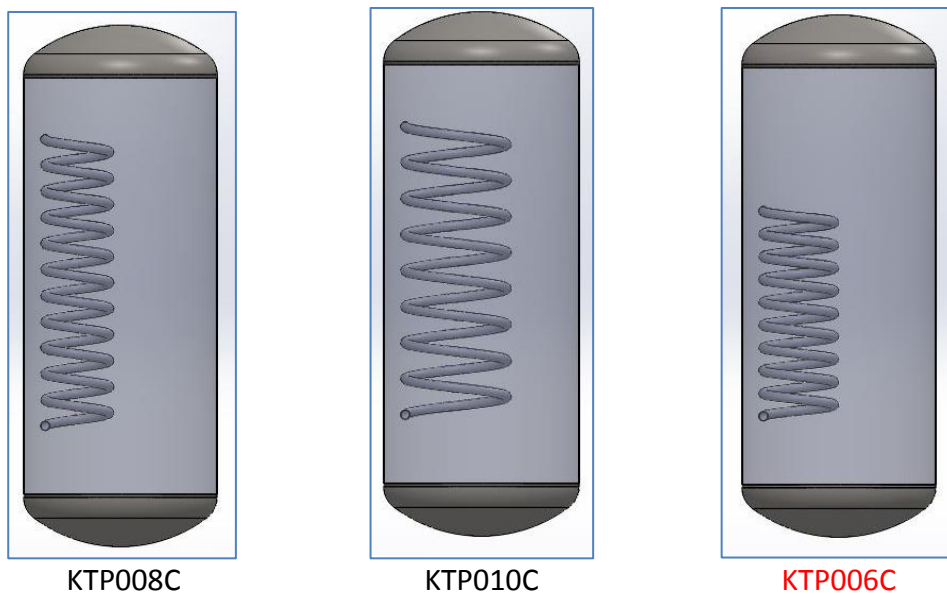
Figure 6.12 – Coil positions for highest U value coils

KTP013C   KTP004B   KTP003B
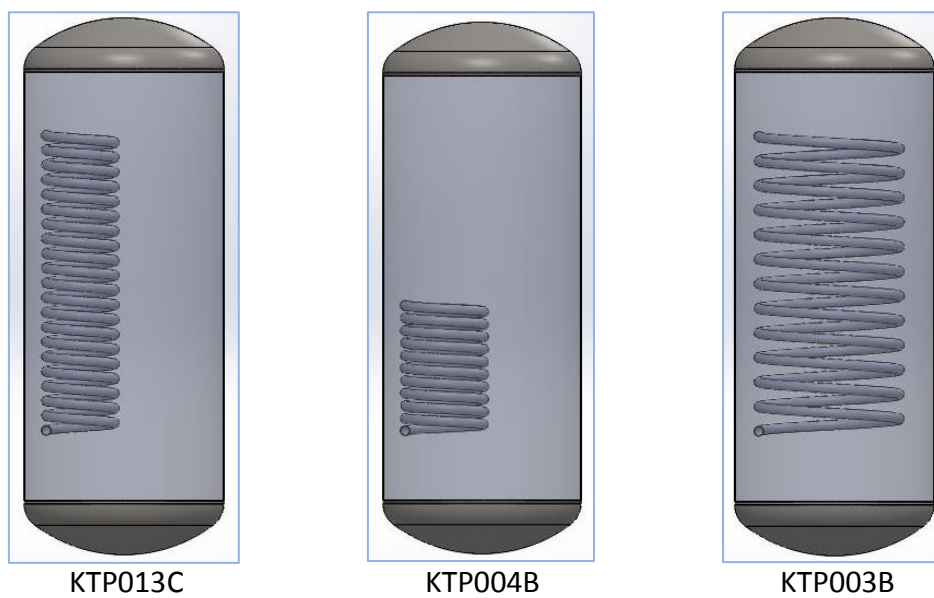
Figure 6.13 – Coil positions for lowest U value coils

Effect of enclosing the coil with a circular chimney

Ducts, baffles and chimneys are a few of the components utilised in practice to promote flow across heat exchangers. A test was carried out to determine the impact of enclosing the coil in a circular chimney on its overall performance. It was hoped that the chimney would increase the flow across the coil and promote an asymmetric convective current within the cylinder. The expected flow pattern is depicted in figure 6.14.
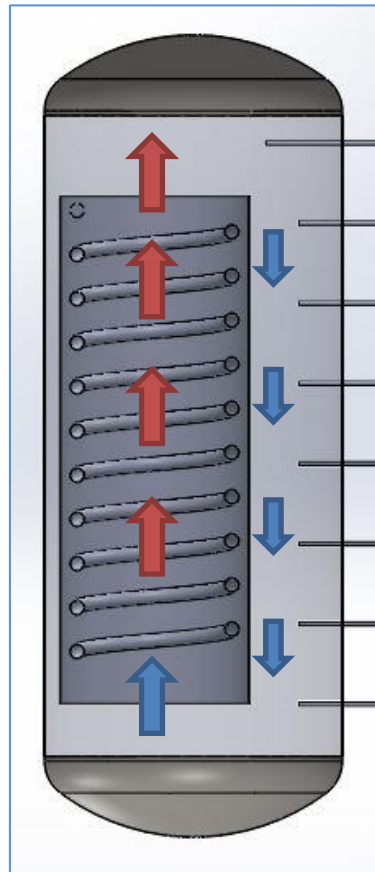
Figure 6.14 – Expected flow pattern with chimney and coil

Figure 6.15 shows the heat up and draw-off plot for the chimney encased coil. It was observed that the water at the bottom of the cylinder was increasing in temperature more rapidly when compared to the heat up plot of the coil without a chimney.
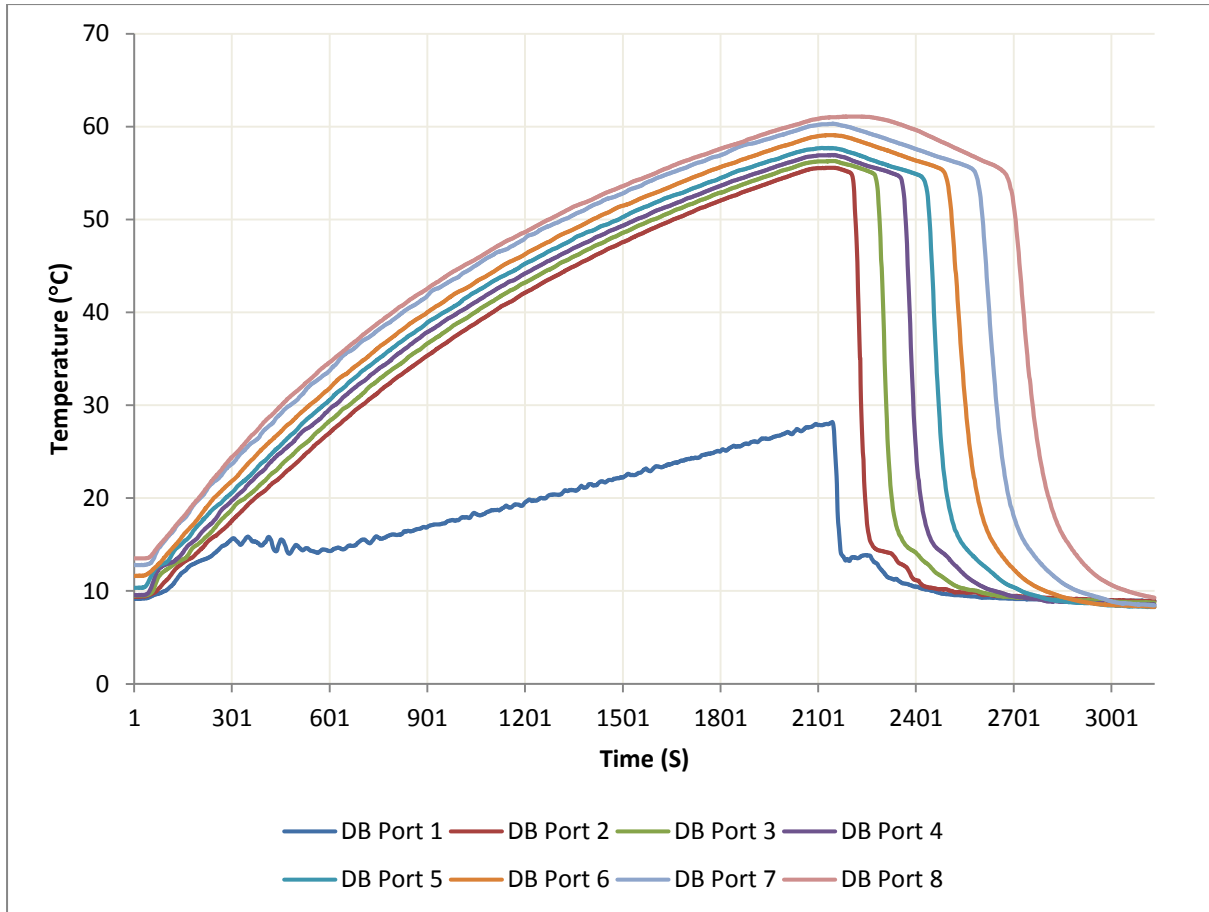
Figure 6.15 – Heat up and draw-off plot for chimney encased coil

The coil used for comparison of the effect of a chimney is from test KTP010C. Table 6.13 gives the performance data of both the coil with and without a chimney. KTP019B is the test with the chimney. As the chimney was placed between the side wall temperature probes and the coil and some mixing was expected, the probe average method was used to compare the results in U value.

Test Reference	Coil Power (kW)	U Values (kW/m²K)	Volume Drawn off over 40°C (l)	Time Taken to heat to 60°C (Decimal Minutes)
KTP006C	13.34	1.280	168.6	37.13
KTP010C	15.94	1.311	166.0	28.58
KTP019B	15.51	1.117	174.0	32.95

Table 6.13 – Performance comparison of coil with chimney

It can be observed that the coil power has reduced and heat up time has increased for the coil with chimney. The U value has also decreased for the coil with chimney.

An increase in the volume of water drawn off above 40°C is also observed. There was an increase in heat up time for the coil when enclosed in the chimney.

Effect of painting the coil surface to be a glossy black

The effect of painting the coil black was investigated as part of the special case testing. The surface of the coil was spray painted with a black gloss paint to achieve the desired black surface. It was expected that the U values would increase due to an increase in the coil surface emissivity when painted black. The black coil was compared with a shiny copper surface. The probe average method was used to obtain the U values for the above tests. This method was selected because it was hoped that a more uniform heating would also take place as the coil surface emissivity increased.

Table 6.14 gives the performance comparison of the black surface coil with the standard unpainted copper coil. The coil with the black surface is denoted by test KTP016A. A single test was considered sufficient as the coil painted was the same coil used in KTP010C and had been tested 3 times before. This would have cleaned the inside of the coil sufficiently.

Test Reference	Coil Power (kW)	U Values (kW/m²K)	Volume Drawn off over 40°C (l)	Time Taken to heat to 60°C (Decimal Minutes)	Average Coil Outlet Temp (°C)
KTP006C	13.34	1.280	168.6	37.13	69.47
KTP010C	15.94	1.311	166.0	28.58	64.67
KTP016A	12.39	0.868	167.1	41.10	68.48

Table 6.14 – Performance comparison of a coil with a black glossy surface

A reduction of 34% in U value was observed. The coil power had also reduced by 22%. The time taken to heat the cylinder contents from 15°C to 60°C was also observed with negligible increase in water drawn-off above 40°C along with an increase in time to heat when the black surfaced coil was used. The average return water temperature from the coil had increased by 5.5% for the test with the black surfaced coil.

Effect of adding a taper to the standard helical coil

The typical coils used in hot water cylinders currently on the market have a vertical helical geometry. This geometry is also the focus in academic study of coiled heat exchangers. A special test was carried out with a vertical helical coil with an added taper angle. It was assumed that a given turn in a standard type coil as tested in the parametric study would interfere with the heat transfer of its neighbouring coil turns. The adjacent coil turns above and below would also cause interference to the coil turn in question by way of boundary layer interactions. To avoid this, issue a taper angle was added to the standard geometry coil to create an unobstructed space above and below a coil turn.

At the larger end of the taper the coil diameter was 400mm and at the smaller end of the taper the coil diameter was 150mm. The Taper angle was approximately 18°C. Figure 6.16 depicts the coil as tested. The probe average method was used to obtain the U values due to the varying distance of coil turns to probes.
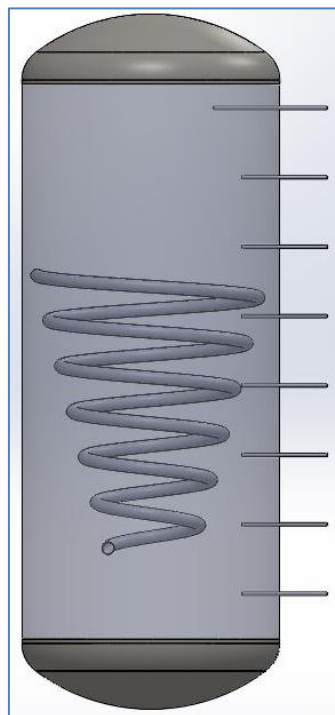
Figure 6.16 – Taper coil position in test cylinder

Table 6.15 gives the performance data of the tapered coil with comparison to straight helical coils of similar area. The test using the tapered coil is denoted by KTP007C.

Test Reference	Coil Diameter (mm)	Coil Height Ratio	Dimensionless Coil Area	Separation Ratio (S_R)	U Values (kW/m²K)
KTP006C	165	0.39	1.00	1.78	1.280
KTP007C	150 to 400	0.39	1.21	3.36	1.195
KTP004B	180	0.24	1.21	0.45	1.178
KTP010C	235	0.55	1.27	3.36	1.313

Table 6.15 – Performance data comparison of tapered coil with standard geometry coils

The tapered coil marginally outperformed the coil used in KTP004B on both coil power and U value with a U value increase of 1.4%.

The coil used in KTP010C has a 9.9% greater U value than the tapered coil. The two coils compared have the same separation ratio.

Comparison of Factors Associated with BS EN 12897:2006

It is useful to have a comparison between the coils tested under the parametric study and a commercially offered coil. The comparison is based on the performance factors used in the British standards. The performance factors under the standards are the values quoted to end users. Table 6.16 compares the commercial coil in KTP002B and the same coil in a commercial cylinder LTR000147T5 with the top three U value coils from the parametric study.

Test Reference	Dimensionless Area	Time (Decimal Minutes)	Volume Over 40°C (litres)	BS EN 12987 Coil Power (kW)	Adjusted Coil Power (kW)
KTP008C	1.11	31.28	165.00	15.49	13.94
KTP010C	1.27	28.58	166.00	17.06	13.47
KTP006C	1.00	37.13	168.60	13.34	13.34
KTP002B	2.09	31.25	205.90	18.89	9.03
LTR000147T5	2.09	32.28	182.10	18.14	8.67

Table 6.16 – Performance comparison of commercial coil with top three U value coils

The coils in the parametric study have comparatively greater coil power values adjusted for coil surface area. The largest difference observed is an increase of 54% from KTP002B to KTP008C. The highest unadjusted kW rating observed for the parametric study coils is for KTP010C with a value of 17.06kW. When comparing KTP002B with KTP010C a 39% reduction on material can be made with a 9.7% reduction in coil power. The reduction in draw-off volume of 19% is observed with a decrease in heat up time of 8.5%.

When comparing KTP010C to LTR000147T5 a commercial cylinder with the same sized coil as KTP002B. The material saving is 39% and the reduction in coil power for KTP010C is 6%. The commercial cylinder provides 9.7% more usable hot water and KTP010C takes 11.5% less time to heat up the contents of the cylinder.

Evaluation of total energy within cylinder over heat up time
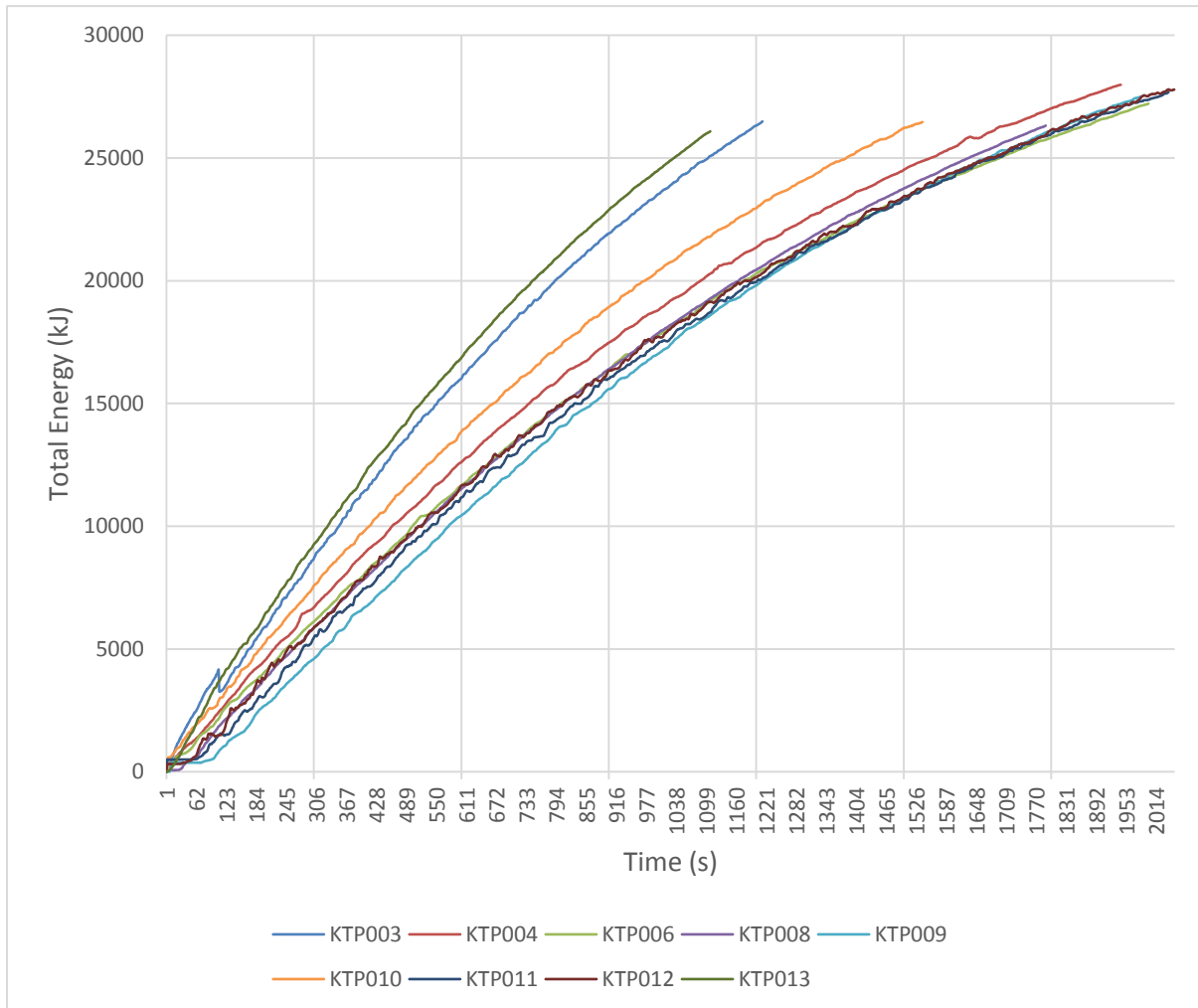
Figure 6.17 – Total energy within cylinder over heat up time for different coils

KTP003 and KTP013 output peak energy faster than other coils in the parametric study. This could be attributed to their larger surface areas. Apart from KTP008, coils that take longer to reach peak energy also have a higher total energy. This could be due to a larger proportion of the cylinder reaching the higher temperatures within the heat up temperature range. This would also suggest that large surface area coils may not be ideal where more usable hot water is a requirement.

KTP010 shows a good compromise between delivering a larger quantity of usable hot water and the time taken to deliver the energy. KTP010 also has a comparatively low surface area.

Evaluation of available hot water above 40°C

Hot water delivery is the ultimate objective of a hot water storage tank. It is useful to understand how the hot water delivery capability would be affected when cylinder size changes. The extremes in this evaluation would be instantaneous water heating and very large storage tanks. Varying the tank size could be compared to varying the size of the heat exchanger in relation to the storage volume if a given size of heat exchanger was to be kept constant. In table 6.17 below, the volume drawn off for two different coil sizes are given. The ratio of storage volume which is a constant 180 litres to coil surface area has reduced by 52% from KTP013C to KTP006C. This would be similar to reducing the storage volume by 52% based on the above approach. The coil geometry is not taken into consideration in the evaluation below.

Test Coil	Dimensionless Area	Heat up time (hours)	Volume drawn off over 40°C (l)	Hot water volume draw off after 1 hour of heating (l)
KTP006C	1.00	0.62	168.60	272.4
KTP013C	2.09	0.31	158.50	506.7

Table 6.17 – Available hot water after 1 hour of heating

KTP006C takes twice as long to reach the target cylinder temperature. However, it does deliver 6.4% more hot water during a single heating and draw off cycle. If the results were evaluated for a hypothetical one hour heating period, KTP013C has the potential to deliver 86% more hot water above 40°C.

When considering only full heating cycles, KTP006C could run a single heating cycle and KTP013C could run two full heating cycles in 0.62 hours. In the time it takes KTP006C to complete one heating cycle, KTP013C can deliver 88% more hot water above 40°C.

The results above looked at the nature of heat up and draw off of a hot water cylinder and highlighted some key characteristic that could prove useful to designers of hot water cylinders for both standard domestic boiler applications and renewable energy applications.

The parametric study undertaken provided some insight on how the effectiveness of a coil would vary given changes in height, diameter and pitch.

Special cases were also investigated. These included the use of a chimney enclosure for the coil to increase recirculation in the cylinder, painting the coil black to increase surface emissivity and adding a taper angle on the coil to reduce vertical obstruction due to coil turns.

The best performing coils in the parametric study were also compared against the current commercial offerings. Most of the analyses were carried out with comparisons of coil U values. However, the commercial aspect of hot water cylinders was also considered and comparisons of the factors directly relevant to the British standards and by extension the end user were investigated.

The novel approach applied to this study was making the coils offset within the cylinder. The level of offset would vary based on the coil diameter but would also be kept at the maximum possible for the geometry. Based on the insights gained above, a high recovery i.e. faster heat up time cylinder design using less coil material was proposed to the host organisation Kingspan Environmental limited. The design is under review for possible commercialisation on larger volume cylinders in the range of 400 and 500 litres.

Conclusions

1. For a diameter ratio of 0.33 the increase in U value is 3.5% when the height ratio is increased by 77%. For lower diameter ratios (<0.4) a marginal improvement in U value is seen for a significant increase in height ratio.

2. For a diameter ratio of 0.52 the increase in U value is negligible (<0.8%) for an increase in height ratio of 29%. For higher diameter ratios (>0.4) virtually no improvement in U value is seen with increase in height ratio

3. For a height ratio of 0.24 the increase in U value is 4.8% for an increase in diameter ratio of 30%. This is the largest U value increase observed. For smaller height ratios (<0.4) an increase in diameter ratio shows an improvement in U values.

4. For a height ratio of 0.55 the increase in U value is negligible (<0.7%) for an increase in diameter ratio of 30%. For greater height ratios (>0.4) an increase in diameter ratio does not improve U values.

5. All improvements in U values are very modest (<5%)

6. The highest U value was observed for a separation ratio of 1.73. Larger separation ratios promote improvement in U value.

7. The second and third lowest U value coils have separation ratios of 0.45 and 0.61 respectively. Very low separation ratios (<1.00) are detrimental to improvements in U value

8. Large diameter ratios combined with high coil surface areas tend to give anomalous results for the calculation methods used

9. The highest U value coil has a height ratio of 0.39 and a diameter ratio of 0.36. When the coil occupies close to 35% of both the vertical and horizontal span of the cylinder, improvements in U value are observed.

10. The lowest U value coil has a height ratio of 0.55 and a diameter ratio of 0.71. Very Large diameter ratios (>0.7) are detrimental to improvements in U value.

11. The highest U value coil has a dimensionless area of 1.00 and coil power of 12.99kW. The lowest U value coil has a dimensionless area of 2.59 and a coil power of 21.09kW. Oversizing the coil area to the cylinder size is detrimental to the coil U value.

12. The top three U value coils from the parametric study have significantly higher coil power outputs adjusted for area when compared with the commercial coil offering

13. The commercial coil offering delivers more usable hot water when compared with the top three U value coils from the parametric study

14. Excluding KTP006C the top performing coils in the parametric study can heat the contents of the cylinder in comparable times or faster than the commercial coil offering.

15. Adding a chimney to the coil increased the water temperature at the bottom of the cylinder and more useful hot water was drawn-off. The chimney is increasing circulation within the cylinder and reducing stratification.

16. Painting the coil surface black significantly reduced the performance of the coil. A performance improvement was expected. The paint layer on the coil acts like an insulator and inhibits conductive heat transfer.

17. On a standard helical coil the obstruction of coil turns above one another does not have as significant impact on U value compared to the obstruction around the coil.

18. Coils with a combination of larger (>0.4) height ratio and diameter ratio do not heat the cylinder as evenly as the other coils

19. A very clear thermocline can be observed below the coils when a chimney is not used. This would mean the recirculation within the cylinder is low.

20. Piston behaviour is observed during hot water draw-off. Little to no mixing occurs when the diffuser is used

21. The LMTD method for calculating UA values deviates considerably from the trend of coil power variation for corresponding coils. Counter flow heat exchanger theory cannot be used in hot water cylinders as the buoyancy flow within the cylinder is not strong enough in all coils.

22. A significant difference in U value and power can be observed for a coil between its first and second test. This difference is much lower from the second to the third test. A heat inhibiting material is coating the inside walls of the coil during production and is getting cleaned during the first and second tests.

23. Excluding the best fit method, all methods for calculating UA could not match the variation in coil power satisfactorily. The thermal plume from the different coils registered differently on the side wall probes. Therefore, the different methods for calculating UA would be suitable for some coils but unsuitable for others.

Discussion

Overall Effects of Coil Parameters

As the height ratio of the cylinder is reduced for higher diameter ratios, the thermocline may be moved to a lower point in the cylinder as well. This is because an increase in water drawn off at 40°C is observed for a comparatively lower height ratio coil. This could be due to a greater concentration of heating further towards the bottom of the cylinder. A lower height ratio could be the preferred option for a cylinder which needs to supply a greater volume of hot water or have a larger solar fraction.

A related observation is that for larger diameter ratios the height of the coil affects the proportion of the cylinder brought to target temperature. The temperature distribution for a shorter coil is more uniform along the height of the cylinder above the thermocline. For taller coils a more visible temperature gradient is observed. This could be due to the power output being more spread out within the cylinder. A cylinder with a comparatively large height ratio could be compared to a cylinder with two smaller coils. Figure 8.1 illustrates the idea.
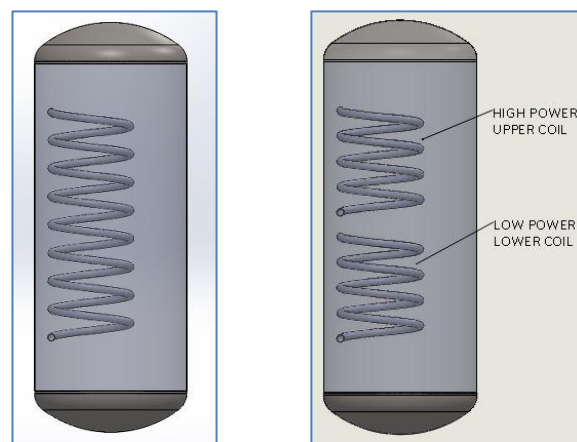
Figure 8.1 – Twin coil analogy of a single coil

The upper coil would most likely have a higher power output compared to the lower coil as it has a higher flow temperature. As the thermal plume tends to move upwards, the upper part of the cylinder would benefit from both top and bottom coils. The lower part of the cylinder may only benefit from the effects of the lower coil leading to uneven heating and an uneven temperature distribution. In a domestic setting the uneven heating can have an impact on the end users experience. In most cases the hot water is blended with cold water using a thermostatic mixing valve. If the temperature of the hot water drops and the response time

for the thermostatic mixing valve is low, the user would see a drop in temperature at the outlet.

All the coils tested under the parametric test were not capable of raising the temperature of the cylinder at the very bottom. No significant re-circulation is observed for all the coils. This could be attributed to the nature of the thermal plume arising from the coil. It is the author's opinion that the strongest thermal plume would arise from the top turn of the coil as the temperature is highest at that point. The coil is positioned offset to the central axis of the cylinder to promote a recirculation condition as indicated in figure 6.15. However, the arising thermal plume might be drifting away from the coil and interfering with the colder fluid travelling downwards. This type of movement was observed in the work done by Devore et al using an express elevator design central coil with a chimney enclosure (Devore et al., 2013).The movement discussed could interrupt the re-circulation and promote stratification and formation of a thermocline. As observed in the particle image velocimetry work carried out by Kuehner et al the thermal plume tends to drift and have vortices attach to it. The coil offset could further contribute to the drift in the plume away from the coil as a horizontal obstruction of the cylinder wall is present on one side.

Effect of Coil Parameters on Performance

For smaller diameter ratios, an increase in the height ratios gives a slight increase in U value. This increase in U value could be attributed to the reduced chance of the thermal boundary layers of the individual coil turns combining or influencing adjacent coil turns. This increase is not present for coils with larger diameter ratios. This may be due to the selected height ratio variation not being significant enough to impact local heat transfer sufficiently. A common theme observed in both cases is the relative space allowed for the free movement of the thermal plume. In the case of the smaller diameter ratios the free space around the central axis is lower. When the height ratio is increased the spacing between the coil turns also increases giving the thermal plume more freedom of movement. For a larger diameter ratio, the coil starts out with a larger space for the thermal plume to move into as the radius of a turn is now larger. Therefore, when the height is also increased and the coil turn spacing increases, due to possibility that the thermal plume initially had more freedom of movement, the added increase in freedom to move could have a less impact and be less noticeable.

The gains in U value are small for an increase in the height of the coil. The effect of coil height variation diminishes with an increase in diameter ratio. When designing hot water cylinders, coil height has a significant impact on the installation of the cylinder as primary pipework must be connected to the coil. The above results may be helpful for the hot water cylinder designer when deciding about the coil height used for a given cylinder.

A slight increase in U value is observed for coils with smaller height ratios when the diameter ratio is increased. There is virtually no improvement in U value when the diameter ratio is increased for larger height ratios. This result further supports the above assumption that if a coil starts out with a relatively high space for the movement of the thermal plume then a further increase in space does not result in higher U values.

This however does not mean that making the coil as tall and as wide as possible is the best course of action for increasing the U values. As observed the coil with the combination of largest diameter ratio and height ratio also has the lowest U value. This could be due to the obstruction caused on the thermal plume by the body of the cylinder itself. The optimum value for height ratio and diameter ratio for this study is 0.39 and 0.36 respectively. The reason for this being an optimum value could be that it is the point at which the cylinder geometry allows for higher thermal plume movement without entering the region where the cylinder shell starts impacting the plume.

The comparably low U values seen for the coil in KTP003B may be due to the above-mentioned factor of the combination of large diameter ratio and height ratio which could be further exacerbated by the its large dimensionless area 2.59. Coil KTP003B may be oversized for the test cylinder both in terms of geometry and surface area.

Comparing KTP013C from table 6.12 with KTP008C from table 6.11, it is observed that the height ratios are the same for both coils and the diameter ratios are very similar. However, the separation ratio is significantly low on KTP013C and it also has a large area in comparison. This indicates that a beneficial diameter ratio and height ratio may be inhibited by not providing sufficient spacing between the turns of the coil and by over-sizing the coil area in relation to the volume of the cylinder.

UA Calculation Methods

Further investigation into the results of the UA value calculation methods have raised a question as to why the variation of the UA values for the different calculation methods couldn't satisfactorily follow the variation for its corresponding coil power. It is the author's opinion that the reason for this when the UA values were calculated by the LMTD method may be due to the coil not acting like a counter flow heat exchanger as previously assumed. The buoyancy driven flow within the cylinder may not have been strong enough to consider a counter flow condition as expected.

The variation in the mid-coil method could be due to a single point measurement of the cylinder temperature not being representative enough for relatively small changes in coil power. Another possibility could be that the effect of the thermal plume originating from the coil is small on the mid-coil probe compared to its effect on another side wall probe such as the best fit probe.

The reason for this shortcoming for the probe average method may be due to the number of measurement probes critical to the calculation of UA values being small compared to the number of probes less directly affected by the heat transfer from the coil. In such a situation, the values from the less critical probes may minimise the prominence of the values from the more critical probes when the average is taken.

The offset of the best fit probe with the mid coil probe was largest for KTP004B with an increase of 4 probe positions above the mid coil probe. The height ratio of 0.24 for the coil used in KTP004B is the smallest observed for all the tests. The diameter ratio of 0.4 for KTP004B is the lowest observed for the D_R of 0.24. This significant offset combined with the low coil height could be facilitating a thermal plume which remains offset while rising through the cylinder and then gradually moving laterally away from the coil and approaching closer to the probes. A vortex effect may also be occurring as observed in the study conducted by Kuehner et al (Kuehner et al., 2012).

This could mean that different probes need to be used to calculate the cylinder temperature depending on the coil geometry. For an example a taller coil with smaller diameter could register its heat input differently on the central probe to a shorter coil with a larger diameter. The level of coil offset from the central axis of the cylinder may also have an impact on which

probe would best detect the heat transferred from the coil. This would be directly related to coil diameter. The nature of the thermal plume arising from the different geometries of coil may be the reason for this.

Variation of U Values between the First Three Tests for a Given Coil

The variation in the U values of the first second and third tests for a given coil could be due to a releasing agent or such other substance from the coil fabrication process being deposited on the inner wall of the coil and forming a layer within the coil. This layer may influence the boundary layer within the coil or act like a weak insulator. The flow within the coil during the first test may reduce a significant amount of the layer and subsequent tests may continue this reduction until the effect of the deposited layer is negligible or non-existent.

Comparison of a Commercial Cylinder to the Test Cylinder

When comparing the commercial cylinder with the test cylinder the results for the heating section of the test are very similar. It is the author's opinion that the results from this study will be representative of a commercial cylinder as the most of the analyses are focused primarily on the heating process. The difference seen in draw-off may be attributed to some unexpected mixing occurring during the draw-off process. Another strong possibility is that the type of coil used is heating up the shells of the cylinders more as it is almost at the bottom of the cylinder and very close to the bottom spinning. The test cylinder has a greater thermal mass than the commercial cylinder and a small amount of the energy output may be stored in the shell of the cylinder and delivered back to the cold water hence a greater volume of drawn-off water at a lower temperature is observed.

Effect of Enclosing Coil with Chimney

A greater increase in the temperature at the lowest probe of the cylinder was observed for the coil with the chimney enclosure. The reason for this could be due to increased mixing at the bottom of the cylinder. It is possible that a convective current is drawing the water up from the bottom of the cylinder past the coil and replacing the water at the bottom of the cylinder with warmer water from the adjacent area above. It is also observed that a very clear thermal gradient is present within the cylinder during heating.

The thermal gradient observed across the remaining probes could be due to a portion of the warmer water being pushed downwards by a convective current and gradually cooling down while it transfers heat to the volume of water outside the chimney.

The increase in the volume of water drawn off above 40°C may be caused by increased mixing by a convective current. In the author's opinion, the lower U values observed may have been caused by the added restriction to the thermal plume from the chimney.

Effect of Painting the Coil Surface Gloss Black

A significant reduction in U value was observed for the coil with its surface painted black. It is thought that the significant reduction in U values could be attributed to the paint layer acting like an insulator on the coil. This can be further confirmed from the higher outlet water temperatures observed.

Effect of Adding a Taper Angle to the Coil

When compared with a KTP004B the tapered coil was marginally better. This could be attributed to a greater spacing in-between the coil turns and the comparatively lower vertical obstruction between the coil turns.

However, the tapered coil had a lower U value when compared with KTP010C. The two coils have the same separation ratio. However, the larger turns on the taper coil having comparatively large diameter ratios in the region of 0.88. This may introduce more horizontal obstruction and have a detrimental impact on the heat transfer. This could mean that overall spacing around the coil may be more important to improving heat transfer compared to spacing around individual coil turns.

When considering a hot water cylinder, householders have a few main requirements. One of the requirements is that the contents of the cylinder can be heated up as quickly as possible. Another requirement is that the chosen cylinder has no interruption in hot water delivery i.e. it can provide enough hot water during the high use periods such as mornings and evenings. It is also important that the cylinder is economical to run as well as it costs less to buy.

Even though the relative increase U values are small across the tests it can provide some insight as to the direction to choose when designing hot water cylinders. Based on the three main requirements of the end user a better hot water cylinder could be developed by applying

the insights gained through this study. Larger height ratios combined with large diameter ratios can be avoided in order to provide more usable hot water and a more uniform temperature within the cylinder. Material can be used more efficiently in manufacture by designing closer to the optimum parameters of height and diameter thus reducing cost of manufacture and cost to end user. Heat up time can also be improved upon by optimising the U values for a given surface area of the coil.

Impact of coil surface area to tank storage volume ratio on hot water draw off volume

As observed in Table 6.17, when the coil surface area to tank storage capacity is increased by 52% it is possible to deliver up to 88% more hot water volume over 40°C. KTP006C can be viewed as the analogy to a large cylinder compared to KTP013C being a smaller cylinder. If the coil surface to storage tank volume ratio was to be kept the same in each case, the large cylinder under investigation would have to be 376.2 litres which is 2.09 times the size of the test cylinder. It could be assumed that the heat up time for the large cylinder would stay the same as coil surface area has also been increased. However, it can be assumed the draw off volume increases by 2.09 times giving the large cylinder a draw off volume of 352.4 litres. If the small cylinder was run for two cycles while the large cylinder runs one cycle, the small cylinder would be able to deliver 317 litres, 10% less than the larger cylinder.

If faster heat up was not a concern and maximising hot water draw off volume was the objective, it would be better to have a larger storage volume tank for a given heat exchanger size. This would be more beneficial for systems with solar collectors as maximising on storage would be the most beneficial scenario. If heat up times faster than large cylinders coupled with similar draw off volumes to large cylinders is the objective, then using two small cylinders would be beneficial. This would allow for 50% reduction in heat up time and would provide 90% of the draw off volume of a larger cylinder.

Parametric Study Coil Comparison with Commercial Coil

While the benefit from the parameter changes in the parametric study was modest, the offset coil has significant improvements over the current commercial coil offering when measured against the British standard BS EN 12897:2006. For a significant reduction in material (39%) the coil used in KTP010C had a comparatively lesser reduction (9.7%) in volume of hot water drawn-off and an even lesser reduction in coil power (6%) when compared with the commercial coil offering. The coil used in KTP010C was also capable of heating the contents of the cylinder 11.5% faster than the commercial coil. The offset coil KTP010C had an improvement of 35.6% on coil power adjusted for area when compared with the commercial coil. Figure 8.2 shows the difference between the offset coil in KTP010C and the commercial coil.
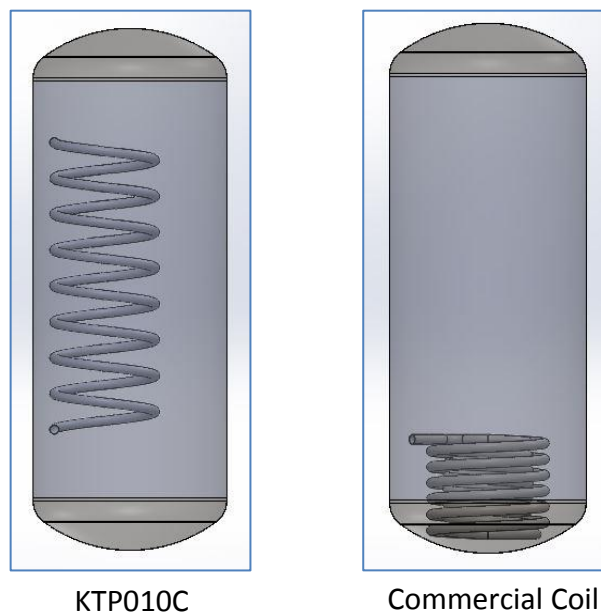

KTP010C   Commercial Coil

Figure 8.2 – Comparison of commercial coil to KTP010C

As it can be observed from figure 8.2, the commercial coil is placed concentric to the cylinder body axis. This may discourage the recirculation within the cylinder. In comparison, the offset coil which is a novel approach to heating in hot water cylinders shows signs of creating recirculation which may be the reason for it significantly higher coil power values when adjusted for area.

The commercial coil is also placed at the lowest possible point in the cylinder. This combined with its higher surface area could be attributed to the higher volume of usable hot water

obtained when using the commercial coil. There may be a possibility to increase the draw-off volume obtained from the offset coil by lowering its position in the cylinder. However, it would need to be carefully examined to not impact the benefit of its faster heat up time which is another important factor for end users.

Furthermore, the difference in performance may also be attributed to the very tight packing of tubes in the commercial coil compared to KTP010C. The commercial coil has a two-pass design where the heating fluid travels downwards on the outer helix and back up through the inner helix and out of the coil outlet. This may cause a leeching of energy out of the cylinder from the inner helix.

There may be significant scope for improving heat up efficiency of current hot water cylinders based on the above, especially if the convective recirculation current can be enhanced.

Future Work

During the work carried out in this study some opportunities for future work have been identified. The first possibility is to carry out the parametric test matrix with the coil flow and return connections reversed. By connecting the hot water flow to the bottom of the coil it is expected that the plume from the lower turns of the coil will create a stronger flow across the upper turns and create an induced forced convection. It is assumed that this flow will increase the U values of the coils significantly.

The parametric test matrix in the study was selected in a way to best represent a wide range of coil diameters, heights and coil turn spacing. To improve on this a more limited range of coil dimeters and heights could be selected. The reason for selecting a more limited range is to increase the resolution of changes from one coil to another.

The two main coil parameters that can be changed are diameter and height. Using these two factors and three pre-specified levels from this study a two factor, three level set of experiments can be conducted. A Taguchi L9 orthogonal array can be selected for this. The reason for conducting the tests is to investigate if any interactions may exist among the factors of coil diameter and height. If interactions do exist, then the relative strength of the interactions can be determined as well.

To further optimise the coil a Taguchi L25 orthogonal array can be selected and 5 levels can be applied to diameter and height. It would be useful to carry out a signal to noise ratio analysis as well.

For future testing, it would be best to replace the k type thermocouples with RTD temperature probes. It would also be good to replace the Picolog TC-08 data loggers with the Signatrol data loggers. This is to obtain a smaller possible error for the measurements.

The parametric test matrix can be re-run with some rig modifications as well. The side wall temperature probes could be made adjustable to maintain a standard distance from the coil as opposed to the existing method of maintaining a set distance from the cylinder wall. The temperature at the centre of the coil along the height could also be recorded.

Particle image velocimetry on the coil in KTP004B could be run to investigate why the best fit probe for its results was considerably higher than its mid-coil probe.

The impact of coil inlet temperature and flow rate could also be investigated. For a given coil inlet flow rate the inlet temperature can be varied for a few coils of different diameter ratio and height ratio combinations. The test can be repeated with varied flow rates for a given inlet temperature. The suggested temperature range is 78°C to 84°C and temperature interval is 0.25°C. The suggested flow rate range is 12 litres/min to 17 litres/min with an interval of 0.25 litres/min.

It would be useful to carry out repeated tests on a given coil to see the total variation in the power output. A minimum number of 8 tests are suggested. Apart from total variation an analysis could be carried out on the variation of the first test with the average of the last 3 tests and the variation of the second test with the average of the last three tests. A statistical analysis could also be carried out on a given coil and the tests could be repeated for a few different coils and the statistical analysis be extended.

References

AB BUILDING PRODUCTS. 2017. *Closed-Cell Versus Open-Cell Polyurethane Spray Foam* [Online]. Available: https://www.abbuildingproducts.co.uk/closed-cell-versus-open-cell-pa-3845.php [Accessed 26/01/2017].

ALTUNTOP, N., ARSLAN, M., OZCEYHAN, V. & KANOGLU, M. 2005. Effect of obstacles on thermal stratification in hot water storage tanks. *Applied Thermal Engineering,* 25**,** 2285-2298.

AMARA, S., BENYOUCEF, B., NORDELL, B., TOUZI, A. & BENMOUSSAT, A. 2003. EXPERIMENTAL STUDY OF A DOMESTIC HOT WATER STORAGE TANK THERMAL BEHAVIOUR. *Unité de Recherche en Energies Renouvelables en Milieu Saharien,* 3**,** 25-32.

ARCON SUNMARK. 2017. *Solar Collector Type HT-HEATboost* [Online]. Available: http://arcon-sunmark.com/products/collector-ht-heat-boost [Accessed 10.01.2017].

ARMSTRONG, P. M., UAPIPATANAKUL, M., THOMPSON, I., AGER, D. & MCCULLOCH, M. 2014. Thermal and sanitary performance of domestic hot water cylinders: Conflicting requirements. *Applied Energy,* 131**,** 171-179.

ATMANE, M. A., CHAN, V. S. S. & MURRAY, D. B. 2003. Natural convection around a horizontal heated cylinder: The effects of vertical confinement. *International Journal of Heat and Mass Transfer,* 46**,** 3661-3672.

AVIV, A., BLYAKHMAN, Y., BEERI, O., ZISKIND, G. & LETAN, R. 2009. Experimental and Numerical Study of Mixing in a Hot-Water Storage Tank. *Journal of Solar Energy Engineering,* 131**,** 011011-011011-8.

AXCELL, B. 1993. *A Water Heating Tank*.

BAEK, S. M., NAM, J. H., HONG, H. & KIM, C.-J. 2011. Effect of brine flow rate on the performance of a spiral-jacketed thermal storage tank used for SDHW systems: A computational fluid dynamics study. *Applied Thermal Engineering,* 31**,** 2716-2725.

BASF CHEMICALS. 2014. *Elastopor® H – Rigid Foam Systems* [Online]. Available: http://www.polyurethanes.basf.com/pu/solutions/en_GB/content/productbrand/elastopor [Accessed 26/01/2017].

BASF CHEMICALS. No Date. BASF Polyurethanes (PU) Rigid Foam.

BAXI 2016. Platinum and Duo-tec combis and Megaflo system boilers.

BERGER, S. A., TALBOT, L. & YAO, L. S. 1983. FLOW IN CURVED PIPES. *Annual Review of Fluid Mechanics,* 15**,** 461-512.

BERGMAN, T. L., INCROPERA, F. P., DEWITT, D. P. & LAVINE, A. S. 2011. *Fundamentals of heat and mass transfer*, John Wiley & Sons.

BIOENERGY TECHNOLOGY LTD. No Date. *How does a biomass boiler work?* [Online]. Available: http://www.bioenergy.org/information/how-does-a-biomass-boiler-work/ [Accessed 09/01/2016].

BRITISH PETROLEUM 2015. BP Statistical Review of World Energy 2015. BP.

BRITISH STANDARDS INSTITUTE 1989. BS 7074-1:1989 Application, selection and installation of expansion vessels and ancillary equipment for sealed water systems. Code of practice for domestic heating and hot water supply.

BRITISH STANDARDS INSTITUTE 2002. BS 1566-1:2002+A1:2011 Copper indirect cylinders for domestic purposes. *Part 1: Open vented copper cylinders - Requirements and test methods.*

BRITISH STANDARDS INSTITUTE 2006. BS EN 12897:2006 Water supply - Specification for indirectly heated unvented (closed) storage water heaters.

BRITISH STANDARDS INSTITUTE 2016. BS EN 12897:2016 Water supply - Specification for indirectly heated unvented (closed) storage water heaters.

CALEFFI S.P.A. 2013. Expansion Vessels.

CENTRE FOR ALTERNATIVE TECHNOLOGY. No Date. *Can I use solar PV panels to heat water?* [Online]. Available: http://info.cat.org.uk/questions/pv/can-i-use-solar-pv-panels-heat-water/ [Accessed 09.01.2017].

CENTRE FOR CLIMATE AND ENERGY SOLUTIONS. 2015. *Historical Global CO2 Emissions* [Online]. Available: https://www.c2es.org/facts-figures/international-emissions/historical [Accessed 23/01/2016].

CHAUVET, L. P., NEVRALA, D. J. & PROBERT, S. D. 1993a. Heat-transfer correlations for an immersed finned heat-exchanger coil transferring heat from a hot-water store. *Applied Energy,* 44**,** 283-314.

CHAUVET, L. P., NEVRALA, D. J. & PROBERT, S. D. 1993b. Influences of baffles on the rate of heat recovery via a finned-tube heat-exchanger immersed in a hot-water store. *Applied Energy,* 45**,** 191-217.

COLE, R. & BELLINGER, F. 1982. Thermally stratified tanks. Argonne National Lab., IL (USA).

CRUICKSHANK, C. A. & HARRISON, S. J. 2010. Heat loss characteristics for a typical solar domestic hot water storage. *Energy and Buildings,* 42**,** 1703-1710.

DEPARTMENT OF ENERGY AND CLIMATE CHANGE 2012. 2012 UK Greenhouse Gas Emissions, Provisional Figures and 2011 UK Greenhouse Gas Emissions, Final Figures Byfuel Type and End-User. *In:* CHANGE, D. O. E. A. C. (ed.).

DEVORE, N., YIP, H. & RHEE, J. 2013. Domestic Hot Water Storage Tank: Design and Analysis for Improving Thermal Stratification. *Journal of Solar Energy Engineering,* 135**,** 040905-040905-7.

ENGINEERINGTOOLBOX.COM. No Date. Available: http://www.engineeringtoolbox.com/water-thermal-properties-d_162.html [Accessed 22.08.2017].

EUROPEAN COMMISSION 2009. DIRECTIVE 2009/125/EC - establishing a framework for the setting of ecodesign requirements for energy-related products.

EUROPEAN COMMISSION 2010. Directive 2010/30/EU - on the indication by labelling and standard product information of the consumption of energy and other resources by energy-related products.

EUROPEAN COMMISSION 2013. Directive 2010/30/EU - Supplement.

EUROPEAN COMMISSION 2015. Guidelines Accompanying Regulations (EU) No 811, 812/2013, 813 & 814/2013.

FAN, J. & FURBO, S. 2012. Buoyancy driven flow in a hot water tank due to standby heat loss. *Solar Energy,* 86**,** 3438-3449.

FERNÁNDEZ-SEARA, J., UHıˊA, F. J. & SIERES, J. 2007a. Experimental analysis of a domestic electric hot water storage tank. Part II: dynamic mode of operation. *Applied Thermal Engineering,* 27**,** 137-144.

FERNÁNDEZ-SEARA, J., UHÍA, F. J. & ALBERTO DOPAZO, J. 2011. Experimental transient natural convection heat transfer from a vertical cylindrical tank. *Applied Thermal Engineering,* 31**,** 1915-1922.

FERNÁNDEZ-SEARA, J., UHÍA, F. J. & SIERES, J. 2007b. Experimental analysis of a domestic electric hot water storage tank. Part I: Static mode of operation. *Applied Thermal Engineering,* 27**,** 129-136.

GLOBAL CARBON PROJECT 2016. Global Carbon Budget Data. *In:* GLOBAL CARBON PROJECT (ed.).

GORMAN, I. M. O., MURRAY, D. B., BYRNE, G. & PERSOONS, T. Natural convection from isothermal horizontal cylinders. ASME 2009 International Mechanical Engineering Congress and Exposition, IMECE2009, 2010 Lake Buena Vista, FL. American Society of Mechanical Engineers (ASME), 1891-1897.

HALES, M. R. 1993. *Water Heaters*.

HAN, Y. M., WANG, R. Z. & DAI, Y. J. 2009. Thermal stratification within the water tank. *Renewable and Sustainable Energy Reviews,* 13**,** 1014-1026.

HEATRAE SADIA 2015. HeatRae Sadia Megaflo Eco Installation Manual.

HEATRAE SADIA No Date. Megaflo Eco Solar PV Ready Installation Manual.

HM GOVERNMENT 2008. Climate Change Act 2008.

HM GOVERNMENT 2013. Domestic Building Services Compliance Guide.

HM TREASURY 2007. Budget 2007: Regulatory Impact Assessment. *In:* TREASURY, H. (ed.).

HOME HEATING GUIDE. No Date-a. *Baxi Heating Bermuda 551 Gas - Boiler Efficiency Ratings* [Online]. Available: http://www.homeheatingguide.co.uk/efficiency-tables.php?model=016496 [Accessed 10.01.2017].

HOME HEATING GUIDE. No Date-b. *Baxi Maxflow Combi WM Efficiency* [Online]. Available: http://www.homeheatingguide.co.uk/efficiency-tables.php?model=008356 [Accessed 25/01/2017].

HOME HEATING GUIDE. No Date-c. *Glow-worm 65-80 65-80 Gas - Boiler Efficiency Ratings* [Online]. Available: http://www.homeheatingguide.co.uk/efficiency-tables.php?model=001248 [Accessed 10.01.2017].

HOUNSFIELD BOILERS. 2016. *Gravity hot water systems* [Online]. Available: http://hounsfieldboilers.co.uk/technical-help/heating-systems-explained/gravity-hot-water-systems [Accessed].

IDEAL BOILERS No Date. Ideal Vogue Combi Specification Sheet.

IEVERS, S. & LIN, W. 2009. Numerical simulation of three-dimensional flow dynamics in a hot water storage tank. *Applied Energy,* 86**,** 2604-2614.

IFS CHEMICALS. 2016. *Reduce Energy Usage with New Insulation Grade, Envirofoam Sustain* [Online]. Available: http://ifs-group.sosclient.com/articles/reduce-energy-usage-with-new-insulation-grade-envirofoam-sustain/ [Accessed 23/01/2017].

INTERNATIONAL ENERGY AGENCY 2011. 25 Energy Efficiency Policy Recommendations.

INTERNATIONAL ENERGY AGENCY. No Date. *Oil - FAQ* [Online]. Available: https://www.iea.org/about/faqs/oil/ [Accessed 23/01/2017].

IPSOS MORI & ENERGY SAVING TRUST 2013. Homeowners' Willingness To Take Up More Efficient Heating Systems. Department of Energy and Climate Change.

JORDAN, U. & FURBO, S. 2005. Thermal stratification in small solar domestic storage tanks caused by draw-offs. *Solar Energy,* 78**,** 291-300.

KINGSPAN ENVIRONMENTAL 2014. Range Tribune HE Installation Manual.

KINGSPAN ENVIRONMENTAL 2015. COMPLETE COMMERCIAL SOLAR THERMAL SOLUTIONS TECHNICAL GUIDE.

KINGSPAN ENVIRONMENTAL 2016a. FPW FLAT PLATE INSTALLATION MANUAL.

KINGSPAN ENVIRONMENTAL 2016b. Kingspan Tribune XE Product Brochure.

KINGSPAN ENVIRONMENTAL. 2017a. *Stainless Vented hot water cylinders* [Online]. Available: https://www.kingspanenviro.com/range/supercal-stainless-vented-hot-water-cylinders [Accessed 08/01/2017].

KINGSPAN ENVIRONMENTAL. 2017b. *Ultrasteel Plus Indirect Hot Water Cylinders* [Online]. Available: https://www.kingspanenviro.com/albion/ultrasteel-plus-indirect-hot-water-cylinders [Accessed 08/01/2017].

KINGSPAN ENVIRONMENTAL No Date. THERMOMAX HP400 & DF400 INSTALLATION MANUAL.

KNUDSEN, S. & FURBO, S. 2004. Thermal stratification in vertical mantle heat-exchangers with application to solar domestic hot-water systems. *Applied Energy,* 78**,** 257-272.

KUEHNER, J. P., PFLUG, J. R., TESSIER, F. A., HAMED, A. M. & MOISO MARIN, F. J. 2012. Velocity measurements in the free convection flow above a heated horizontal cylinder. *International Journal of Heat and Mass Transfer,* 55**,** 4711-4723.

KULACKI, F. A., DAVIDSON, J. H. & HEBERT, M. 2007. On the Effectiveness of Baffles in Indirect Solar Storage Systems. *Journal of Solar Energy Engineering,* 129**,** 494.

LAND ENERGY. No Date. *Renewable Energy Heating & Hot Water Systems* [Online]. Available: http://www.land-energy.com/heating-and-hot-water [Accessed 09.01.2017].

LAVAN, Z. & THOMPSON, J. 1977. Experimental study of thermally stratified hot water storage tanks. *Solar Energy,* 19**,** 519-524.

LIN, C. & EBADIAN, M. 1997. Developing turbulent convective heat transfer in helical pipes. *International Journal of Heat and Mass Transfer,* 40**,** 3861-3873.

MACLEAY, I., HARRIS, K., ANNUT, A. & CHAPTER AUTHORS 2010. Digest of United Kingdom Energy Statistics 2010. *In:* CHANGE, D. O. E. A. C. (ed.).

MACROTRENDS. 2017. *Crude Oil Prices - 70 Year Historical Chart* [Online]. Available: http://www.macrotrends.net/1369/crude-oil-price-history-chart [Accessed 23/01/2017].

MOTE, R., MINÉ, T., PROBERT, D. & CHAUVET, L. 1989. Comparison of designs and performances of heat exchangers for use in a hot water store. *Applied Energy,* 32**,** 155-169.

MOTE, R., PROBERT, S. D. & NEVRALA, D. 1991. The performance of a coiled finned-tube heat-exchanger submerged in a hot-water store: The effect of the exchanger's orientation. *Applied Energy,* 38**,** 1-19.

MOTE, R., PROBERT, S. D. & NEVRALA, D. 1992. Rate of heat recovery from a hot-water store: Influence of the aspect ratio of a vertical-axis open-ended cylinder beneath a submerged heat-exchanger. *Applied Energy,* 41**,** 115-136.

OFGEM. 2017. *About the Domestic RHI* [Online]. Available: https://www.ofgem.gov.uk/environmental-programmes/domestic-rhi/about-domestic-rhi [Accessed].

OLIVIER, J. G. J., JANSSENS-MAENHOUT, G., MUNTEAN, M. & PETERS, J. A. H. W. 2015. Trends in global CO2 emissions: 2015 Report. PBL Netherlands Environmental Assessment Agency.

PERSOONS, T., GORMAN, I. M., BYRNE, G. & MURRAY, D. B. Time-resolved heat transfer and fluid dynamic analysis of natural convection from isothermal horizontal cylinders. 2010 14th International Heat Transfer Conference, 2010. American Society of Mechanical Engineers, 131-138.

POWELL, C. S. & HALES, M. R. 2004. *Unvented Water Heater*.

PRINGLE, D. L. 2008. *Aluminium Hot Water Cylinder with Internal Piston-like Baffle*.

RANGE CYLINDERS 1950. Photograph from Range Cylinders Conference.

RESDEVON. 2015. *BIOMASS/WOOD BOILERS* [Online]. Available: http://www.res-devon.co.uk/technologies/biomass/ [Accessed 09.01.2017].

RHEE, J., CAMPBELL, A., MARIADASS, A. & MORHOUS, B. 2010. Temperature stratification from thermal diodes in solar hot water storage tank. *Solar Energy,* 84**,** 507-511.

SIMPSON, A. & CASTLES, G. 1992. Measurements of heat losses from an insulated domestic hot water cylinder. *Building Services Engineering Research and Technology,* 13**,** 43-47.

THE GREEN AGE. No Date. *Biomass Boilers Versus Conventional Gas Boilers* [Online]. Available: http://www.thegreenage.co.uk/tech/biomass-boilers-versus-conventional-gas-boilers/ [Accessed 10.01.2017].

UNITED STATES DEPARTMENT OF ENERGY. No Date. *Estimating the cost and energy efficiency of a solar water heater* [Online]. Available: https://energy.gov/energysaver/estimating-cost-and-energy-efficiency-solar-water-heater [Accessed 23/01/2017].

VIESSMANN 2016. Solar thermal and PV systems.

WALKER, A. 2016. *Natural Ventilation* [Online]. Whole Building Design Guide. Available: http://www.wbdg.org/resources/natural-ventilation [Accessed 29/01/2017].

WALMSLEY, M. R., ATKINS, M. J. & RILEY, J. 2009. Thermocline management of stratified tanks for heat storage.

WORLD HEALTH ORGANISATION 2007. Legionella and the Prevention of Legionellosis.

YAGHOUBI, M., ASHJAEE, M., ESHTIAGHI, A. H. & YOUSEFI, T. 2009. Thermal study of an array of inline horizontal cylinders below a nearly adiabatic ceiling. *Experimental Thermal and Fluid Science,* 33**,** 232-239.

Appendices

Appendix I - Height Difference Between Coil Connection Ports and Temperature Probe Ports

Probe	Coil Connection Port Number							
	1	**2**	**3**	**4**	**5**	**6**	**7**	**8**
DB Port 1	77	173	269	365	461	557	653	749
DB Port 2	-45	51	147	243	339	435	531	627
DB Port 3	-167	-71	25	121	217	313	409	505
DB Port 4	-289	-193	-97	-1	95	191	287	383
DB Port 5	-411	-315	-219	-123	-27	69	165	261
DB Port 6	-533	-437	-341	-245	-149	-53	43	139
DB Port 7	-655	-559	-463	-367	-271	-175	-79	17
DB Port 8	-777	-681	-585	-489	-393	-297	-201	-105

Table A.1 - Height difference in mm between coil connection ports and temperature probe ports

Appendix II – Comparison of a Vented and Unvented Test

Test Reference	Time (Decimal Minutes)	Volume Over 40°C (litres)	Coil Power (kW)	Remarks
LTR00119A	29.46	196	19.24	
LTR00119B	28.83	196	19.42	Vented recovery test
LTR00119C	29.85	196	19.04	
LTR00120A	28.88	198	19.86	
LTR00120B	30.05	196	19.1	Unvented recovery test
LTR00120C	30.4	196	18.77	

Table A.2 – Comparison of vented and unvented test for same coil

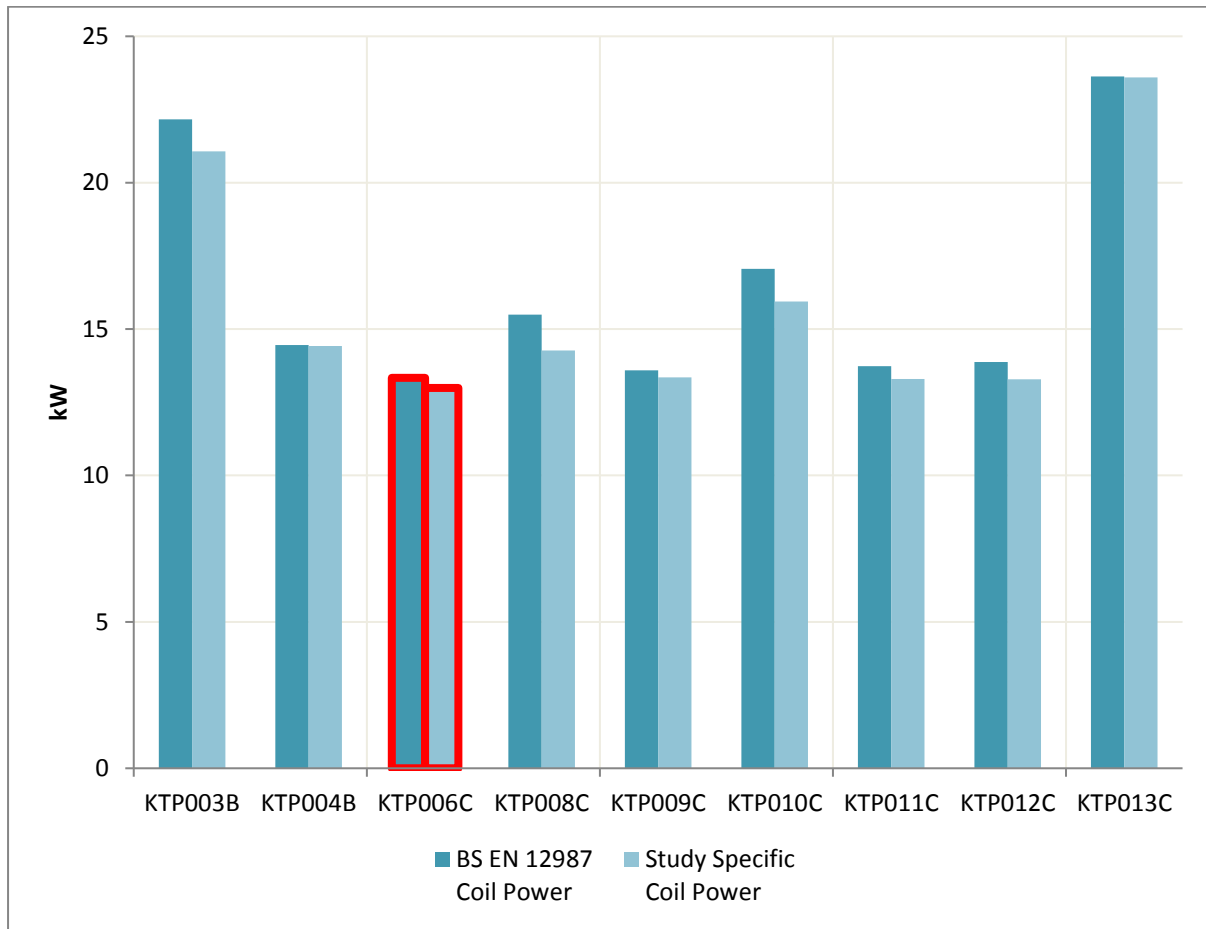## Appendix III – Coil Power Comparison for Two Methods of Calculation

Figure A.1 – Coil power comparison for BS EN 12897:2006 calculation method and study specific calculation method

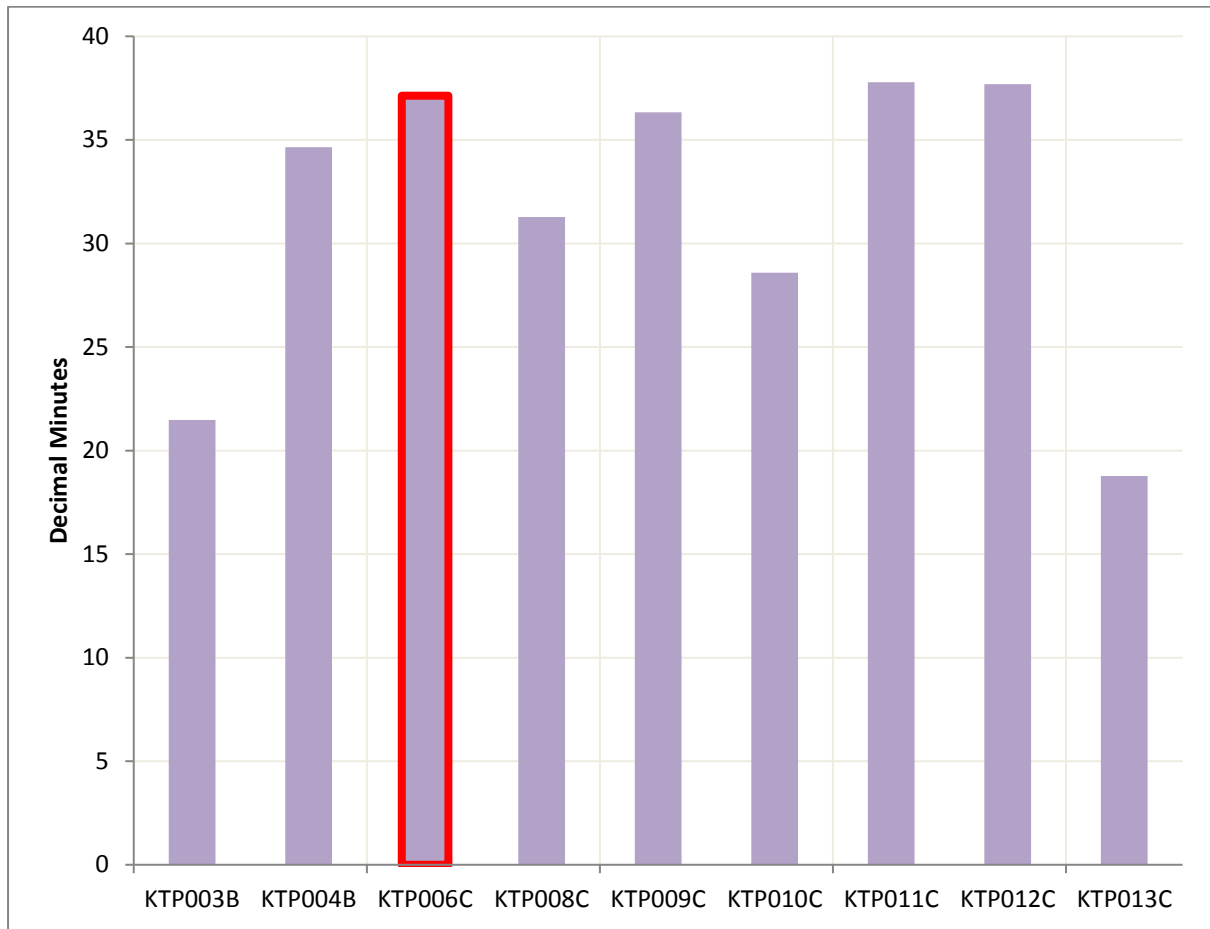# Appendix IV – Heat up time comparison for parametric study tests

Figure A.2 – Heat up time from 15°C to 60°C for parametric study tests

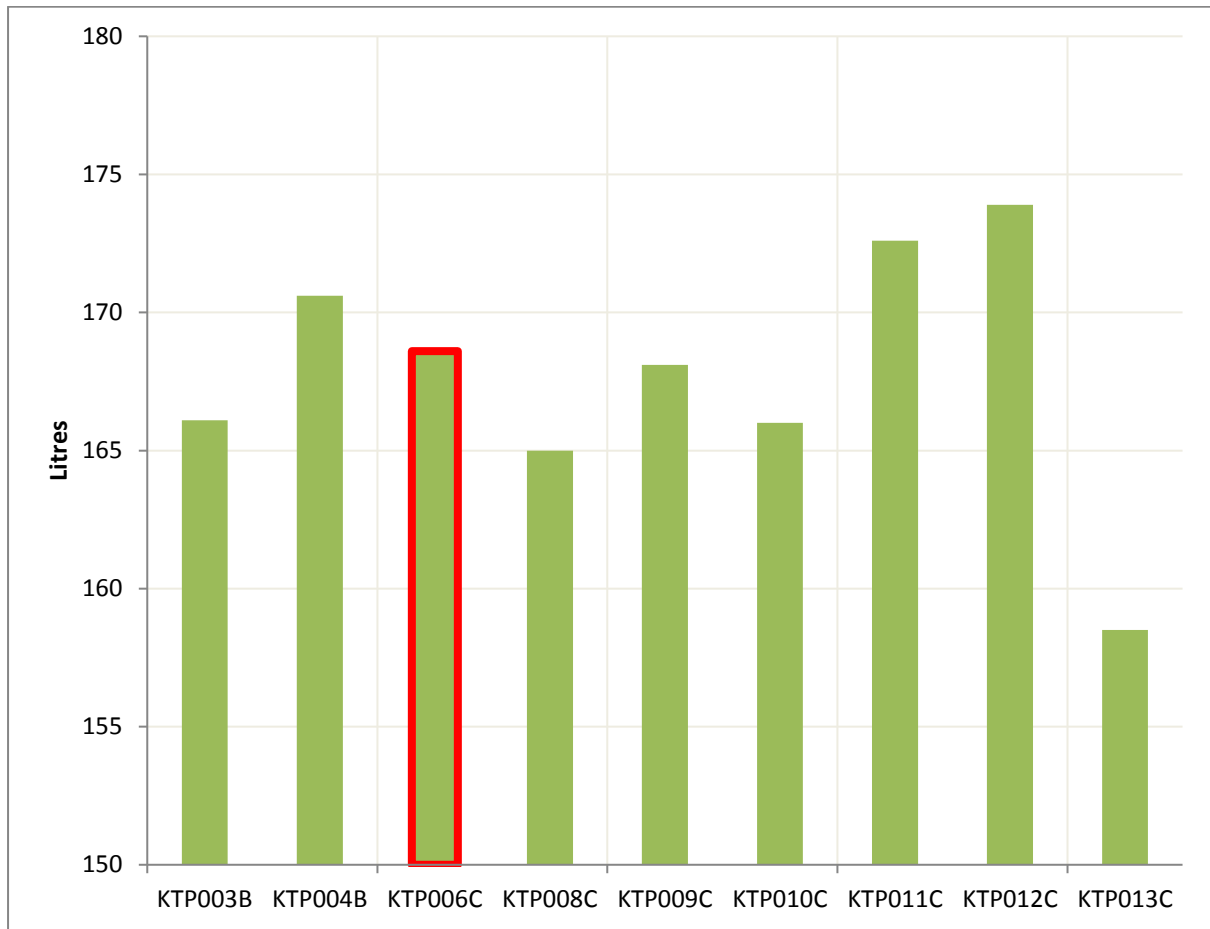# Appendix V – Comparison of Volume Drawn-off for Parametric Study Tests

Figure A.3 – Volume of hot water drawn-off above 40°C for parametric study tests